

Attachment A

Replace page 5.4-1 with attached 5.4-1 through 5.4-5.

8404100124 840402
PDR ADOCK 05000244
P PDR



1. 1990年12月25日，在“九七”香港回归前，香港各界人士纷纷发表文章，就香港前途问题提出自己的看法。

5.4 Fuel Storage

Specification

- 5.4.1 The new and spent fuel pit structures are designed to withstand the anticipated earthquake loadings as Class I structures. The spent fuel pit has a stainless steel liner to ensure against loss of water.
- 5.4.2 The spent fuel storage racks are divided into two regions as depicted on Figure 5.4-1. In Region 1 it is impossible to insert fuel assemblies in other than the prescribed locations. The fuel is stored vertically in an array with sufficient center to center distance between assemblies to assure $K_{eff} \leq 0.95$ for (1) unirradiated fuel assemblies delivered prior to January 1, 1984 (Region 1-15) containing no more than 39.0 gms U-235 per axial cm, and (2) unirradiated fuel assemblies delivered after January 1, 1984 containing no more than 41.9 gms U-235 per axial cm.
- 5.4.3 In Region 2 of the spent fuel storage racks, fuel is stored in a close packed array utilizing fixed neutron poisons in each of the stored locations. For discharged fuel assemblies to be stored in Region 2, (1) 60 days must have elapsed since the core reached hot shutdown prior to discharge and (2) the combination of assembly average burnup and initial U-235 enrichment must be such that the point identified by these two parameters on Figure 5.4-2 is above the line applicable to the particular fuel assembly design, therefore assuring that $K_{eff} \leq 0.95$.

5.4.4 The spent fuel storage pit is filled with borated water at a concentration to match that used in the reactor cavity and refueling canal during refueling operations whenever there is fuel in the pit.

Basis

The center to center spacing of Region 1, insures that $K_{eff} \leq 0.95$ for the enrichment limitations specified in 5.4.2¹, and for a postulated missile impact the resulting dose at the EAB would be within the guidelines of 10CFR100².

In Region 2, $K_{eff} \leq 0.95$ is insured by the addition of fixed neutron poison (boraflex) in each of the Region 2 storage locations, and a minimum burnup requirement as a function of initial enrichment for each fuel assembly design. The 60 day cooling time requirement insures that for a postulated missile impact the resulting dose at the EAB would be within the guidelines of 10CFR100.

The two curves of Figure 5.4-2 divide the fuel assembly designs into two groups. The first group is all fuel delivered prior to January 1, 1984. This incorporates all Exxon and Westinghouse HIPAR designs used at Ginna⁴. The second curve is for the Westinghouse Optimized Fuel Assembly design delivered to Ginna beginning in February 1984³.

The assembly average burnup is calculated using INCORE generated power sharing data and the actual plant operating history. The calculated assembly average burnup should be reduced by 10% to account for uncertainties. An uncertainty of 4% is associated with the measurement of power sharing. The additional 6% provides additional margin to bound the burnup uncertainty

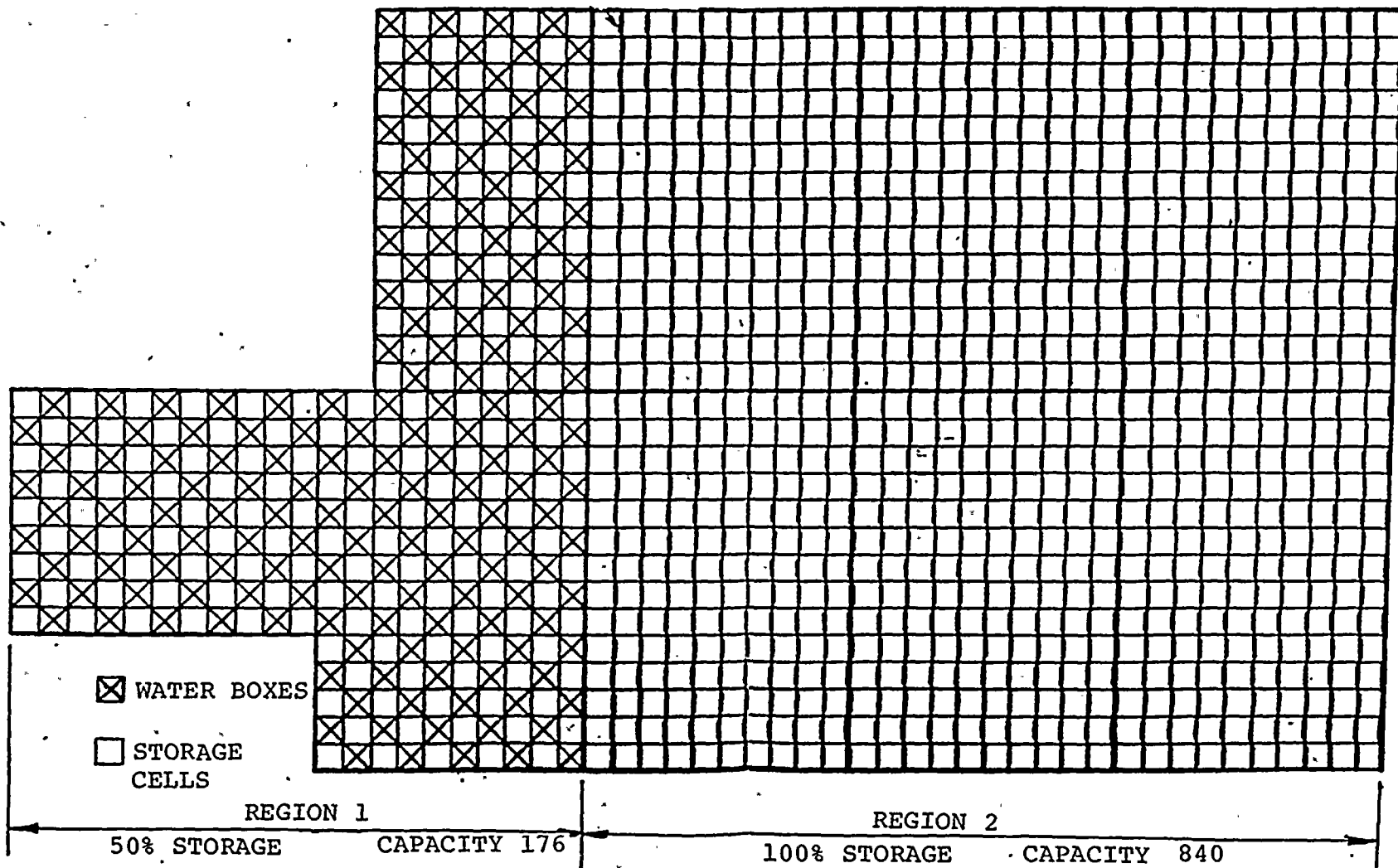
associated with the time between measurements and updates of core burnup. The curves of Figure 5.4-2 incorporate the uncertainties of the calculation of assembly reactivity.³

References

1. Letter, J.E. Maier to H.R. Denton, January 18, 1984.
2. Letter J.E. Maier to H.R. Denton, January 18, 1984.
3. Criticality Analysis of Region 2 of the Ginna MDR Spent Fuel Storage Rack, Pickard, Lowe and Garrick, Inc.
March 8, 1984.
4. Letter, T.R. Robbins, Pickard, Lowe and Garrick, Inc. to J.D. Cook, RG&E March 15, 1984.

FIGURE 4-1

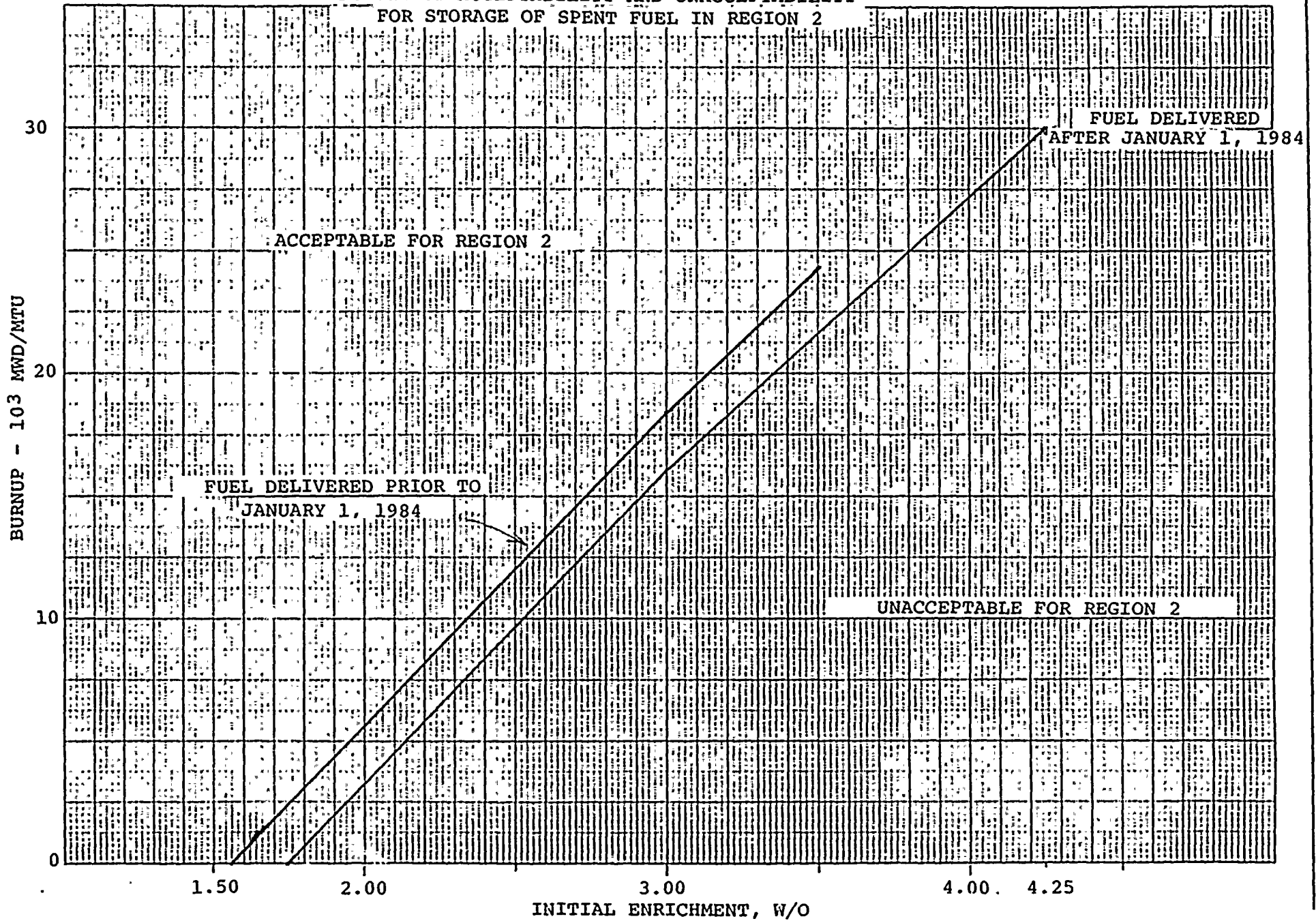
SPENT FUEL STORAGE RACKS



TOTAL CAPACITY 1016

FIGURE 3.4-2

REGIONS OF ACCEPTABILITY AND UNACCEPTABILITY
FOR STORAGE OF SPENT FUEL IN REGION 2



Appendix B

Background

The original spent fuel storage racks provided capacity for the storage of 210 fuel assemblies. In 1976 RG&E requested, and the NRC approved, the replacement of the original racks with higher density racks provided by Wachter and Associates.^{1,2} This expanded the storage capability from 210 to 595 fuel assemblies.

In 1980, RG&E requested³ and the NRC approved⁴ modifications to the spent fuel cooling system to provide heat removal capacity of 16×10^6 BTU/HR. This modification provides sufficient heat removal capability for all predicted fuel discharges in addition to a full core discharge at least to the year 2010.

Recently RG&E has submitted changes to the Technical Specification to establish new limitations on unirradiated fuel enrichment⁵ (which has been approved) and to delete a restriction on the spacing of recently discharged fuel⁶.

General

The proposed modification to the spent fuel storage racks will involve only the six west-most rack modules (Figure 1-1). These racks will be removed from pool and modified so that fuel assemblies can be stored in what were the water box locations. The remaining three rack modules will not be modified. The modifications will provide an additional 420 storage locations resulting in a total capacity of 1016*. The six modified racks will be designated Region 2 and will be used for fuel that satisfies certain burnup criteria and has cooled for at least 60 days. The

* A mechanical plug previously installed in a storage cell will be removed.



remaining three racks will be designated Region 1 and will be used for low burnup and/or recently discharged fuel.

The enclosed analysis conforms to the NRC guidance of April 14, 1978. This relies on past analyses (References 1 thru 6) for those components which are not modified or are not impacted by the modification. The analysis is separated into 7 sections.

1. Description of the Modification
2. Nuclear
3. Thermal-Hydraulic
4. Mechanical, Material and Structural
5. Cost/Benefit Assessment
6. Radiological Evaluation
7. Accident Evaluation

Rochester Gas & Electric utilized U.S. Tool & Die as a contractor to perform the mechanical, structural and material analyses. U.S. Tool & Die previously merged with Wachter and Associates, the suppliers of the current storage racks. The nuclear analysis was performed by Pickard, Lowe and Garrick, Inc.

The description of the modification notes an exception to the Technical Specifications (Section 3.11.3) that will be required to remove the west most racks in the pool. While the trolley of the auxiliary building crane or its transported rack will not travel over any spent fuel, the trolley will pass over 2-3 empty rows of a rack containing spent fuel. The distance between the area underneath the transported rack and the stored spent fuel will be maximized to insure the fuel would not be damaged if the load was dropped.

1. Description of the Modification

A description of the current spent fuel storage racks are contained in reference 1 and subsequent responses to NRC staff questions by RG&E. A general layout of the racks in the pool is at Figure 1-1. The racks as currently configured are composed of three major components.

- a. The rack modules, which are rectangular arrays of cells of which one out of two are storage cells. The others are water boxes.
- b. The support bases, on which the rack modules rest, are a rectangular construction of I beams. Figure 1-2 gives a general layout of the support bases in the pool and Figure 4-2 provides a sketch of the rack and support base. At each corner of the base a jack screw provides a leveling mechanism and lifts the base a minimum of 2 inches off the pool floor. To facilitate cooling water flow, holes are cut into the support base I beams. The jack screws bottom hemispherical head rests on steel plates which rest on the pool floor.
- c. Seismic supports between the bases and the pool walls provide a means to transmit horizontal loads from the racks to the walls (see figure 1-2).

Task Description of Modification

1. Shuffle spent fuel to the east most position in the pool to allow access to the two west most racks.

2. Divers loosen the four mounting bolts fastening the rack to the base in the two west most racks.

Comment: As a result of step 1, at least 8 empty rows of fuel cells will be between the divers and any spent fuel (Figure 1-1).

3. Install the lifting rig in the rack and using the auxiliary building crane remove it from the pool. As the racks clear the pool surface decontaminate with high pressure water. Move rack over the decontamination pit directly to the south of the spent fuel pool and place on J skid. Perform additional decontamination as required.

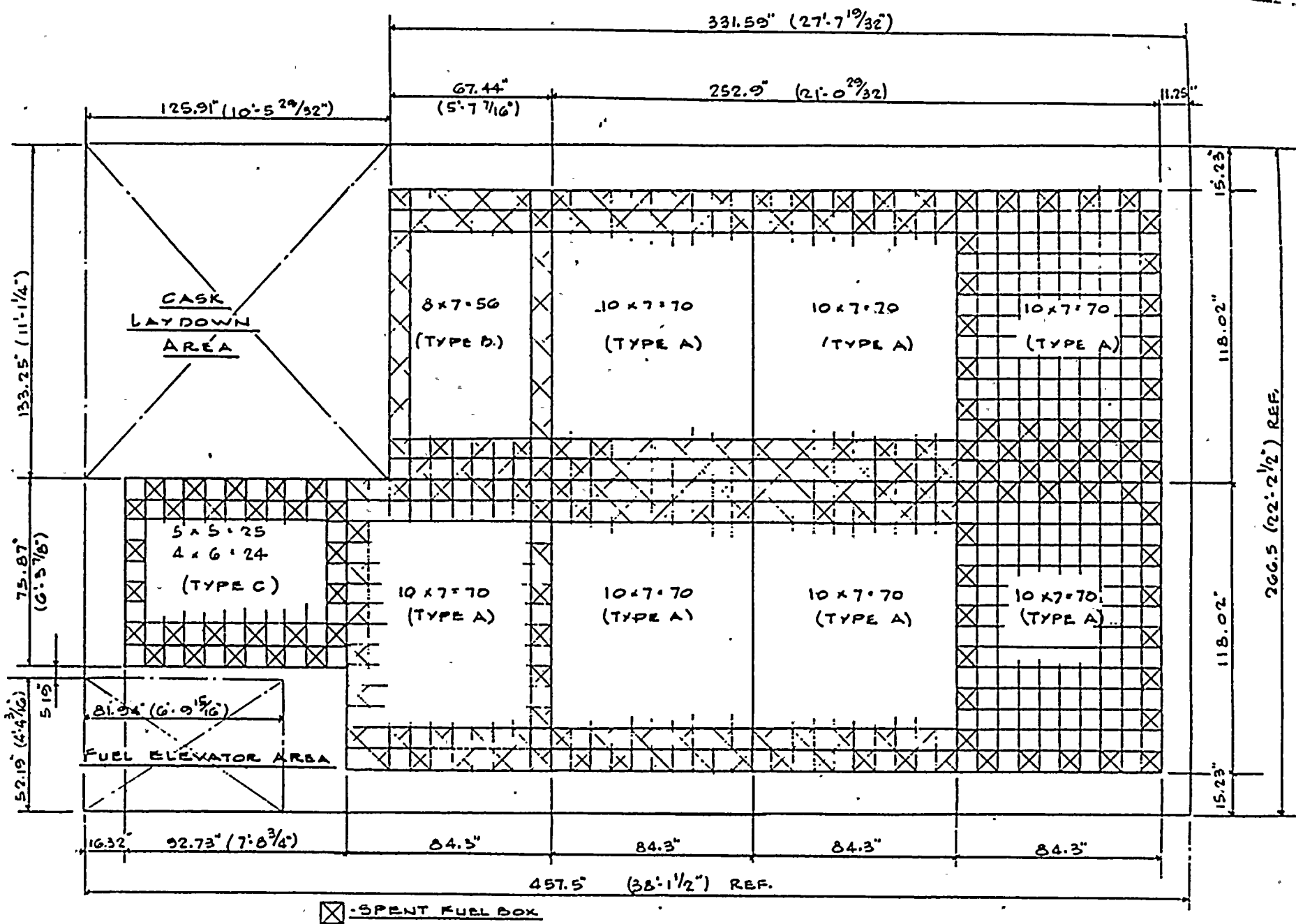
Comment: Both the spent fuel pool and the decontamination pit sit on bed rock, therefore, the safety significance of a rack drop during transfer is minimized (See Figure 1-3). For the modification, a temporary platform will be built over the decontamination pit on which the work will be performed. The Ginna Technical Specifications prohibits the trolley of the Auxiliary Building crane from moving over racks containing spent fuel (Section 3.11.3). For the first two west most racks this will be violated. However, the trolley or the transported rack will not pass over any spent fuel, but 2 to 3 empty rows of a rack containing spent fuel. Should a load drop occur the distance between these rows and cells containing spent fuel will prevent fuel damage. During the decontamination process over the pool, the pool boron concentration will be checked frequently.

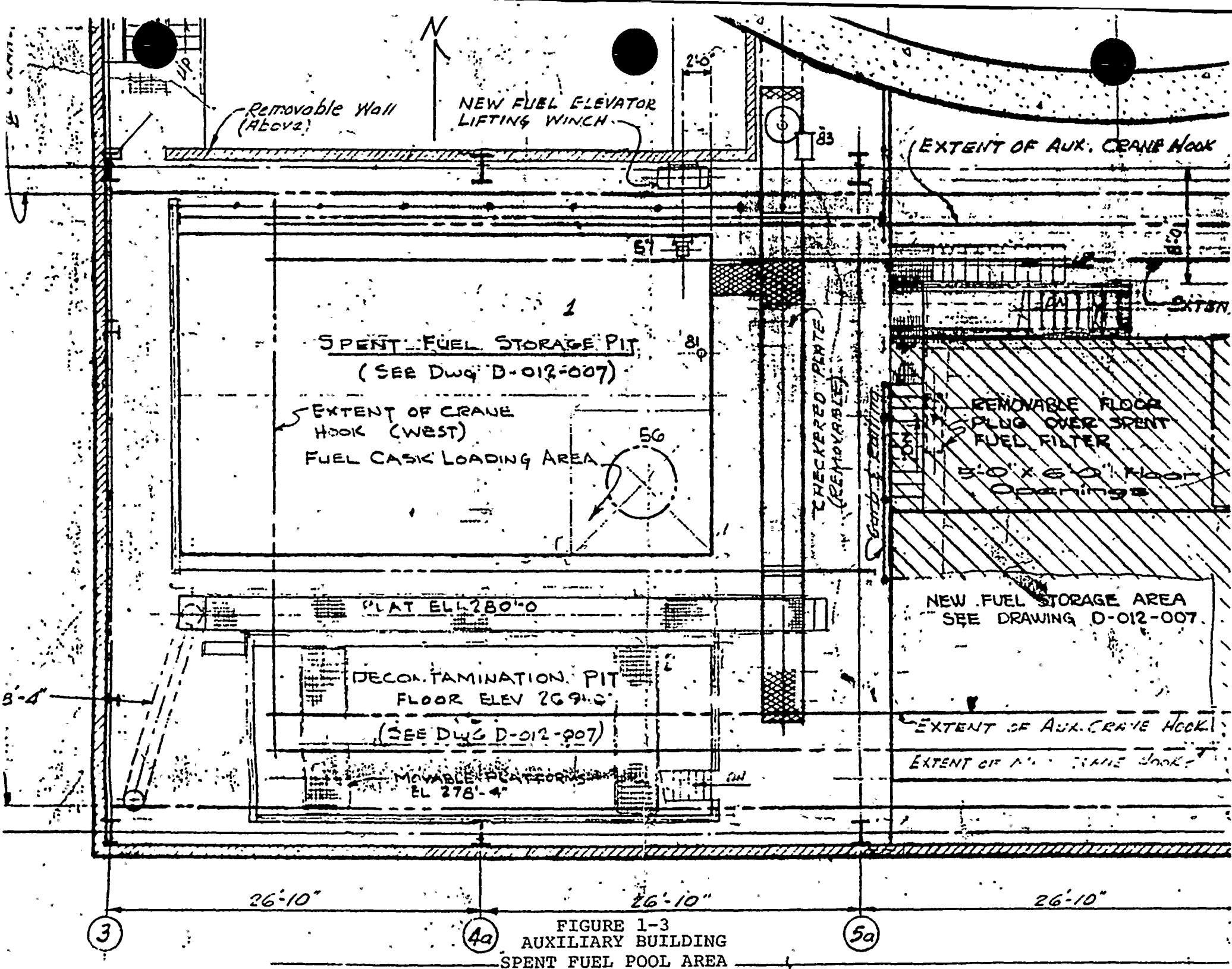
4. Using a special cutting machine remove 70 guide funnels and 28 guide angles over the water boxes.
5. Remove 4 lifter assemblies and install modified bottom plates with lifting slots.
6. Enlarge the flow holes in the bottom plates, and install additional 1/2" bottom plates to the former water boxes.
7. Install the right-angled poison assemblies in each cell of the rack.
8. Divers install shims at the corners of the support base and retract jack screws. Base and rack loads will rest on the shims.
9. Set racks in pool on support bases without the mounting bolts.
10. Repeat the above steps until the six west most racks in the pool have been modified.
11. Remove all (both Region 2 and Region 1) seismic supports between the rack bases and the walls.

In order to remove the two west most racks the spent fuel pool cooling system discharge pipe will have to be removed where it descends the west wall of the spent fuel pool. The decay heat load during the time period of the modification will be small (<2MBTU/HR) because the projected start time for the modification of October 1984 will be at least six months after the discharge of the last reload batch. The heat capacity of the pool is such that a heat up rate assuming no heat losses due to evaporation or other mechanisms is less than 1°F per hour. A temporary fitting and hose will be used to return cooling water to the pool.

Should coolant flow be lost, the slow heat up rate and the typically low initial temperature of the pool will ensure adequate time is available for the normal backup (skid mounted pump and heat exchanger) emergency cooling system to be put into operation. As soon as possible after the two west most racks are re-installed, the normal cooling path will be restored.

FIGURE 1-1





2. Nuclear Analysis

Attached is a nuclear analysis of Region 2 rack configuration performed by Pickard, Lowe and Garrick. This analysis establishes the minimum burnups as a function of initial enrichment required in order for a fuel assembly to be stored in Region 2. This analysis was performed for the Westinghouse Optimized Fuel Assembly. Reference 23 added the Exxon zircaloy guide tube design (Regions 13-15). The Exxon Regions 13-15 differ from the earlier Exxon Regions 10-12 only in that the later regions incorporate zircaloy guide tubes while the earlier regions had stainless steel guide tubes. The later Exxon region of fuel will be more reactive than the earlier region at any burnup because of this design change. Therefore, the minimum burnup criteria for Region 2 generated for Exxon Regions 13-15 will be bounding. The other fuel design used at Ginna was the Westinghouse HIPAR design which incorporated inconel grids and stainless steel guide tubes. Table 2-1 shows a comparison of design parameters for those fuel assemblies used at Ginna. Reference 23 documented that the Westinghouse HIPAR design is less reactive than the Exxon Regions 13-15 design at any burnup, therefore the minimum burnup criteria generated for the Exxon design will be bounding for the Westinghouse HIPAR.

In order to determine the burnup of an individual assembly following discharge, RG&E will use its Nuclear Fuel Accountability Code (NFAC) which was established in the early 1970's to record the isotopic content of the fuel and other specific parameters such as burnup for use in future fuel reprocessing. NFAC uses as input the burnup rate data (Mw-hrs per 1000 core Mw-hrs) generated

by INCORE results from flux measurements. Every assembly irradiated at Ginna is followed with NFAC beginning with insertion and proceeding through core life to discharge. These burnups generated by INCORE-NFAC will be reduced by a factor of 10% to conservatively bound measurement uncertainties. This reduced burnup will be compared to the curve (Figure 5.4-2 of proposed Technical Specification) to determine if a fuel assembly is acceptable for storage in Region 2.

As described in Section 1, every cell of the modified racks will have Boraflex neutron poison inserts installed. Specific quality control procedures will be used to insure the presence of the Boraflex in every cell. Proper documentation from the manufacturers of Boraflex will be obtained to assure the minimum ^{10}B density. A discussion of mechanical stability of Boraflex is at Section 5, Mechanical Analysis.

Referring to Figure 4-4, Poison Assembly Installation, the length of the poison material in the cell is 132 inches. This compares to a maximum fuel assembly active fuel length of 142 inches. The ends of the active fuel region will be at a burnup lower than the assembly average. However, this positive reactivity effect will be offset by the increased neutron leakage at the ends of the fuel region. Additional calculations are being performed to quantify the net reactivity effect of the poison configuration. The results of these calculations will be forwarded when available and the poison material region extended if required.

Table 2-1

Comparison of Design Parameters

	*Westinghouse HIPAR REGIONS 1-9	Exxon REGIONS 10-12	13-15	Westinghouse OFA REGION 16
Rod Array	14 x 14	14 x 14	14 x 14	14 x 14
Rods per Assembly	179	179	179	179
Rod Pitch, In.	.556	.556	.556	.556
Assembly Pitch	7.803	7.803	7.803	7.803
Active Fuel Height, In.	141.4-142.0	142.0	142.0	141.4
Clad O.D., In.	.422	.424	.424	.400
Clad Thickness, In.	.0243	.030	.030	.243
Clad Material	SS-304	ZRC	ZRC	ZRC
Pellet Diameter, In.	.3659	.3565	.3565	.3444
Annular Gap, In.	.0075	.0075	.0075	.0070
Pellet Density, %	94	94	94	95
Guide Tube O.D., In.	.5375	.540	.541	.5280
I.D., In.	.5075	.510	.507	.4825
GT Material	SS-304	SS-304	ZRC	ZRC
Instrument Tube O.D., In.	.422	.424	.424	.4015
I.D., In.	.3455	.346	.346	.3499
IT Material	SS-304	SS-304	ZRC	ZRC
# Grids	9	9	9	9
Grid Material	INCONEL	ZRC w INCONEL SPRINGS	ZRC w INCONEL SPRINGS	7-ZRC 2 - INCONEL

*These are Region 8 parameters. There were minor variations in some of these parameters over the regions.

3. Thermal Hydraulic

Reference 4 contains the NRC safety evaluation of proposed spent fuel pool cooling system modifications and approval that these would provide sufficient cooling capacity for projected discharges through year 2009 with a full core discharge in year 2010 (1360 fuel assemblies total). This cooling capacity exceeds the maximum that would be required under the proposed modifications (1016 fuel assemblies total). The current projected refueling cycles are consistent with the assumptions of this safety analysis.

It is anticipated that this modification will be completed during 1986. The current spent fuel pool cooling system capacity is 9.3×10^6 BTU/HR. This is far in excess of what will be required under normal conditions prior to 1986 (discharge of only one region of fuel at end of each cycle). If a full core discharge is required prior to the new spent fuel pool cooling system being in operation, the in-reactor decay time will be extended in order to ensure the pool temperature limitations in the Technical Specifications are satisfied.

In response to NRC questions concerning the previous storage rack modification, RG&E calculated the maximum cladding temperature for the hottest fuel assembly of a recently discharged batch, discharged in conjunction with a full core. This calculation showed a margin of over 80°F to the saturation temperature. This assumed a recently discharged batch grouped together at a storage location farthest from the cooling system cold water inlet. This analysis is still valid for Region 1 where, in accordance with the proposed Technical Specification (Section 5.4.4), recently

discharged fuel would be stored for a period of at least 60 days after reactor shutdown. After 60 days of cooling time the fuel could be moved to Region 2's higher density storage. As part of the modification, the flow hole at the bottom of the former water boxes would be enlarged to equal that of the other storage locations. As indicated in the analysis, adequate flow will be available to the hotter than average assemblies and there is no limiting thermal requirement which would prevent the grouping of these assemblies?

4. Structural, Mechanical, Material Analyses

A. Seismic Analysis

Objectives

The objectives of this seismic analysis are to determine the following during OBE and SSE seismic events:

1. The maximum loads imposed on the fuel storage racks.
2. The maximum distance the racks will slide and/or lift off.

The results of this analysis will be used in the mechanical analysis to evaluate the structural integrity of the racks when subjected to these loads and movements.

Scope

The loadings considered in this report for the modified racks using both standard fuel assemblies and consolidated fuel with a 2:1 compaction ratio are:

1. Deadweight of the fuel storage racks and the fuel assemblies.
2. Submerged weights of the fuel storage racks and the fuel assemblies.
3. Seismic loading, both OBE and SSE, as provided by the acceleration time history at the pool floor.

Horizontal responses to the seismic accelerations of the racks are obtained by evaluating the loadings for two different boundary conditions.

1. The horizontal motion is restrained by a horizontal force equal to 0.2 times the normal force. This is the minimum anticipated friction factor between the rack

and the support stand, (Ref. 13). These results give the maximum distance the racks will move during a seismic event.

2. Differential motion between the rack and the support stand is prevented. This is modeled in the finite element representation by placing a horizontal spring, representing the rack flexibility, between the rack and a fixed point.

Methods of Analysis

The vertical seismic analysis was performed using the equivalent static response spectra method. This consists of determining the vertical natural frequency to be greater than 33 HZ, then using accelerations of 0.23 g for OBE and SSE taken from the response spectra curves²⁴. These values were applied to the deadweight to obtain the total vertical forces. The vertical reaction loads were combined with the horizontal seismic loads using the square root sum of the squares method as specified in Ref. 8.

Horizontal seismic analysis was performed using the time history method of analysis in conjunction with time history data. The OBE time history data was obtained by dividing the SSE time history data by two. This accounts for the non-linearities inherent in the spent fuel storage racks which include:

1. Fuel-to-rack wall impacts
2. Rack sliding
3. Vertical impact due to rack tipping.

The time history analysis was performed using a special purpose computer program "RACKOE"*. This program was developed

* RACKOE is an acronym for rack analysis considering kinetics of earthquakes, a non linear finite element program developed by Prof. W.F. Stokey of Carnegie-Mellon University, Pittsburgh.



specifically to analyze fuel storage rack behavior resulting from seismic disturbance. This program solves the equations of motion explicitly using Euler's Extrapolation Formula.

The fuel rests in the cell base. It is assumed to act as a pinned beam, centered in the cell, with a gap between the cell and the fuel along its length. The gaps between the fuel and the cell walls can close causing impact to the walls. The space between the fuel and the wall is filled with water. As the fuel and the wall move relative to each other, hydrodynamic forces are set up due to the acceleration of the water. These forces are exerted on the fuel and rack structure, tending to mitigate impact forces. Hydrodynamic forces are generated between the racks and the pool walls. Methods described by Fritz (Ref. 9), Dong (Ref. 10) and Stokey (Ref. 11) are used to quantify these hydrodynamic forces.

Damping values used for this analysis are taken from Regulatory Guide 1.61, (Ref. 12). The rack boxes are welded together. When the welds are stressed there will be some localized deformation. The damping values are between those for welded steel and bolted steel structures. In the interest of conservatism the lower values for welded steel structures are used.

Friction, between the rack and the pool support stand, is handled by a special friction element of the model. The normal force on this element is the force in the vertical supports which, due to rack tipping, can be greater than the deadweight of the rack.

Equipment Description and Material Properties

Equipment Description

Section 1 provides a description of the modification. As shown in Figure 4-1, the west six racks will be modified to allow storage of spent fuel in what are currently water box locations. These racks will be designated Region 2 and will incorporate neutron absorbing material in each location. Shims are added under the rack bases in Region 2 to provide an increased load transfer area. Sliding is accommodated in the Region 2 racks between the rack and the base support by removal of the bolts between the two (Fig. 4-2). The Region 1 racks are unmodified and their storage density and loads remain the same. In this case sliding would occur between the jack screws at each corner of the support bases and the 11" x 11" plates which rest on the spent fuel pool floor.

In addition, all the seismic supports (both in Region 1 and Region 2) between the support bases and the spent fuel pool walls will be removed, therefore no loads will be transmitted to the walls by either region of racks as indicated by the results below. The amount of sliding is insignificant compared to the rack to wall clearance or the dimensions of the plates on which the Region 1 support base jack screws rest. Also the racks respond in-phase to seismic events, thus there will be no added impact loads at the Region 1 - Region 2 interface.

The analysis is performed for the 140 cell size rack which is common for all six in Region 2. The cell cross-section is shown on Figure 4-3 and the longitudinal section on Figure 4-4.

Two storage arrangements are analyzed. One is referred to as "standard" wherein one fuel assembly (179 fuel rods) is stored in each cell. The other is referred to as "consolidated" wherein the fuel rods from two assemblies (358 fuel rods) contained in a storage canister are stored in each cell. Figure 4.5 shows the arrangement of the fuel rods in the canister.

Material Properties

Applicable from 70 to 200 degrees F. The spent fuel racks are fabricated from type 304 stainless steel. The 304 SS rack material properties used in the seismic analysis are: (Ref. 14)

Density	=	501.0	PCF
Young's Modulus	=	27.8E06	PSI
Shear Modulus	=	10.7E06	PSI

The fuel assemblies contain clad constructed of Zircaloy whose properties are: (Ref. 15):

Density	=	409.0	PCF
Young's Modulus	=	13.0E06	PSI
Shear Modulus	=	5.0E06	PSI

Other densities used in the analysis are:

Water	=	62.4	PCF
UO2	=	643.0	PCF



Results

A finite element representation of a rack with fuel assemblies is shown on Figure 4-6 where:



Represents Mass Nodes

- 1 Rack at Base (Horizontal)
- 2-6 Rack (Horizontal)
- 7-11 Fuel Assy. (Horizontal)
- 12 Rotary Inertia
- 13 Rack & Fuel Assy's (Vertical)



Represents Flexible Elements

- 1-5 Rack
- 6-10 Fuel Assy.
- 11 Horizontal Support
- 12,13 Vertical Supports



Represents Gap Elements

MHrw = Hydrodynamic Mass (Rack to Wall)

MHrf = Hydrodynamic Mass (Rack to Fuel)

The results are summarized for:

- a. Standard Rack-140 Fuel Assy's-179 Fuel Rods Per Assy.
- b. Consolidated Rack-140 Fuel Canisters-358 Fuel Rods Per Canister.

The tabulated results are grouped and identified by "sets" numbered 1 thru 5. The values in each set are explained below.

SET #1 - Maximum Forces (KIPS).

SET #2 - Loads on Individual F/A's (LBS) and Support (KIPS).

The maximum contact forces are the forces of set #1 divided by the number of fuel assemblies in the rack. The support forces are the forces of set 1 divided by two. Two supports take the given reaction.

SET #3 - Maximum Forces (LBS) at the Rack Support.

The Fvert Values, NS, EW, VT, are the values of set 1 minus the submerged weight. (Ex. 271,700 - 208,190 = 63,510)

The Fhoriz Values, NS and EW, are taken from set 1.

The Vertical Forces, VT, are determined by using:

$$OBE = 0.23g$$

$$SSE = 0.23g$$

From the response spectra curve corresponding to 33 HZ²⁴.

$$VT (OBE) = (1.23 \text{ DWT} - \text{BUOYANT FORCE}) - \text{SUBMERGED WT.}$$

$$VT (SSE) = (1.23 \text{ DWT} - \text{BUOYANT FORCE}) - \text{SUBMERGED WT.}$$

The RMS Values are calculated using:

$$RMS = \text{SUBMERGED WEIGHT} + \sqrt{Fns^2 + Few^2 + Fvt^2}$$

SET #4 - Maximum Forces (LBS) on Each Support. These values are the values of Set #3 divided by 2.

SET #5 - Horizontal and Vertical Movement of the Rack (Inches)

ELASTIC - The amount the rack will deform as a result of the internal flexibility of the rack when restrained from horizontal motion.

SLIDING - The amount the rack will move when the rack is considered rigid and a 0.2 friction factor is used to restrain movement in the horizontal direction.

LIFTOFF - The maximum values the rack will move vertically off of the base, or tip, during the seismic event.

The Values DWT, BWT and SWT are Deadweight, Buoyant Weight, and Submerged Weight respectively.

The friction forces are the maximum horizontal forces developed at the base of rack using a minimum friction factor of 0.2.

PROJECT 8369

SUMMARY OF RESULTS FOR 140 CELL RACK - STANDARD. FILE RGSUM.1

-----SET #1 - MAX. FORCES (KIPS)-----
AT GAP ELEMENT#

DIR	EVT	1	2	3	4	5	SUPPORT	
							Fvt	Fhz
NS	OBE	31.4	53.2	53.3	64.4	83.5	271.7	170.0
EW	OBE	0.0	55.6	72.4	73.2	73.2	393.3	156.2
NS	SSE	8.9	62.0	98.3	77.7	97.6	404.7	231.5
EW	SSE	16.6	66.5	115.8	83.9	103.3	381.6	164.2

-----SET #2 - LOADS ON INDIVIDUAL F/A'S (LBS) AND SUPPORTS (KIPS)-----

NS	OBE	224.	380.	381.	460.	596.	135.9	85.0
EW	OBE	0.	397.	517.	523.	523.	196.7	78.1
NS	SSE	64.	443.	702.	555.	697.	202.4	115.8
EW	SSE	119.	475.	827.	599.	738.	190.8	82.1

-SET #3 - MAX. FORCES AT SUPPORT (LBS)

	Fvert	Fhoriz
NS OBE	63,510.	170,000.
EW OBE	185,110.	156,200.
VT OBE	53,728.	00,000.
RMS	411,133.	230,865.
NS SSE	196,510.	231,500.
EW SSE	173,410.	164,300.
VT SSE	53,728.	00,000.
RMS	475,723.	283,878.

-SET #5- MOVEMENT AT BASE (INS)

ELASTIC	SLIDING	LIFTOFF
0.019	0.080	0.009
0.046	0.088	0.048
0.026	0.308	0.050
0.048	0.513	0.067

-SET #4 - MAX. FORCES ON SUPPORT (LBS)--

NS OBE	31,755.	85,000.
EW OBE	92,555	78,100
VT OBE	26,864.	00,000.
RMS	205,567.	115,432.
NS SSE	98,255	115,750.
EW SSE	86,705.	82,150.
VT SSE	26,864.	00,000.
RMS	237,862.	141,939.

DWT = 233,600. LBS.
BWT = 25,410. LBS.
SWT = 208,190. LBS.

FRICTION FORCES
@ 0.2 FACTOR (LBS)

NSOBE = 41,640.
EWOBE = 82,210.
NSSSE = 59,760.
EWSSE = 101,600.

PROJECT 8369

SUMMARY OF RESULTS FOR 140 CELL RACK - CONSOLIDATED. FILE RGSUM.2

-----SET #1 - MAX. FORCES (KIPS)-----									
AT GAP ELEMENT#						SUPPORT			
DIR	EVT	1	2	3	4	5	Fvt	Fhz	
NS	OBE	0.0	0.0	100.0	98.4	159.3	312.4	160.2	
EW	OBE	0.0	53.6	178.3	176.0	180.1	405.2	153.0	
NS	SSE	14.8	214.9	225.6	217.5	250.7	455.7	239.3	
EW	SSE	0.0	148.4	249.3	223.2	235.0	512.1	184.7	
-----SET #2 - LOADS ON INDIVIDUAL F/A'S (LBS) AND SUPPORTS (KIPS)-----									
NS	OBE	00.	00.	714.	703.	1138.	156.2	80.1	
EW	OBE	00.	383.	1274.	1257.	1286.	202.6	76.5	
NS	SSE	106.	1535.	1611.	1554.	1791.	227.9	119.7	
EW	SSE	00.	1060.	1781.	1594.	1679.	256.1	92.4	
-SET #3 - MAX. FORCES AT SUPPORT (LBS)					-SET #5- MOVEMENTS AT BASE (INS)				
		Fvert		Fhoriz		ELASTIC SLIDING		LIFTOFF	
NS	OBE	* 00.		160,200.		0.018	0.028	0.000	
EW	OBE	64,140.		153,000.		0.045	0.024	0.015	
VT	OBE	89,470.		00,000.					
RMS		451,146.		221,524.					
NS	SSE	114,640.		239,300.		0.027	0.094	0.017	
EW	SSE	171,040.		184,700.		0.054	0.128	0.072	
VT	SSE	89,470.		00,000.					
RMS		565,564.		302,289.					
-SET #4 - MAX. FORCES ON SUPPORT (LBS)--									
NS	OBE	00.		80,100.					
EW	OBE	32,070		76,500					
VT	OBE	44,735.		00,000.					
RMS		225,573.		110,762.					
NS	SSE	57,320.		119,650.					
EW	SSE	85,520.		92,350.					
VT	SSE	44,735.		00,000.					
RMS		282,782.		151,144.					
						DWT = 389,000. LBS.			
						BWT = 47,940. LBS.			
						SWT = 341,060. LBS.			
						FRICTION FORCES			
						@ 0.2 FACTOR (LBS)			
						NSOBE = 49,640.			
						EWOBE = 51,630.			
						NSSSE = 68,210.			
						EWSSE = 68,210.			
						* BECAUSE OF NO LIFTOFF.			

B. Mechanical Analysis

Introduction

The spent fuel storage racks are classified as category 1 per NRC Regulatory Guide 1.29. Their primary function is to maintain stored fuel assemblies in a subcritical array while protecting them from mechanical damage during all credible storage conditions. The mechanical analysis presents analytical proof of structural integrity.

The analysis follows NRC guidance as delineated in the position paper "Review and Acceptance of Spent Fuel Storage and Handling Applications", dated April 14, 1978 and modified January 18, 1979. The design calculations are based on subsection NF of ASME Boiler and Pressure Vessel Code, Section III and Appendix D of the Standard Review Plan (SRP) 3.8.4. The permissible weld stresses are taken from Table NF-3324.5(a)-1, 1983 edition. This is the same as Table NF-3292-1, 1977 edition, referred to in the position paper and in NF-3321. This table no longer exists in the 1983 edition.

The load combinations used in this analysis are only submerged deadweight plus SRSS combinations of OBE and SSE loads. These load combinations are the RMS values taken directly from the seismic analysis (Section 4A). The racks are not subjected to live loads nor to thermal loads. Thus the load combinations, $D+L+T_o(\text{or } T_a)+E$ and $D+L+T_a+E'$ become $D+E$ and $D+E'$.

Analyses are performed for two storage arrangements, one referred to as "standard" wherein one fuel assembly (179 fuel rods) is stored in each cell in Region 2, the other referred to as "consolidated" wherein the fuel rods from two assemblies (358 fuel rods) in a canister are stored in each cell in Region 2.

The interface between the racks and bases is the cruciform bottom plate at the rack corners which span three boxes in each direction. Thus the plane at the third row location, as shown on Figures 4-7 and 4-8, and the three-box corner square are the weld planes analyzed.

Floor loads for Region 2 are transferred through the base to the 11" x 11" floor plates. Because of the increased storage in Region 2, shims are installed between the base corner and each floor plate to provide greater load transfer area than the present jackscrews (Fig. 4-9). In Region 1, however, since no change in storage is being made there is no change in base to floor plates, i.e. The jackscrews remain. The region 1 racks are not being moved from their present locations, and with the jackscrews centered on the 11" x 11" floor plates there is enough distance to the edge to take care of any sliding.

There are no calculations for wall loads because, as freestanding racks and bases, due to removal of the wall seismic restraints, there are relatively large dimensions between the racks and walls and consequently small hydrodynamic forces. These approximate dimensions are indicated on Figure 4-1 and are large compared to the maximum sliding distance of .5 inches.

References 1 and 2 provided an evaluation of fuel handling accidents and concluded that the rack structure protects stored fuel from the impact of a dropped fuel assembly.

A postulated drop accident of a fuel assembly straight down into a storage cell is included in the report because it was not previously addressed.

Equipment Description

Six of the nine presently installed racks will be modified for 100% storage density, and designated as Region 2 for storage of depleted fuel. The remaining three racks, unmodified, are designated Region 1 for storage of unirradiated or freshly discharged fuel at 50% storage density.

All six racks in Region 2 are the same size, 140 storage cells. The modification consists of removing the present bolt connections between racks and bases and the wall seismic restraints, resulting in a free-standing array. The wall seismic restraints are also removed from Region 1. Additionally, a full-length right angle poison insert is welded in each Region 2 cell, as shown on Figure 4-3 and Figure 4-4 of the seismic analysis (Section 4A).

A sketch of rack, base, shims, and floor plates is represented in Figure 4-9. The shims are added between the base and floor plates in order to provide more load carrying area than the present jackscrews.

Loads from the Seismic Analysis

Tabulation of loads from the seismic analysis are in Section 4A. The load combinations of D+E (OBE) and D+E' (SSE) are the RMS

values listed at Set #3. Maximum vertical loads are those occurring on 2 of the 4 rack corners at return impact following lift-off. Set #4 is half of set #3 or the load on a single corner.

The stresses are summarized in Table 4-1 for:

- a. Shear in welds no. 1, 2, & 3 shown on Figures 4-7 and 4-8.
- b. Shear out of the corner 9 boxes (shaded area, Fig. 4-7).
- c. Buckling of the box walls
- d. Floor loads under the 11" x 11" base plate

The stresses in welds no. 1, 2, & 3 are determined by calculating the RMS values of the shear load, vertical and horizontal, to get the NS, EW, VT and SWT loads. The force in the weld is calculated by:

$$F = \text{SWT} \pm \sqrt{F_{\text{NS}}^2 + F_{\text{EW}}^2 + F_{\text{VT}}^2} \quad (\text{SWT is Submerged Weight})$$

The shear out of the corner, the buckling load on the plate and the floor load are determined by using the RMS values for the individual supports given in Section 4A.

The maximum stresses in welds 1, 2, & 3 are:

STD. Rack, E-W Plane, OBE, 19,970 psi, Weld #2
STD. Rack, N-S Plane, SSE, 21,700 psi, Weld #2
CON. Rack, E-W Plane, OBE, 16,940 psi, Weld #2
CON. Rack, E-W Plane, SSE, 23,340 psi, Weld #1

The maximum shearout stresses in the corners are:

STD. Rack, OBE, 11,940 psi
STD. Rack, SSE, 13,800 psi
CON. Rack, OBE, 13,110 psi
CON. Rack, SSE, 16,430 psi

The maximum floor loads in the 11" x 11" base plate are:

STD. OBE, 1700 psi

STD. SSE, 1965 psi

CON. OBE, 1860 psi

CON. SSE, 2340 psi

The allowable weld OBE shear stress is 24,000 psi. (Ref. 14),
Sect. NF 3000, Table NF-3292 1-1)

The allowable weld SSE shear stress is 38,400 psi (1.6 OBE
(USNRC, SRP 3.8.4.5(b))

The critical buckling stress is 19,140 psi (Ref. 21 pg. 2.12)

Floor Loads

The six modified racks are in Region #2. Using the submerged
weight for the rack and contained fuel assemblies the total floor
loads are:

Standard Rack 1,249,000 LBS.

Consolidated Rack 2,046,360 LBS.

THE BEARING STRESS ON THE CONCRETE UNDER THE
11" X 11" X 3/4" SUPPORT PLATES ARE:

	STANDARD RACK		CONSOLIDATE RACK	
	<u>OBE</u>	<u>SSE</u>	<u>OBE</u>	<u>SSE</u>
FLOOR LOAD (lbs)	205,567	237,862	225,573	282,782
BEARING STRESS (PSI)	1700	1965	1864	2337

The allowable concrete bearing stress is 3570 psi (Ref. 22).

TABLE 4-1

SUMMARY OF STRESSES

	STRESS (PSI) NORTH-SOUTH PLANE				STRESS (PSI) EAST-WEST PLANE			
	STANDARD		CONSOLIDATED		STANDARD		CONSOLIDATED	
	<u>OBE</u>	<u>SSE</u>	<u>OBE</u>	<u>SSE</u>	<u>OBE</u>	<u>SSE</u>	<u>OBE</u>	<u>SSE</u>
WELD #1	11680	16200	7980	17330	18480	18660	14260	21260
WELD #2	14800	21700	11280	22100	19970	20270	16940	23340
WELD #3	11350	17700	12170	17200	18880	19320	16720	22430
CORNER* SHEAROUT	11,950	13,800	13,110	16,430	11,950	13,820	13,100	16,430
BOX* BUCKLING STRESS	8,800	10,200	9,670	12,120	8,800	10,200	9,670	12,120
MAX.* FLOOR LOADS	1,700	1,965	1,860	2,340	1,700	2,000	1,860	2,340

* These values are common to both planes.

Straight Drop of a Fuel Assembly Through an Individual Cell

An analyses was performed to determine the affect of a fuel assembly being dropped onto or into a spent fuel rack. The consequences of a drop onto a rack, in which the assembly impacts the top of the fuel boxes, has previously been addressed and found acceptable (Ref. 1, 2). It was shown that a fuel assembly is not damaged by this drop. An assessment is provided below of a fuel assembly being dropped directly into a fuel box. Since the clearance between a fuel assembly and a fuel box, even in the maximum box size considering tolerances, is on the order of .2 inches, it is unlikely that this would occur. It is most likely that the fuel bundle will strike the top of the fuel box and be deflected so that the energy is dissipated in deformation of the box or fuel bundle itself.

This postulated drop accident would cause the fuel assembly to impact the bottom plate in the cell. The clearance between fuel dimensions and box dimensions are quite close; thus the fuel assembly would act as a leaky piston and the fuel box would act as a leaky cylinder. The hydraulic forces generated when the fuel assembly initially enters the fuel box would be quite large and would serve to retard the fuel assembly during the next 13.25 feet of its descent. The 0.090" welds which attach the bottom plate to the cell would be plastically deformed to failure if loaded high enough. This failure load estimate is based on

30,000 psi ultimate shear strength and a typical plastic deformation of 20%. The area in shear is

$$0.090" \times 4(8.25") = 2.97 \text{ in.}$$

$$\text{Energy} = 30,000 \text{ psi} \times (20\% \times 0.090") \times 2.97 \text{ in.} = 1604 \text{ in-lbs.}$$

Comparing this value to the energy available from the straight drop on the rack, which is 43,500 in-lb when the fuel assembly is considered as a rigid body for a 30" drop, the bottom plate welds would fail.

Since each bottom plate of a fuel location is individually welded to its fuel box, failure of one bottom plate would not affect any other fuel location of stored fuel. Thus, the postulated fuel drop would only result in one storage location being rendered unuseable. In addition, the consequences from a radiological standpoint are unchanged since only one assembly would be affected. Also, since the physical configuration of the spent fuel storage cells will not be changed, the sub-critical array of the rack is maintained.

Neutron Absorbing Material

The neutron material, Boraflex, to be used in the Ginna modified spent fuel rack construction will be manufactured by Brand Industrial Services, Inc., and fabricated to safety related nuclear criteria of 10CFR50, Appendix B. Boraflex is a silicone based polymer containing fine particles of boron carbide in a homogeneous, stable matrix. Boraflex contains a minimum ^{10}B density of 0.2 gm/cm^3 .

Boraflex has undergone extensive testing to study the effects of gamma irradiation in various environments, and to verify its

structural integrity and suitability as a neutron absorbing material.¹⁸ Tests were performed at the University of Michigan exposing Boraflex to 1.03×10^6 rads gamma radiation with a substantial concurrent neutron flux in borated water. These tests indicate that Boraflex maintains its neutron attenuation capabilities before and after being subjected to an environment of borated water and 1.03×10^6 rads gamma radiation.¹⁹

Long term borated water soak tests at high temperatures were also conducted.²⁰ It was shown that Boraflex withstands a borated water immersion of 240°F for 260 days without visible distortion or softening. Boraflex maintains its functional performance characteristics and shows no evidence of swelling or loss of ability to maintain a uniform distribution of boron carbide.

During irradiation a certain amount of gas may be generated. However, the absorber will not be sealed within the storage cell and vent paths will be available to the pool. This will prevent gas induced swelling of the inserts and interference with the fuel assembly.

The actual tests verify that Boraflex maintains long-term material stability and mechanical integrity, and can be safely utilized as a poison material for neutron absorption in spent fuel storage racks.

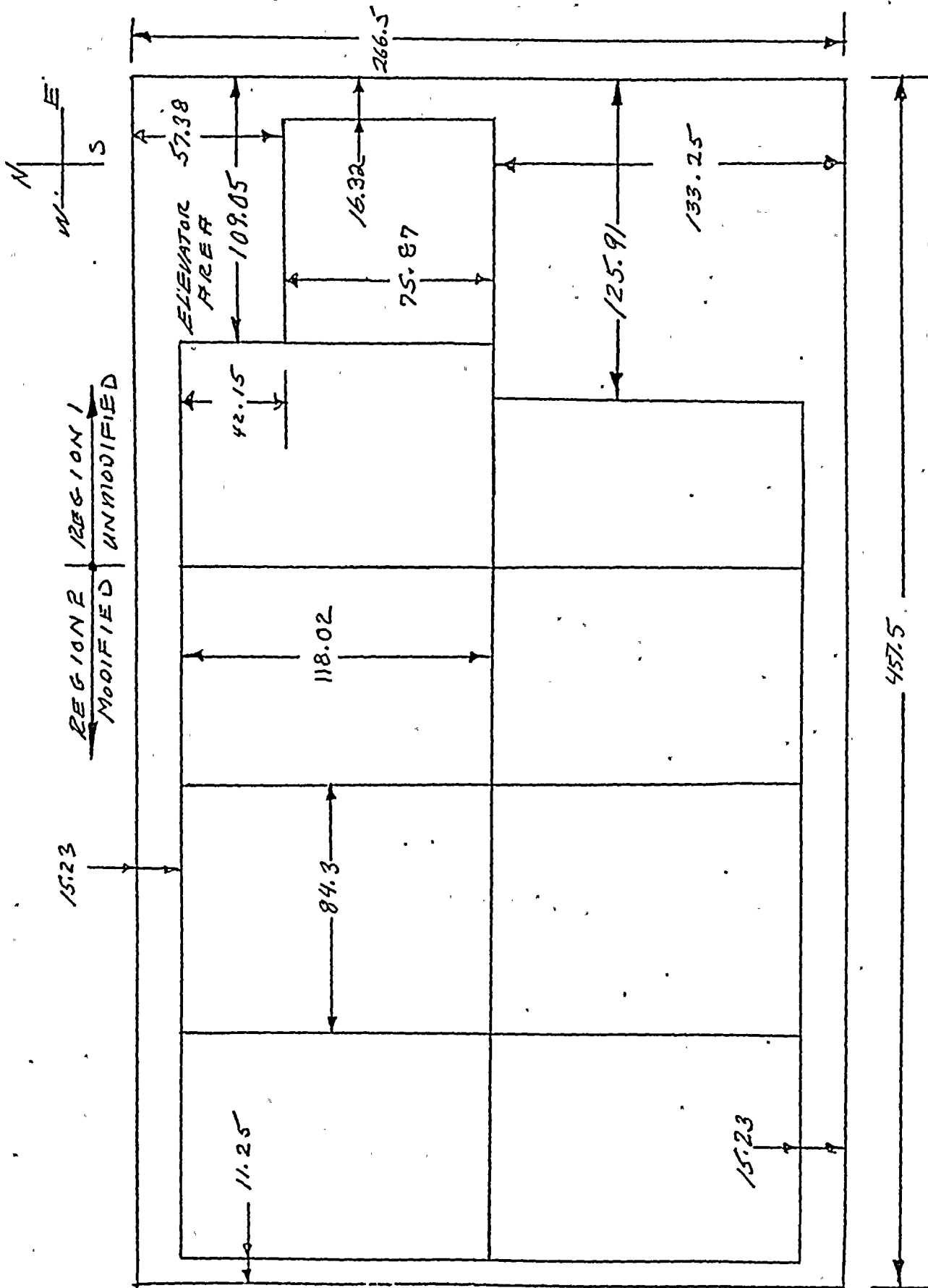
Beyond the extensive testing conducted, Boraflex is broadly used in high density spent fuel storage racks in the United States and in Europe. It was first installed at Point Beach Unit

1 in 1979. A partial list of operating power reactor users of Boraflex follows:

Point Beach Units 1 & 2	Calvert Cliffs II
Nine Mile Point Unit 1	Quad Cities Units 1 & 2
Oconee Units 1 & 2	H.B. Robinson Unit 2
Prairie Island Units 1 & 2	

The extensive testing and the broad industry experience with the use of Boraflex obviates the need for a Ginna specific surveillance program of the neutron absorber. Any potential long term problems will develop at other plants before it would be evident at Ginna.

BY ALW DATE 11/27/83 SUBJECT FIGURE 4-1 SECT. 2 SHEET 4 OF 8
 CHKD. BY WMM DATE 12/27/83 POOL LAYOUT PROJ. NO. 8369



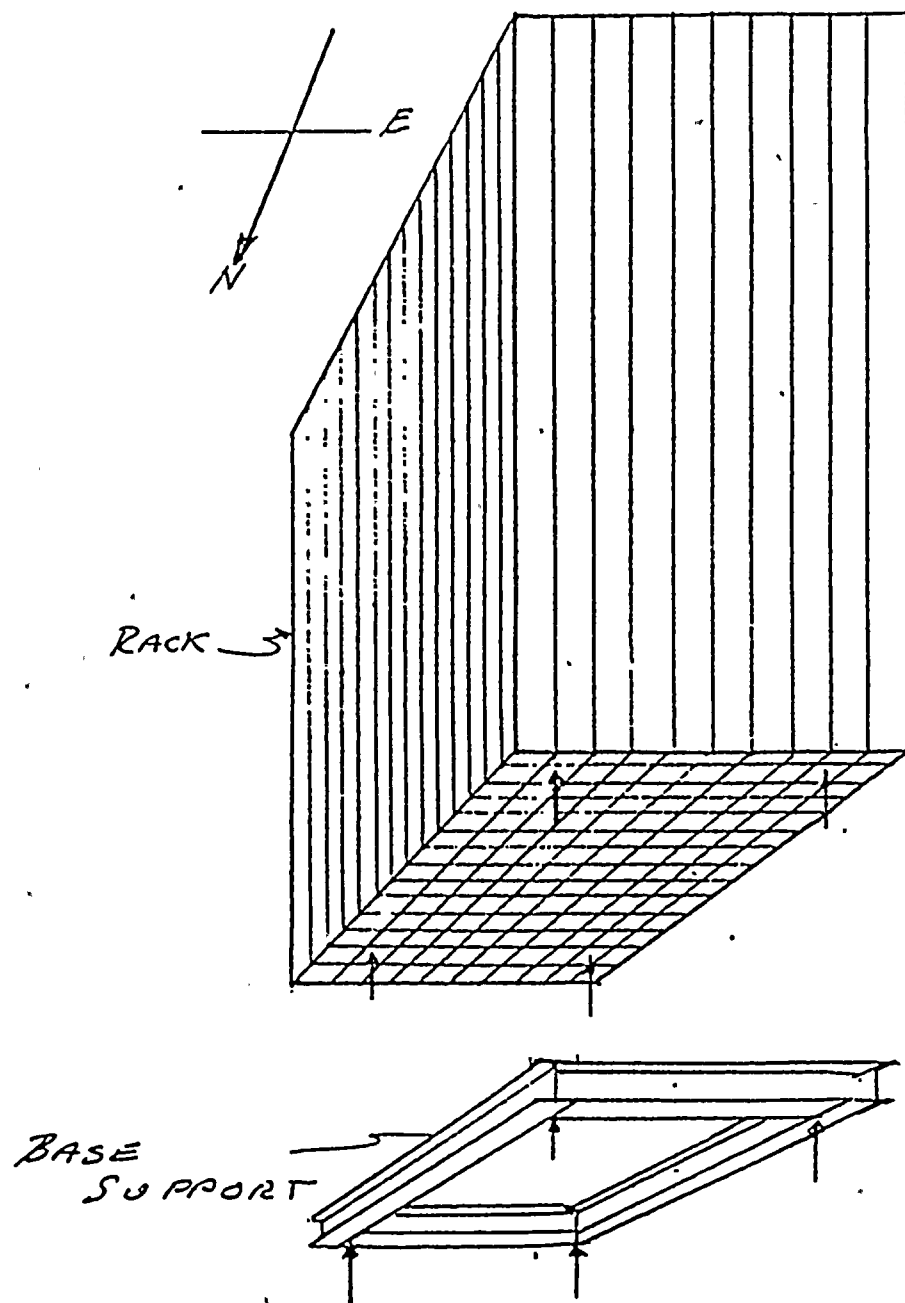


FIGURE 4-2
RACK-BASE SUPPORT

BY R. J. L. DATE 10/13/83 SUBJECT

CHKD. BY W. H. H. DATE 10/22/83

MUR STRETCH DESIGN.

PROJ. NO. 8369

CROSS-SECTION (FULL SIZE)

REVISED 10/22/83 TR

FIGURE 4-3

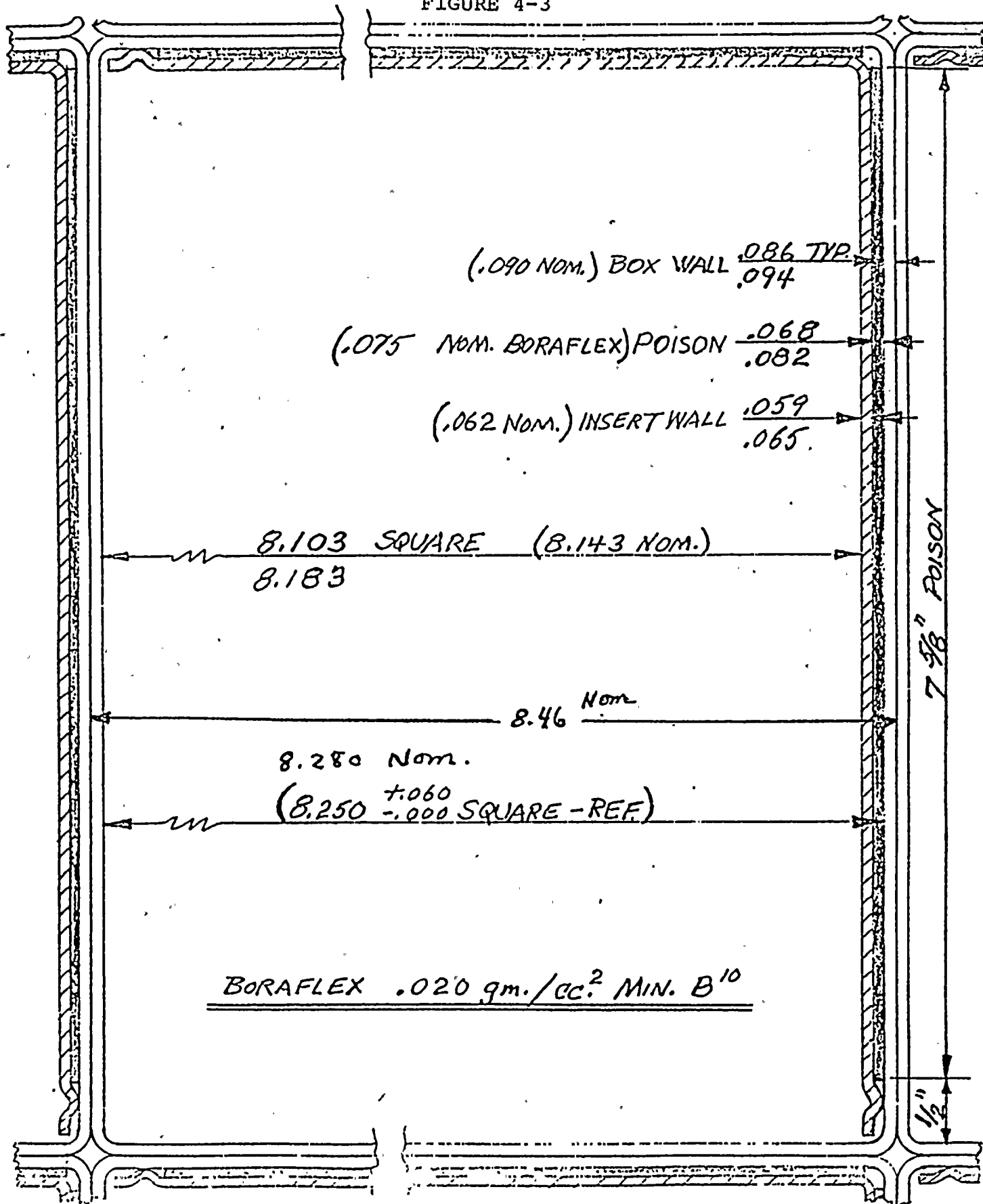
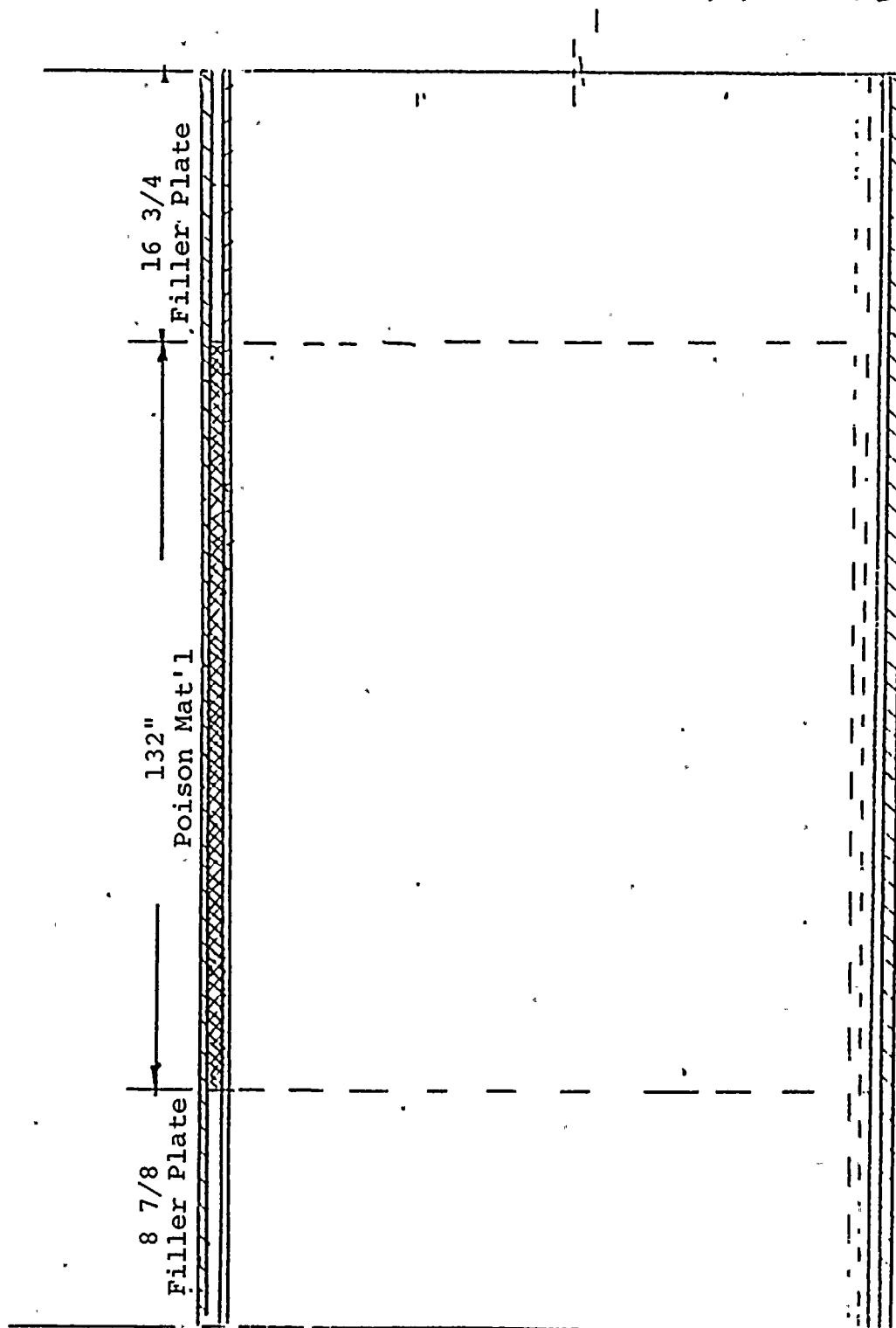


FIGURE 4-4

POISON ASSEMBLY INSTALLATION

REF. DWG B369-5



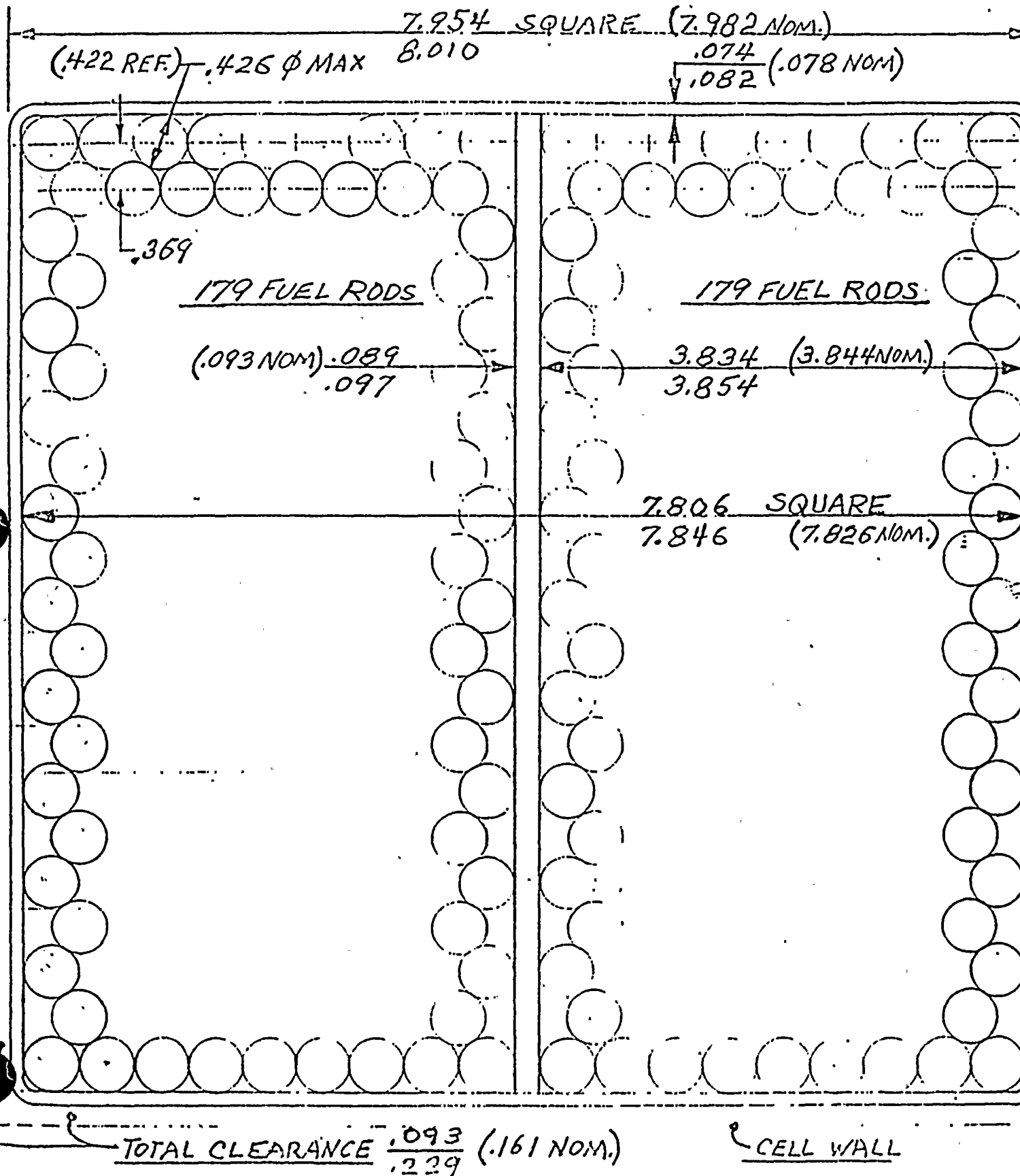
BY Ray L. L... DATE 10/22/83 SUBJECT
 CHKD. BY J... DATE 12/15/83

FIGURE 4-5

8 OF 8
 8369

ROD CONSOLIDATION

CROSS-SECTION (~FULL SIZE)



PROJECT 8369

DIRECTION OF LOAD

FIGURE 4-6
FINITE ELEMENT REPRESENTATION

FIGURE 4-7
RACK WELDS
EAST-WEST PLANE

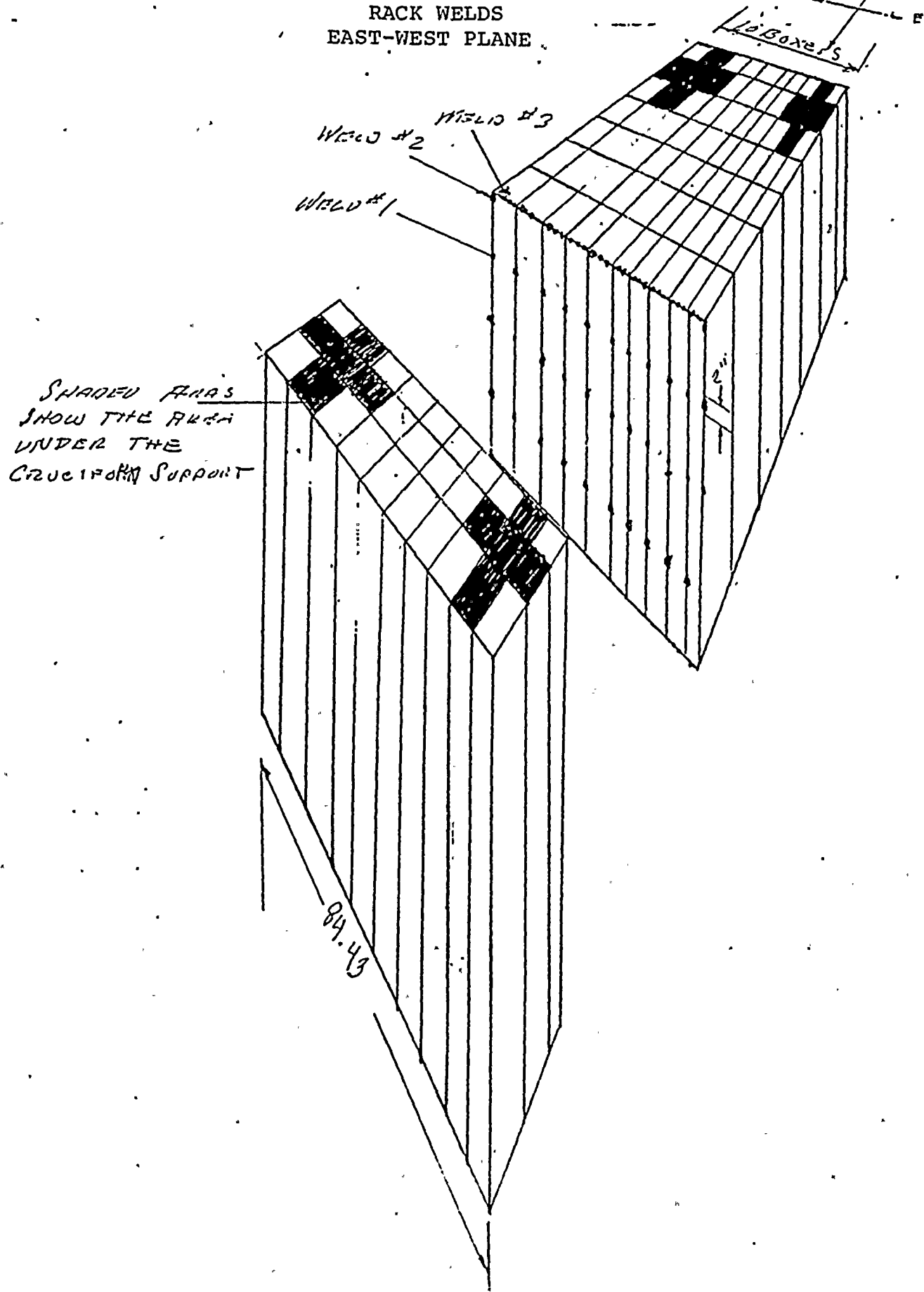
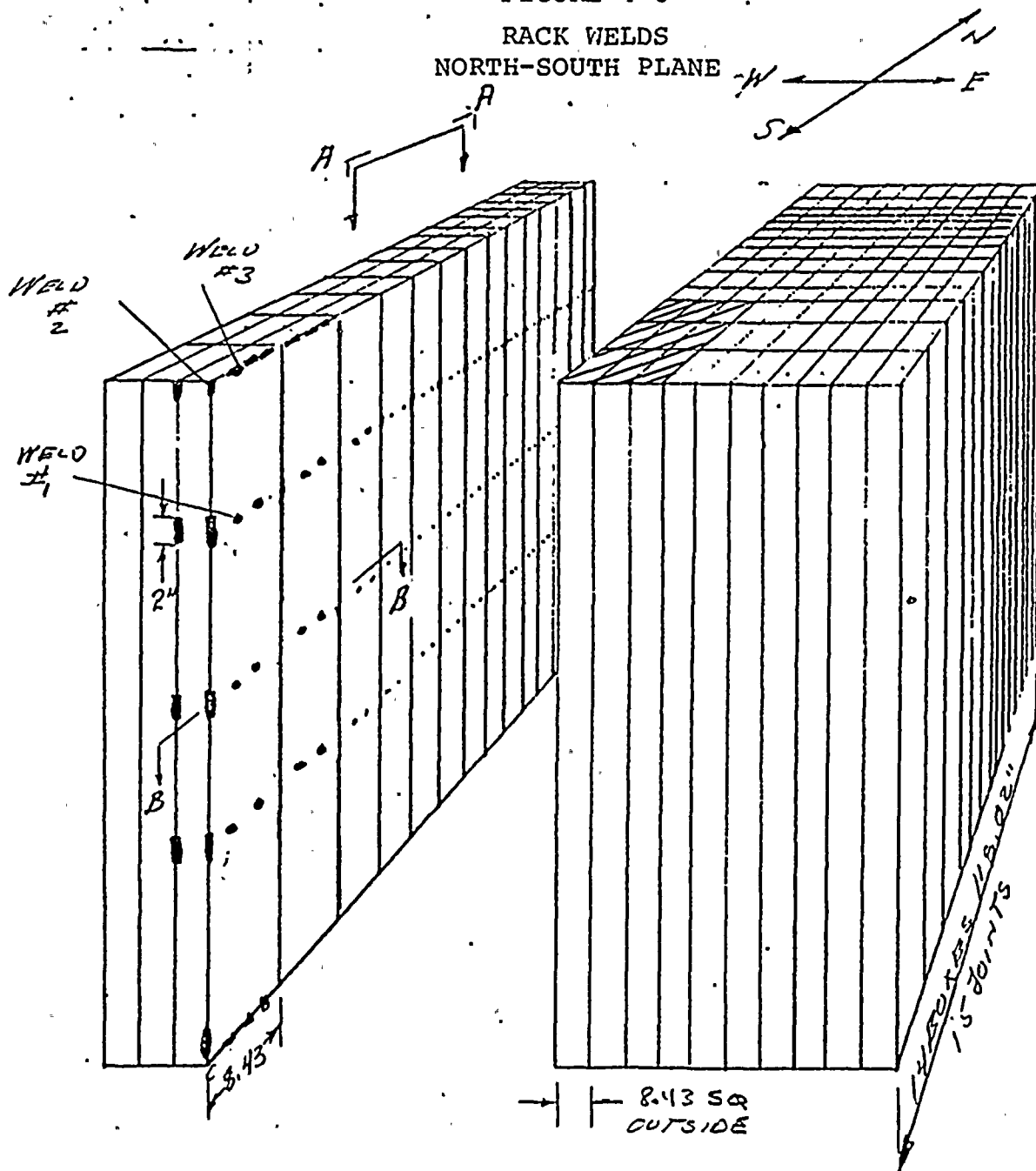


FIGURE 4-8
RACK WELDS
NORTH-SOUTH PLANE



VIEW A-A

SECTION B-B

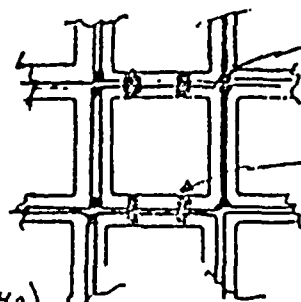
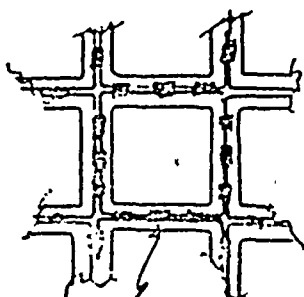
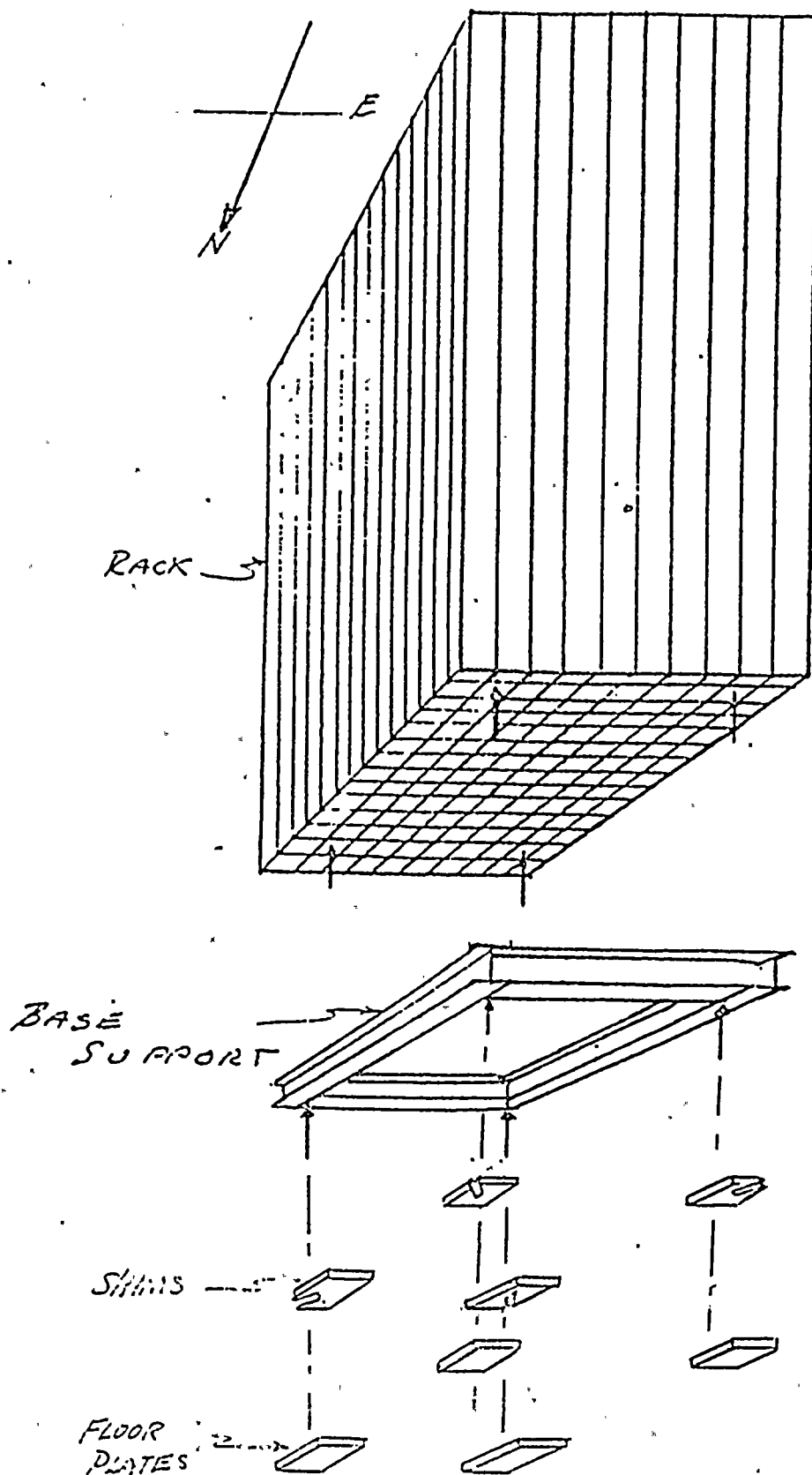


FIGURE 4-9
RACK-BASE SUPPORT



5. Cost/Benefit Assessment

The capacity of the spent fuel storage racks in their current configuration is 595 fuel assemblies. At the completion of the Spring, 1984 refueling outage 332 fuel assemblies will be stored in the pool. Assuming future average reload sizes of 28 fuel assemblies full core discharge capability would be lost after the Spring 1990 refueling outage. Rochester Gas and Electric also has 81 fuel assemblies stored at what was formerly the Nuclear Fuel Services facility at West Valley, New York. RG&E is required by the state of New York to have this fuel removed from West Valley by September, 1985. The addition of this fuel to the storage pool would cause a loss of full core discharge capability after refueling in the Spring 1987.

With the proposed modification, 420 storage locations would be added. At the projected average of 28 fuel assemblies discharged at the end of an annual cycle in the Spring of each year, the loss of full core discharge capability would occur after the Spring, 2002 refueling outage. It is the intent of RG&E that this modification extend the capability to store spent fuel at the Ginna site until a final repository is available in accordance with the interim storage provisions of the Nuclear Waste Policy Act of 1982. It is expected that a disposal facility will be available and shipments will begin by the mid to late 1990's.

RG&E's sole contractual arrangement for the storage of spent fuel is with the New York State Energy Research and Development Authority (NYSERDA) covering the 81 fuel assemblies at West



Valley, New York. NYSERDA has demanded the fuel be removed and in accordance with the Contract, RG&E must comply.

The attached Table 5-1 and 5-2, provides information on schedule of projected fuel discharges and core components stored in the SFP.

A discription of the modification is at Section 1 of this attachment. Preliminary estimates of the costs of the modification are outlined below.

Engineering	125,000
Construction	
Material	500,000
Installation	825,000
AFDC	50,000
Contingency	400,000
Total	<u>\$1,900,000</u>

This is equivalent to about \$4500 per storage location (or \$13 per kgU). These estimates are preliminary and will be updated upon request.

The alternatives to increasing the capacity of the spent fuel pool are few. There is no fuel reprocessing facility available now and no indication that one would be available during this decade. There are no government operated away-from-reactor storage facilities. Independent spent fuel storage exists only in the General Electric, Morris, Illinois facility. This is not generally available to non-G.E. customers nor is it currently available to new customers. Costs for transport of one fuel assembly alone, assuming a three day turnaround time and a 600 mile trip one way, would be on the order of \$10,500 per fuel

assembly or \$30/KgU. The annual charge to store the fuel and labor and material costs for loading and unloading would be additional. Another alternative, that of shipping to another reactor site is not available to RG&E because the company operates only the Ginna Nuclear Plant.

Shutting down the reactor as an alternative to increasing spent fuel storage capacity would impose a financial hardship on the customers of RG&E. The Ginna Plant supplies approximately 45 per cent of RG&E's electric generation. The replacement power costs would depend on whether company coal fired generation was available to pick up the load. Estimates range from \$23 per MWH to \$45/MWH for incremental costs of replacement power. This is equivalent to about \$280,000 to \$540,000 per day.

In terms of the material resources required to complete the modification, the amount needed is low relative to that required to either replace the storage racks entirely with all new high density racks, or use dry storage cask technology. As discussed in Section 1, the modification consists of removing the lead-ins and guide funnels from the water boxes, adding bottom plates to the former water boxes, and right angled boraflex poison inserts with SS-304 filler plates and liners. Table 5-3 lists the material requirement for the modification.

In References 3 and 4, the additional heat loads that would be anticipated assuming normal discharges up to an end of plant life in 2009 were calculated. This analysis (Reference 4) assumed normal annual discharges of 36 fuel assemblies 100 hours after

reactor shutdown. The resulting heat loads for normal discharges were calculated to increase incrementally from 7.07×10^6 BTU/HR in 1981 to 9.96×10^6 BTU/HR in the year 2010. By increasing the cooling time to 14 days in the case of a full core discharge in year 2010 the decay heat load on the spent fuel pool cooling system will remain below 16×10^6 BTU/HR. At this maximum heat load, the analysis concluded that, assuming 80°F service water with a flow rate of 1600 gpm, the maximum pool temperature would be 150°F and the increase in service water temperature would be within the environmental guidelines of 20°F. The potential for an increase in the heat released to the environment due to the modification is the increment from 7.07×10^6 BTU/HR to 9.96×10^6 BTU/HR or about 3×10^6 BTU/HR. During the assumed normal operation of cooling system (80°F service water @ 1000 gpm) this increment represents about a 6°F increase in service water temperature through the heat exchanger. As stated above even given the maximum heat load for a full core discharge the 20°F environmental guideline for total plant discharge would be met.

Table 5-1

Schedule of Anticipated Fuel Discharges

<u>Month/Year</u>	<u>Discharged</u>	<u>Total Stored</u>	<u>Capacity Existing</u>	<u>Remaining Proposed</u>
March 1984	28	332	263	683
March 1985	28	360	235	655
*Sept 1985	81	441	154	574
March 1986	28	469	126	546
March 1987	28	497	**98	518
March 1988	28	525	70	490
March 1989	28	553	42	462
March 1990	28	581	14	434
March 1991	28	609	-	406
March 1992	28	637		378
March 1993	28	665		350
March 1994	28	693		322
March 1995	28	721		294
March 1996	28	749		266
March 1997	28	777		238
March 1998	28	805		210
March 1999	28	833		182
March 2000	28	861		154
March 2001	28	889		126
March 2002	28	917		**98

* 81 fuel assemblies from West Valley

** Loss of full core discharge capability

Table 5-2

Non-Fuel Components Stored in SFP*

Control Rod Assemblies	<u>5</u>
Burnable Poison Rods	<u>46</u>
Thimble Plugging Devices	<u>19</u>
Primary/Secondary Sources	<u>2</u>

* After 1984 refueling

Table 5-3

<u>Component</u>	<u>Material</u>	<u>Volume</u>	<u>Weight</u>
Bottom Plates (420)	SS-304	12,259 in ³	3555 lbs
Neutron Poison	Boraflex .020 gm/cc min ¹⁰ B	126,819 in ³	7990 lbs
Filler Plates (3360)	SS-304	24,619 in ³	7140 lbs
Liner Plates (840)	SS-304	135,804 in ³	39,383 lbs

6. Radiological Evaluation

The SFP purification system consists of a demineralizer and filter. A surface skimmer system consisting of a pump and filter is also used to maintain water clarity. Presently the demineralizer generates 28 cubic feet of solid waste annually from two resin bed changes. The SFP filter and skimmer filter are changed annually generating 7 cubic feet of waste. This represents approximately 0.3% of the average solid radioactive waste volume generated each year. Since the previous SFP rack modification was completed in 1977, the number of spent fuel assemblies stored has increased from 92 to 302 as of 1983 for an average increase of 30 per year. From 1977 through 1983, the waste volume generated by the SFP has remained the same, while the number of stored spent fuel assemblies increased a factor of 3.28. Even if the generated solid radioactive waste increases linearly, which it has not, with the number of spent fuel assemblies in the SFP, the solid waste would increase by a factor of 2.96 with 894 assemblies in the SFP (to maintain full core discharge capability only $1015 - 121 = 894$ fuel assemblies can be stored in the SFP). The solid waste generated by the SFP would then be less than 1% of the total yearly generated solid radioactive waste.

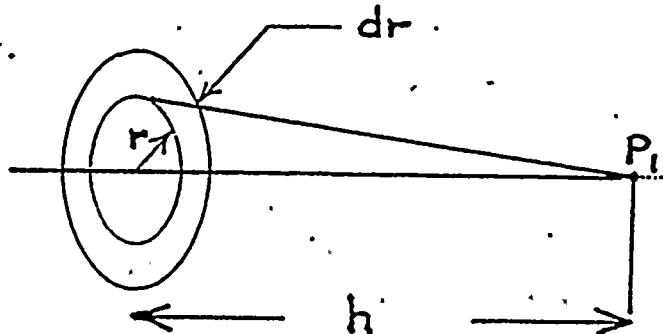
The fuel storage area ventilation is combined with the auxiliary and intermediate building ventilation. The Kr-85 measured in this system was 9.9 curies in 1982 and 15.7 curies in 1983. All of the kr-85 measured could be attributed to the release of decayed waste gas tanks.

The table below provides the results of a recent gamma isotopic analysis (Nov. 22, 1983) of the Ginna SFP water, and identifies principal radionuclides and their respective concentrations. Values obtained from the analysis are representative both in terms of typical gross radioactivity, and the relative concentrations of major radionuclides present in the pool water.

<u>Isotype</u>	<u>Concentration ($\mu\text{Ci/cc}$)</u>	<u>Percent Contribution To Total Water Activity</u>
Cs-137	7.7 E-5	3
Cs-134	2.9 E-5	1
Co-60	2.1 E-3	93
Co-58	5.8 E-5	3

Since the previous SFP rack modification in 1977, dose equivalent rates above and at the sides of the pool have remained the same, between 1 and 2 mrem/hour. The dose equivalent rate above the SFP can also be determined from the following model.

The radiation dose rate from the SFP at a point above the pool surface was calculated from the effective water surface activity, allowing for self-absorption by the water medium in which the isotopes were assumed to be uniformly mixed. Dose models used were those by Cember (1969)*. The basic geometry applied in the calculations consists of a modified plane source as shown below.



*Cember, H., Introduction to Health Physics, Chapter 10, Pergamon Press (1969).

The equation for the dose rate D at point P_1 from a planar source similar to the above is:

$$D_i = \int_0^R \frac{\Gamma_i \times C_{ai} \times 2\pi r \, dr}{r^2 + h^2} = \pi \times \Gamma_i \times C_{ai} \times \frac{\ln \frac{R^2 + h^2}{h^2}}{h^2} \quad (1)$$

where: D_i = dose rate (rem/hr) of the i^{th} isotope

Γ_i = gamma source strength of i^{th} isotope
(rem/hr at 1 m/Ci)

C_{ai} = effective surface activity
(Ci/m²) of i^{th} isotope

R = radius of source (m)

h = distance above source along central axis (m)

In the fuel pool dose calculations, the pool surface was conservatively assumed to have a disc configuration whose radius equaled one half the longest actual pool dimension.

Since the pool containing mixed radioactivity more closely resembles a large slab source, Equation 1 was modified to account for the pool depth (t), the mixed radionuclide concentration C_r (Ci/m³), and the attenuation coefficient of the pool water μ (m⁻¹). The pool surface activity due to radioactivity in the layer dx at a depth of x is:

$$d(C_{ai}) = C_{ri} \cdot dx \cdot e^{-\mu x} \quad (2)$$

Integrating Equation (2) over the total thickness t gives the effective surface activity:

$$C_{ai} = \int_0^t C_{ri} \times e^{-\mu x} dx = \frac{C_{ri}}{\mu} (1 - e^{-\mu t}) \quad (3)$$

By substituting Equation 3 into Equation 1, the following relationship is obtained for calculating dose rate:

$$D(\text{rem/hr}) = \sum D_i = \sum \pi \Gamma_i \frac{C_{ri}}{\mu} (1 - e^{-\mu t}) \ln \frac{R^2 + h^2}{h^2}$$

This equation gives the dose rates at the center of the pool where personnel would experience the highest radiation levels from the water. The dose rates calculated for the nuclides listed on the table below are less than 5 mrem/hr.

Dose rates at the edge of the pool would be slightly less than the dose rates at the center of the pool because of the smaller radiation contributions from one side. Routine radiation surveys performed in the spent fuel pool area have confirmed that dose levels at the pool edge are not in excess of those at the center.

The table below gives the results of analyses performed in 1983 to determine the principal airborne radionuclides and their respective concentrations in the spent fuel pool area.

<u>Isotope</u>	<u>μCi/cc</u>
I-131	<1E-12
I-133	<1E-12
H-3	5.0 E-07
Cs-134	<1E-13
Cs-137	<1E-13
Co-58	<1E-13
Co-60	<1E-13

The annual radiation dose to a specified organ from inhalation of radioactive material is calculated using the following relationship:

$$\text{Dose} = 365 (C_i)(R_b)(DCF_i)$$

where:

Dose = annual dose (mrem/yr)

365 = units conversion constant

C_i = airborne concentration of isotope
i ($\mu\text{Ci/cc}$)

R_b = assumed breathing rate (cc/d)

DCF_i = dose conversion factor relating organ dose
to intake of an isotope by inhalation (mrem/ μCi).

Values for DCF_i are based upon ICRP recommendations (ICRP Publication II, 1959) and are calculated in the following manner:

$$DCF_i = \frac{D_{\text{ref}}}{(C_{\text{ref}})(2.0 \text{ E}+7)(365)}$$

where:

D_{ref} = ICRP recommended maximum permissible dose to a specified organ of an adult occupationally exposed to radiation (mrem/yr)

C_{ref} = ICRP recommended concentration of an isotope in air which, if breathed by an adult at the rate of $2.0 \text{ E}+7$ cc/day for 50 years, will result in a 50th-year dose of D_{ref} mrem to the specified organ ($\mu\text{Ci/cc}$)

$2.0 \text{ E}+7$ = adult breathing rate assumed in ICRP calculations (cc/day)

365 = units conversion constant (days/yr)

Where ICRP II gives no values of C_{ref} for certain organs, the lowest value of C_{ref} listed for other organs is taken as the value of C_{ref} for the unlisted ones. For added conservatism, those isotopes whose concentrations were reported as "less than" values, were assumed to be present at detection limit levels.

Since individuals will spend only a portion of their time in the spent fuel pool area, doses are expected to be considerably less than if continuous exposure is assumed. If a 100-hour annual occupancy time is assumed for a maximally exposed worker in the spent fuel pool area, the resulting total body and organ doses are less than 10 mrem per year.

The spent fuel pool modification will result in longer term storage of well cooled fuel. The present pool temperature limitations will still apply. The operation of the pool purification system and the building ventilation equipment will not change. Therefore, the present airborne isotopic concentrations are not expected to change significantly after the modification. Thus, resulting potential dose increases both in the spent fuel pool area and any offsite locations will be quite small.

The potential increase in annual man-rem from more frequent resin and filter changes was estimated by scaling present personnel exposure values linearly with the number of future added spent fuel assemblies in the pool. Spent fuel pool filter cartridge and demineralizer resin changes associated with the existing 302 stored fuel assemblies contribute less than 0.1 percent of Ginna's total annual man-rem burden. If filter and resin change frequencies are conservatively assumed to increase linearly with increased numbers of assemblies in the pool, resultant personnel exposures could be raised by a factor of 2.96, or to less than 0.3 percent of Ginna's total annual man-rem. Thus, increases in occupational doses from these related operations, when compared to the plant's total yearly exposure burden, will be negligible.

Routine radiation surveys of the Ginna spent fuel pool have shown dose rates typically less than 5 mR/hr along the pool edges. No trend is apparent in past and current survey data which would reflect dose rate increases from crud buildup. Further, no future increases in radiation levels from crud in the pool are anticipated as a result of additional fuel. Should accumulation along the pool walls begin to produce higher exposures of any significance, these will be indicated by routine radiation surveys. At that time methods will be developed to reduce radiation levels at the pool edge to as low as is reasonably achievable.

Based upon average personnel occupancy times in the fuel pool area, the annual man-rem resulting from all related operations is estimated to be less than one percent of the total plant man-rem. Future total occupational exposure at Ginna is not expected to be significantly affected by either a) more frequent changing of demineralizer resin and filters, or b) crud buildup along the sides of the pool, as a result of the proposed spent fuel pool modification.

Radiation dose rates above the pool resulting from submerged spent fuel assemblies placed in any configuration will be negligible when compared to background. The contribution from this source to total annual personnel exposure is therefore negligible.

The radiation protection program will utilize routine survey information to determine changes in SFP area radiation levels and airborne radioactive material concentrations to maintain personnel exposure ALARA.

As stated in Section 1, the modification of the storage racks will include removal of the lead in guides over the water boxes and the seismic supports between the support bases and the pool walls. These two components are fabricated from SS-304 and represent the waste material that will be produced by the modification. The total weight of this material is approximately 8000 lbs. This material will be disposed of as either low level radioactive waste or decontaminated and disposed of as normal (non-radioactive) waste.

7. Accident Evaluation

Currently Ginna Technical Specifications prohibit the movement of a spent fuel cask with the auxiliary building crane. RG&E has submitted an application to delete this restriction based upon a proposed modification to the crane to meet the single-failure-proof requirements of NUREG-0554²⁵. Modifying the crane to be single-failure-proof would obviate the need to analyze the cask drop. For those loads that can not be moved in a single failure proof mode, RG&E will continue to satisfy the requirements of NUREG-0612 by some combination of load drop analysis, load height restriction and safe load path. In either case, the Ginna Technical Specification prohibits the trolley of the auxiliary building crane to be stationed above or pass over a spent fuel storage rack containing spent fuel. This requirement along with installed interlocks prevents the movement of loads over spent fuel by the auxiliary building crane.

The overhead hoist attached to spent fuel pool bridge is used to transfer spent fuel within the pool area. Use of this hoist is limited to single fuel assemblies and their handling tools. The rack structure protects stored fuel from the impact of a dropped fuel assembly². A weight limitation on the hoist (2000 lbs), the physical position of the overhead hoist, and an up-stop limit switch prevents the potential impact energy of a load from substantially exceeding that of a dropped spent fuel assembly.⁷



References

1. Application for Amendment to Operating License, January 30, 1976.
2. Letter, A Schwencer to L.D. White, November 15, 1976.
3. Letter, L.D. White to D.L. Ziemann, February 13, 1980.
4. Letter, D.M. Crutchfield to L.D. White, November 3, 1981.
5. Application for Amendment to Operating License, February 23, 1982.
6. Application for Amendment to Operating License, January 18, 1984.
7. Letter, J.E. Maier to D.M. Crutchfield, June 9, 1981.
8. U.S. Nuclear Regulatory Commission, Standard Review Plan 3.7.2 "Seismic System Analysis," Revision 1, July, 1981.
9. Fritz, R.J., "The Effects of Liquids on the Dynamic Motions of Immersed Solids, "ASME February, 1972.
10. Dong, R.G., "Effective Mass and Damping of Submerged Structures", UCRL-52342, L.L.L., April, 1978.
11. Stokey, W.J., Scavuzzo, R.J. and Radke, E.E., "Dynamic Fluid Structure Coupling of Rectangular Modules in Rectangular Pools," ASME Special Publication PVP-39, 1979.
12. Regulatory Guide 1.61, "Damping Values for Seismic Design of Nuclear Power Plant", October, 1973.
13. Rabinowicz, E., "Friction Coefficients of Water-Lubricated Stainless Steels for a Spent Fuel Rack Facility", Study performed for Boston Edison, Co. November, 1976.
14. ASME Boiler and Pressure Vessels, NUCLEAR VESSELS, Section III, 1980 ed.
15. G.E. Technical Paper 22A5866, Rev. Dec. 26, 1979. Appendix II, FUEL ASSEMBLY STRUCTURAL CHARACTERISTICS.
16. R.D. Blevins, Ph.D, FORMULAS FOR NATURAL FREQUENCY AND MODE SHAPE, Van Nostrand Reinhold Co., N.Y., N.Y., 1979.
17. R.J. Roark, W.C. Young, FORMULAS FOR STRESS AND STRAIN, MCRAW-HILL BOOK CO., N.Y. 5th Ed., 1975.



18. J.S. Anderson, "Boraflex Neutron Shielding Material -- Product Performance Data," Brand Industries, Inc., Report 748-30-1, (August, 1979).
19. J.S. Anderson, "Irradiation Study of Boraflex Neutron Shielding Material," Brand Industries, Inc., Report 748-10-1, (July, 1979).
20. J.R. Anderson, "A Final Report on the Effects of High Temperature Borated Water Exposure on BISCO Boraflex Neutron Absorbing Material," Brand Industries, Inc., Report 748-21-1, (August, 1978).
21. O.W. Blodgett, Design of Welded Structures, J.F. Lincoln Arc Welding Foundation, Cleveland, Ohio, 7th Printing 1975.
22. American Concrete Institute, Manual of Concrete Practice, 329-32, Detroit, Michigan.
23. Letter T.R. Robbins to J.D. Cook, March 15, 1984.
24. Gilbert Associates, Inc., Ginna Station Seismic Upgrading Program - Auxiliary Structures Seismic Analysis, May 15, 1980.
25. Application for Amendment to Operating License, January 18, 1984.



For
U.S. Tool & Die, Inc.

Criticality Analysis of Region 2 of the Ginna MDR
Spent Fuel Storage Rack

Final Report

by
Pickard, Lowe & Garrick, Inc.
Washington, D.C.

TABLE OF CONTENTS

	<u>Page</u>
1.0 THE MAXIMUM DENSITY RACK (MDR) DESIGN CONCEPT	1
1.1 Introduction	1
2.0 CRITICALITY ANALYSIS OF REGION 2 (ASSUMES IRRADIATED FUEL)	2
2.1 Analytical Technique	3
2.2 Calculational Approach	8
2.3 Manufacturing and Thermal Considerations	9
2.4 Design Conservatisms	10
2.5 Accident Analysis	11
2.6 Required Exposure as a Function of Initial Enrichment for Region 2 Spent Fuel	11
REFERENCES	13

TABLE OF CONTENTS (continued)

List of Tables

<u>Table</u>	<u>Title</u>
1	Region 2 Design Criteria
2	Fuel Assembly Technical Information for Ginna Nuclear Plant
3	Summary of Leopard Results for Measured Criticals
4	Westinghouse UO ₂ Zr-4 Clad Cylindrical Core Critical Experiments
5	Battelle Fixed Neutron Poison Criticals
6	Saxton PuO ₂ -UO ₂ Critical Experiments
7	ESADA PuO ₂ -UO ₂ Critical Experiments
8	Summary of Predictions for k_{eff} in Criticality Experiments
9	Summary of Reactivity Biases and Uncertainties for Ginna Region 2 MDR
10	Computed Infinite Multiplication Factors for Ginna MDR



TABLE OF CONTENTS (continued)

List of Figures

<u>Figure</u>	<u>Title</u>
1	Ginna MDR Spent Fuel Rack Design
2	Net Destruction of U-235 Versus Burnup in the Yankee Asymptotic Neutron Spectrum
3	Specific Production of U-236 Versus Burnup in Yankee Asymptotic Neutron Spectrum
4	Net Destruction of U-238 Versus Burnup in the Yankee Asymptotic Neutron Spectrum
5	Specific Production of Pu-239 Versus Burnup in Yankee Asymptotic Neutron Spectrum
6	Specific Production of Pu-240 Versus Burnup in Yankee Asymptotic Neutron Spectrum
7	Specific Production of Pu-241 Versus Burnup in Yankee Asymptotic Neutron Spectrum
8	Specific Production of Pu-242 Versus Burnup in Yankee Asymptotic Neutron Spectrum
9	Specific Production of Total Pu and Fissile Pu Versus Burnup in Yankee Asymptotic Neutron Spectrum
10	Atom Percent of Total U Versus Exposure
11	Pu-239/U-238 Atom Ratio Versus Exposure
12	Atom Percent of Total Pu Versus Exposure
13	Fission Product Absorption Cross-Sections as a Function of Time After Shutdown
14	One-Quarter Rack Cell Model for Ginna MDR
15	Four-Quarter Rack Cell Model for Ginna MDR
16	Variation of k_{∞} with Assembly Pitch for Ginna MDR
17	Variation of k_{∞} with Steel Thickness for Ginna MDR

TABLE OF CONTENTS (continued)

List of Figures

<u>Figure</u>	<u>Title</u>
18	Variation of k_{∞} with Pellet Diameter for Ginna MDR
19	Variation of k_{∞} with Pellet Density for Ginna MDR
20	Variation of k_{∞} with Water Density for Ginna MDR
21	Variation of k_{∞} with Temperature for Ginna MDR
22	Configuration Used to Determine the Effects of the Region 1 - Region 2 Interface
23	Regions of Acceptability and Unacceptability for Region 2 Spent Fuel

1.0 THE MAXIMUM DENSITY RACK (MDR) DESIGN CONCEPT

1.1 Introduction

Historically, spent fuel rack designs have been based on conservative assumptions that could be easily accommodated since it was not planned to store large numbers of high exposure spent fuel assemblies on-site. Previously it was anticipated that only small amounts of high exposure fuel assemblies (1/4 to 1/2 of a full core load) would normally be stored in the spent fuel pool at any one time. Additionally, it was anticipated that occasionally (e.g., for inservice inspection of the reactor vessel internals) the entire core would be unloaded and temporarily stored in the spent fuel pool. Therefore, the spent fuel storage rack design was based on the conservative assumption that all fuel rack storage positions would be occupied by fresh unirradiated fuel assemblies of the highest initial enrichment that was foreseen as being useable in that facility.

The penalty in achievable spent fuel storage density associated with this conservative design assumption was relatively small under the circumstances anticipated and easily accommodated by a conservative spent fuel rack design. The potential penalty associated with this conservative design basis is no longer small when long term on-site storage of spent fuel is a necessity.

It is not conceivable that more than one full core load of fresh unirradiated fuel assemblies could be stored in the spent fuel storage pool. Therefore, it is unnecessary and wasteful to base the entire spent fuel storage rack design on the assumption of fresh unirradiated fuel of the highest initial enrichment.

In the MDR design concept, the spent fuel pool is divided into two separate and distinct regions which for the purpose of critically considerations may be considered as separate pools. Suitability of this design assumption regarding pool separability is assured through appropriate design restrictions at the boundaries between Region 1 and Region 2. The smaller region, Region 1, of the pool is designed on the

basis of currently accepted conservative criteria which allow for the safe storage of a number of fresh unirradiated fuel assemblies (including a full core unloading if that should prove necessary). The larger region of the pool, Region 2, is designed to safely store irradiated fuel assemblies which will be discharged from the reactor in large quantities.

The criteria for Region 2 of the pool are specifically listed in Table 1. The only change in criteria is the recognition of actual fuel and fission product inventory accompanied by a system for checking fuel prior to moving any fuel assembly from Region 1 to Region 2.

During a normal refueling operation, each fuel assembly is first moved from the core to Region 1. After the refueling operation is complete and the suitability of each spent fuel assembly for movement into Region 2 is verified, this fuel will be moved into Region 2.

Region 2 is designed to store fuel which does not exceed pre-established reactivity criteria. Consequently, the limit on acceptable initial enrichment varies with the exposure at the time of storage. For instance, 4.25 w/o fuel is acceptable for storage only after a predetermined minimum exposure has been reached. A somewhat lower minimum exposure would be acceptable for fuel with a lower initial enrichment. This resulting curve of initial fuel assembly enrichment versus minimum acceptable exposure defines a curve of constant spent fuel rack reactivity. The major purpose of this study is the determination of this curve.

2.0 CRITICALITY ANALYSIS OF REGION 2 (ASSUMES IRRADIATED FUEL)

The fuel assemblies used in this analysis are characterized in Table 2. The Ginna as built spent fuel rack cell is shown in Figure 1. The following discussion summarizes the design of the spent fuel racks with respect to the criticality design. The analytical techniques described here are similar to those used to successfully license spent fuel racks for several other plants.

2.1 Analytical Technique

The LEOPARD⁽¹⁾ computer program was used to generate macroscopic cross sections for input to four energy group diffusion theory calculations which are performed with the PDQ-7⁽²⁾ program. LEOPARD calculates the neutron energy spectrum over the entire energy range from thermal up to 10 Mev and determines averaged cross sections over appropriate energy groups. The fundamental methods used in the LEOPARD program are those used in the MUFT⁽³⁾ and SOFOCATE⁽⁴⁾ programs which were developed under the Naval Reactor Program and thus are well founded and extensively tested techniques. In addition, Westinghouse Electric Corporation, the developers of the original LEOPARD program, demonstrated the accuracy of these methods by extensive analysis of measured critical assemblies consisting of slightly enriched UO_2 fuel rods.⁽⁵⁾

In addition, Pickard, Lowe and Garrick, Inc. (PLG) has made a number of improvements to the LEOPARD program to increase its accuracy for the calculation of reactivities in systems which contain significant amounts of plutonium mixed with UO_2 . PLG has tested the accuracy of these modifications by analyzing a series of UO_2 and PuO_2 - UO_2 critical experiments. These benchmarking analyses not only demonstrate the improvements obtained for the analysis of PuO_2 - UO_2 systems but also demonstrate that these modifications have not adversely affected the accuracy of the PLG-modified LEOPARD program for calculations of slightly enriched UO_2 systems.

The UO_2 critical experiments chosen for benchmarking include variations in H_2O/UO_2 volume ratios, U-235 enrichments, pellet diameters and cladding materials. Although the LEOPARD model also accurately calculates the reactivity effects of soluble boron, these experiments have not been included in the LEOPARD benchmarking criticals since the spent fuel pool calculations do not involve soluble boron.

Neutron leakage was represented by using measured buckling input to infinite lattice LEOPARD calculations to represent the critical assembly. A summary of the results is shown in Table 3 for the 27 measured criticals chosen as being directly applicable for benchmarking

the LEOPARD model for generating group average cross sections for spent fuel rack criticality calculations. The average calculated k_{eff} is 0.9979 and the standard deviation from this average is 0.0080 Δk . Reference 5 raised questions concerning the accuracy of the measured buckling reported for the experiments number 12 through 19. If these data are excluded, the average calculated k_{eff} for the remaining 19 experiments is 1.0006 with a standard deviation from this value of 0.0063 Δk . In all of these experiments; there are significant uncertainties in the measured bucklings which are necessary inputs to the LEOPARD analysis. These uncertainties are the same order of magnitude as the indicated errors in the LEOPARD results, and therefore a more definitive set of experimental data is used to establish the accuracy of the combined LEOPARD/PDQ-7 model used for the criticality analysis of the spent fuel racks.

The PDQ series of programs have been extensively developed and tested over a period of 20 years and the current version, PDQ-7, is an accurate and reliable model for calculating the subcritical margin of the proposed spent fuel rack arrangement. This code or a mathematically equivalent method is used by all the U.S. suppliers of light water reactor cores and reload fuel. In addition, this code has received extensive utilization in the U.S. Naval Reactor Program.

As a specific demonstration of the accuracy of the calculational model used for the spent fuel rack calculations, the combined LEOPARD/PDQ-7 model has been used to calculate fourteen measured just critical assemblies. The criticals are high neutron leakage systems with a large variation in U/H₂O volume ratio and include parameters in the same range as those applicable to the proposed fuel rack design. Experiments including soluble boron are included in this demonstration since the ability of PDQ-7 to calculate neutron leakage effects is of primary interest. The use of soluble boron allows changes in the neutron leakage of the assembly while maintaining a uniform lattice and thus allows a better test of the accuracy of the model. Furthermore, it eliminates the error associated with the measured bucklings which is inherent in the LEOPARD benchmarks, thus permitting determinations of the actual calcu-

lational uncertainty which must be accounted for in the spent fuel rack criticality analysis.

These combination LEOPARD/PDQ-7 calculations result in a calculated average k_{eff} of 0.9928 with a standard deviation about this value of 0.0012 Δk . These results, as shown in Table 4 demonstrate that the proposed LEOPARD/PDQ-7 calculational model can calculate the reactivity of the proposed spent fuel rack arrangements with an accuracy of better than 0.010 Δk at the 95 percent confidence level.

The cross sections for the Boraflex neutron absorbing material which is an integral part of the design are calculated using fundamental techniques that have been successfully applied in the past to thin heavily absorbing mediums such as control rods.

This procedure is straightforward and is comprised of several well defined steps:

1. The B^{10} from the thin Boraflex sheets is homogenized in an appropriate amount of water, and LEOPARD is used to obtain unshielded macroscopic B^{10} cross sections.
2. Integral transport theory is applied in slab geometry using They's method for calculating flux depressions and shielding factors to determine an appropriate B^{10} number density. This approach is similar to that of Amouyal and Benoist.
3. The B^{10} number density calculated in Step 2 is homogenized in water, and LEOPARD is used to obtain corrected microscopic B^{10} cross sections.
4. Blackness theory is applied to obtain macroscopic cross sections which will produce the required boundary conditions at the surface of the Boraflex sheets.

In addition to the fourteen critical assemblies in Table 4, the LEOPARD/PDQ model was used to calculate the k_{eff} for twelve additional critical assemblies, seven of which incorporated thin, heavily-absorbing materials for which the procedure just described was used to determine the macroscopic cross sections.

These twelve criticals were performed by Battelle Pacific Northwest Laboratories specifically for the purpose of providing benchmark critical experiments in support of spent fuel criticality analysis. They are described in detail in Reference 18. The results of these critical experiments are summarized in Table 5. The first seven of these twelve experiments include fixed neutron poison absorber plates, and the average k_{eff} calculated for these just critical assemblies was 0.9935, with a standard deviation around this value of $0.0007 \Delta k$. The other five critical experiments in this series do not include absorber plates and the average k_{eff} calculated for these just critical assemblies was 0.9944, with a standard deviation around this value of $0.0007 \Delta k$. The overall average k_{eff} calculated for these twelve just critical assemblies was 0.9939, with a standard deviation around this value of $0.0008 \Delta k$.

This extensive series of UO_2 critical experiments further supports the applicability of the methods described above for use in calculating the subcritical margin of these fuel storage rack designs, and demonstrates that the accuracy of better than $0.010 \Delta k$ at the 95 percent confidence level established for the LEOPARD/PDQ-7 model applies equally well to designs incorporating fixed neutron absorbers for which blackness theory is used to calculate the macroscopic cross sections and also to assemblies containing plutonium.

As a result of this approach to separately benchmark both the cross sections and the diffusion theory calculations against applicable critical assemblies, the "transport theory correction factor" is implicitly included in the derived calculational uncertainty factor.

The analytical methods used for Region 2 must also account for the depletion of U-235 and buildup of various plutonium isotopes and fission products. The isotopic composition is calculated as a function of irradiation time, assembly average exposure, and subsequent decay using the LEOPARD⁽¹⁾ and CINDER⁽⁶⁾ computer programs. Once the isotopic compositions of the fuel assemblies are known, the subsequent criticality calculations for the spent fuel racks in Region 2 are performed in the manner given above.

The accuracy of the exposure dependent isotopic concentrations calculated with the LEOPARD program is demonstrated in Figure 2 through Figure 12. Figures 2 through 9 show comparisons of LEOPARD calculated data with measured data from a UO_2 fuel assembly irradiated in the Yankee-Rowe reactor while Figures 10 through 12 show corresponding data for a mixed oxide (PuO_2 - UO_2) fuel assembly irradiated in the SAXTON reactor.

Except for the data labeled PLG calculation, the data and curves on Figures 2 through 9 and Figures 10 through 12 are taken directly from References 7 and 8, respectively. In all cases, the accuracy of the calculations labeled PLG is within the uncertainty in the measured data.

The accuracy of reactivity calculations for irradiated fuel can be demonstrated in part by the analysis of critical arrays of mixed oxide fuel rods which contain high concentrations of the plutonium isotopes. Tables 6 and 7 show results of criticality analyses for the SAXTON⁽⁹⁾ and ESADA⁽¹⁰⁾ sets of experiments which cover a wide range of water-to-oxide volume ratios. A summary of these data is shown in Table 8. For the mixed oxide criticals, the calculated mean k_{eff} is 0.9969 with a standard deviation about this value of $0.0066 \Delta k$. Using the 95% probability at 95% confidence level criterion (one-sided) with 11 data points, this implies a possible error of $2.82 = 0.0186 \Delta k$ with an offset of $+0.0031 \Delta k$.

The analytical methods used for Region 2 must also account for the depletion of U-235 and buildup of various plutonium isotopes and fission products. The isotopic composition is calculated as a function of irradiation time, assembly average exposure, and subsequent decay using the LEOPARD⁽¹⁾ and CINDER⁽⁶⁾ computer programs. Once the isotopic compositions of the fuel assemblies are known, the subsequent criticality calculations for the spent fuel racks in Region 2 are performed in the manner given above.

The accuracy of the exposure dependent isotopic concentrations calculated with the LEOPARD program is demonstrated in Figure 2 through Figure 12. Figures 2 through 9 show comparisons of LEOPARD calculated data with measured data from a UO_2 fuel assembly irradiated in the Yankee-Rowe reactor while Figures 10 through 12 show corresponding data for a mixed oxide ($\text{PuO}_2\text{-UO}_2$) fuel assembly irradiated in the SAXTON reactor.

Except for the data labeled PLG calculation, the data and curves on Figures 2 through 9 and Figures 10 through 12 are taken directly from References 7 and 8, respectively. In all cases, the accuracy of the calculations labeled PLG is within the uncertainty in the measured data.

The accuracy of reactivity calculations for irradiated fuel can be demonstrated in part by the analysis of critical arrays of mixed oxide fuel rods which contain high concentrations of the plutonium isotopes. Tables 6 and 7 show results of criticality analyses for the SAXTON⁽⁹⁾ and ESADA⁽¹⁰⁾ sets of experiments which cover a wide range of water-to-oxide volume ratios. A summary of these data is shown in Table 8. For the mixed oxide criticals, the calculated mean k_{eff} is 0.9969 with a standard deviation about this value of 0.0066 Δk . Using the 95% probability at 95% confidence level criterion (one-sided) with 11 data points, this implies a possible error of $2.82 = 0.0186 \Delta k$ with an offset of $\pm 0.0031 \Delta k$.

The other major uncertainty in the calculations for Region 2 is associated with the calculated reduction in fuel assembly reactivity associated with the depletion of the heavy metals and the accumulation of fission products as a function of fuel assembly exposure. As an example, consider a 4.25 w/o (initial enrichment) Ginna fuel assembly at 30,000 MWD/MT. The total reactivity loss from the fresh unirradiated case is $0.225 \Delta k/k$, of which approximately 50% can be attributed to the build-up of fission products. Calculations of reactor reactivity lifetimes using the same analytical methods as used in this analysis demonstrate an accuracy of better than $\pm 5\%$. Therefore, the resulting uncertainty in the calculated fuel assembly k_{∞} associated with fuel depletion would be conservatively estimated at $0.0112 \Delta k/k$ ($= .05 \times .235 \Delta k/k$). The corresponding uncertainty in the calculated Region 2 multiplication factor is $0.0102 \Delta k$ on a base case Region 2 k_{∞} of 0.9072.

In order to provide further assurance of the conservative nature of these calculations, the decay of all fission products following discharge of the fuel assembly was taken into account. This was accomplished with the aid of the CINDER⁽⁸⁾ code which treats a total of 186 nuclides in 84 linear chains. The fission product inventory for each fuel assembly was decayed for thirty years following its removal from the reactor core, and the time point of minimum fission product absorption within that thirty year period was used at the basis for determining the fission produce macroscopic absorption cross sections for that particular fuel assembly at that specific exposure. That minimum occurs at approximately 100 days into the decay and from then on continues to increase as illustrated in Figure 13. Reduction in the fission product inventory due to leakage or escape to the plenum has been found to be negligible.⁽¹¹⁾

2.2 Calculational Approach

The PDQ-7 program is used in the final predictions of the reactivity of the spent fuel storage racks. The calculations are performed in four energy groups and take into account all the significant geometric details of the fuel assemblies, fuel boxes, and major structural components. The



geometry used for most of the calculations is a basic cell representing one-quarter of the area of a repeating array of stainless-steel boxes. The specific geometry of this basic cell is shown in Figure 14.

The calculational approach is to use the basic cell to calculate the reactivity of an infinite array of uniform spent fuel racks and to account for any deviations of the actual spent fuel rack array from this assumed infinite array as perturbations on the calculated reactivity of the basic cell. The effects of manufacturing tolerances, as well as thermal uncertainties, including fuel and water temperature and density variations, are also treated as perturbations on the calculated reactivity of the basic cell.

The adequacy of the calculational mesh selected for this type of cell calculation has been verified by comparison with the results of an identical geometry which used a finer calculational mesh (two times the number of mesh intervals in each direction). The finer calculational mesh resulted in little change in the value of k_{∞} with an observed increase of $+0.0002 \Delta k$.

A further check on the calculational model used was the use of a more accurate spatial model encompassing the corners of four adjacent rack cells as shown in Figure 15. The use of this model had the effect of increasing k_{∞} by $0.0005 \Delta k$.

2.3 Manufacturing and Thermal Considerations

Several perturbations of the basic cell were performed to determine the effects of changes in the physical cell and component dimensions, due to manufacturing tolerances, changes in water density, and changes in temperature. All cases were performed on 4.25 w/o fuel at an exposure of 30,000 MWD/tonne.

The following changes in specifications due to manufacturing tolerances were considered: Reducing assembly pitch by .060" leaving other dimensions constant (water gap reduced); reducing steel wall thickness of both box (by .009") and boraflex retaining device (by .003") (increased water gap); reducing pellet diameter .0010", and increasing pellet density by 1.5% of the theoretical value. These variations represent the full range of possible variations in the mechanical design of the fuel rack and fuel. The reduction in pitch results in an increase in k_{∞} of 0.0019 Δk . The reduction in steel thickness results in a decrease of k_{∞} of 0.0002 Δk . The reduction in pellet diameter results in a decrease in k_{∞} of 0.0005 Δk , while the increase in pellet density increases k_{∞} by 0.0015 Δk . These effects are shown in Figures 16-19.

The results of decreases in water density and increases in temperature are shown in Figures 20 and 21. In both cases, it is clear that the base case (68°F, water at full density) represents the maximum reactivity.

The effect of the interface between Region 1 and Region 2 was evaluated assuming fresh 4.25 w/o fuel in Region 1 and 4.25 w/o fuel at an exposure of 30,000 MWD/MT in Region 2. This resulted in a computed k_{∞} of 0.9195, or a change of +0.0123 Δk over the computed k_{∞} basis rack cell used to represent Region 2. The model used is shown in Figure 22.

A summary of the biases and uncertainties in the computed values of k_{∞} is given in Table 9. The uncertainties have been combined statistically. These results show that a basic cell computed k_{∞} of less than 0.9108 will assure an actual k_{∞} below 0.95 with 95% probability at the 95% confidence level.

2.4 Design Conservatism

While the MDR concept reduces some of the design conservatisms inherent in the earlier spent fuel storage concepts (e.g., assumption of fresh unirradiated fuel), the design and analyses for the MDR as implemented in Region 2 are still very conservative in nature.

The use of assembly average exposures is one example of this conservative approach. Axially, more than 80% of the fuel assembly will normally have reached exposures greater than the average and this will occur along the central, higher worth region of the assembly. The lower exposure regions would normally account for less than 20% of the fuel assembly length distributed at the ends of the fuel assembly active length which are lower worth regions. The result is a neutronicly higher exposure assembly than represented by the simple assembly average exposure. The use of the simple assembly average exposure can result in an over-estimate of the fuel assembly k_{eff} by $+0.015 \Delta k/k$.

2.5 Accident Analysis

The Region 2 fuel racks are designed to prevent a dropped fuel bundle from penetrating and occupying a position other than a normal fuel storage location. The only positive reactivity effect of such a bundle on the multiplication factor of the rack would be by virtue of a reduction in axial neutron leakage from the rack. Since the calculations reported here take no credit for axial neutron leakage, the effect of a dropped fuel assembly could not be expected to exceed the reported maximum possible reactivity of the spent fuel storage rack. This is because the reported maximum possible reactivity of the rack is based on infinite array calculations (both laterally and vertically).

2.6 Required Exposure as a Function of Initial Enrichment for Region 2 Spent Fuel

As shown above, a computed k_{∞} of 0.9108 will assure that the actual k_{∞} is below 0.95 with a probability of 0.95 at the 95% confidence level. These computations were performed for 4.25 w/o fuel with an exposure of 30,000 MWD/MT. For lower enrichments with the same computed value of k_{∞} , the amount of exposure will be reduced, reducing the reactivity uncertainties due to depletion of fuel and buildup of fission products, and thus reducing the total uncertainty. Thus the computed k_{∞} value of 0.9108 should be conservative for all enrichments not exceeding 4.25 w/o. In

order to allow for possible interpolation errors, however, a target value of 0.9050 for k_{∞} will be used for other enrichments. The results shown in Table 10 may be interpolated to estimate the required exposure to reach a computed k_{∞} value of 0.9050. For 4.25 w/o fuel the required exposure is 30,000 MWT/MT, for 3.00 w/o fuel it is 15,960 MWT/MT. For 1.75 w/o fuel, even fresh fuel has a computed k_{∞} of less than 0.9050. The resulting curve, shown in Figure 23, gives the required exposure as a function of enrichment to assure that the value of k_{∞} in the spent fuel has a probability of 95% of not exceeding 0.95 at the 95% confidence level.

Because of the well-founded, conservative technique used for determination of the infinite multiplication factor, there is assurance that this spent fuel rack design will not cause undue risk to the public health and safety resulting from criticality considerations.

REFERENCES

1. R.F. Barry, "LEOPARD--A Spectrum Dependent Non-Spatial Depletion Code for the IBM-7094," WCAP-3269, September 1963.
2. W.R. Caldwell, "PDQ-7 Reference Manual," WAPD-TM-678, January 1967.
3. H. Bohl, E. Gelbard and G. Ryan, "MUFT-4-- Fast Neutron Spectrum Code for the IBM-740," WADP-TM-72, July 1957.
4. H. Amster and R. Suarez, "The Calculation of Thermal Constants Averaged Over a Wigner-Wilkins Flux Spectrum: Description of the SOFOCATE Code," WAPD-TM-39, January 1957.
5. L.E. Strawbridge and R.F. Barry, "Criticality Calculations for Uniform Water-Moderated Lattices," Nuclear Science and Engineering, 23, 58, 1965.
6. Electric Power Research Institute, "Fission Product Data for Thermal Reactors, Part 1 and Part 2: Data Set for EPRI-CINDER and Users Manual for EPRI-CINDER Code and Data," EPRI NP-356, Final Report (1976).
7. R.J. Nodvik, "Evaluation of Mass Spectrometric and Radiochemical Analyses of Yankee Core I and Core II Spent Fuel," WCAP-6068 (1965).
8. R.J. Nodvik, "Saxton Core II Fuel Performance Evaluation of Mass Spectrometric and Radiochemical Analyses of Irradiated Saxton Plutonium Fuel," WCAP-3385-56 Part II (1970).
9. W.L. Orr, H.I. Sternberg, P. Deramaix, R.H. Chastain, L. Binder and A.J. Impink, "Saxton Plutonium Program, Nuclear Design of the Saxton Partial Plutonium Core," WCAP-3385-51, December 1965. (Also EURAEC-1490).
10. R.D. Leamer, W.L. Orr, R.L. Stover, E.G. Taylor, J.P. Tobin and A. Bukmir, "PuO₂-UO₂ Fueled Critical Experiments," WCAP-3726-1, July 1967.
11. R.A. Lorenz, et al., "Fission Product Release from Highly Irradiated LWR Fuel," NUREG/CR-0722, February 1980.
12. P.W. Davison, et al., "Yankee Critical Experiments Measurements on Lattices of Stainless Steel Clad Slightly Enriched Uranium Dioxide Fuel Rods in Light Water," YAE-94, Westinghouse Atomic Power Division (1959).
13. V.E. Grob and P.W. Davison, et al., "Multi-Region Reactor Lattice Studies - Results of Critical Experiments in Loose Lattices of UO₂ Rods in H₂O," WCAP-1412, Westinghouse Atomic Power Division (1960).

REFERENCES (continued)

14. W.J. Eich and W.P. Kovacic, "Reactivity and Neutron Flux Studies in Multiregion Loaded Cores," WCAP-1433, Westinghouse Atomic Power Division (1961).
15. W.J. Eich, Personal Communication (1963).
16. T.C. Engelder, et al., "Measurement and Analysis of Uniform Lattices of Slightly Enriched UO_2 Moderated by D_2O-H_2O Mixtures," BAW-1273, the Babcock & Wilcox Company (1963).
17. A.L. MacKinney and R.M. Ball, "Reactivity Measurements on Unperturbed, Slightly Enriched Uranium Dioxide Lattices," BAW-1199, the Babcock & Wilcox Company (1960).
18. Battelle Pacific Northwest Laboratories, "Critical Separative Between Subcritical Clusters of 2.35 Wt % ^{235}U Enriched UO_2 Rods in Water With Fixed Neutron Poisons," PNL-2438.

TABLE 1

REGION 2 DESIGN CRITERIA

1. Actual irradiated fuel and fission product inventory is assumed.
2. $k_{eff} < 0.95$
3. Credit may be taken for presence of borated water for abnormal (accident) conditions.
4. Multiple checks required for each fuel assembly prior to transfer from Region 1 to Region 2.

TABLE 2

FUEL ASSEMBLY TECHNICAL INFORMATION FOR
GINNA NUCLEAR PLANT

Rod Array	14 x 14 W
Rods Per Assembly	179
Rod Pitch, In.	0.556
Overall Dimensions, In.	7.784
Active Fuel Height, In.	141.4
Clad Thickness, In.	.0243
Fuel Rod O.D., In.	.400
Pellet Diameter, In.	.3444
Diametral Gap, In.	.0070
Pellet Density (% theoretical)	95
Control Rod Guide Tubes	
Outer Diameter, In.	0.5280
INSIDE DIAMETER, IN	0.4900
Instrument Tube	
Outer Diameter, In.	0.4015
INSIDE DIAMETER, IN	0.3499

TABLE 3

SUMMARY OF LEOPARD RESULTS FOR MEASURED CRITICALS

Case** Number	Reference Number	Enrichment (atom %)	H ₂ O/U Volume	Fuel Density (g/cm ³)	Pellet Diameter (cm)	Clad Diameter (cm)	Clad Thickness (cm)	Lattice Pitch (cm)	Critical Buckling m ⁻²	Calculated k _{eff}
1	12	2.734	2.18	10.18	0.7620	0.8594	0.04085	1.0287	40.75	1.0015
2	12	2.734	2.93	10.18	0.7620	0.8594	0.04085	1.1049	53.23	1.0052
3	12	2.734	3.80	10.18	0.7620	0.8594	0.04085	1.1938	63.28	1.0043
4	13	2.734	7.02	10.18	0.7620	0.8594	0.04085	1.4554	65.64	1.0098
5	13	2.734	8.49	10.18	0.7620	0.8594	0.04085	1.5621	60.07	1.0118
6	13	2.734	10.13	10.18	0.7620	0.8594	0.04085	1.6891	52.92	1.0072
7	14	2.734	2.50	10.18	0.7620	0.8594	0.04085	1.0617	47.5	1.0008
8	14	2.734	4.51	10.18	0.7620	0.8594	0.04085	1.2522	68.8	0.9987
9	14	3.745	2.50	10.37	0.7544	0.8600	0.0406	1.0617	68.3	1.0010
10	14	3.745	4.51	10.37	0.7544	0.8600	0.0406	1.2522	95.1	1.0025
11	15	3.745	4.51	10.37	0.7544	0.8600	0.0406	1.2522	95.68	1.0009
12	16	4.099	2.55	9.46	1.1278	1.2090	0.0406	1.5113	88.0	0.9889
13	16	4.099	2.14	9.46	1.1278	1.2090	0.0406	1.450	79.0	0.9830
14	17	4.099	2.59	9.45	1.1268	1.2701	0.07163	1.555	69.25	0.9999
15	17	4.069	3.53	9.45	1.1268	1.2701	0.07163	1.684	85.52	0.9958
16	17	4.069	8.02	9.45	1.1268	1.2701	0.07163	2.198	92.84	1.0040
17	17	4.069	9.90	9.45	1.1268	1.2701	0.07163	2.381	91.79	0.9872
18	17	3.037	2.64	9.28	1.1268	1.2701	0.07163	1.555	50.75	0.9946
19	17	3.037	8.10	9.28	1.1268	1.2701	0.07163	2.198	68.81	0.9809
20	9	0.714*	1.68	9.52	0.8570	0.9931	0.0592	1.3208	108.8	0.9912
21	9	0.714*	2.17	9.52	0.8570	0.9931	0.0592	1.4224	121.5	1.0029
22	9	0.714*	4.70	9.52	0.8570	0.9931	0.0592	1.8669	159.6	0.9944
23	9	0.714*	10.76	9.52	0.8570	0.9931	0.0592	2.6416	128.4	1.0008
24	10	0.729*	1.11	9.35	1.2827	1.4427	0.0800	1.7526	89.1	0.9902
25	10	0.729*	3.49	9.35	1.2827	1.4427	0.0800	2.4785	104.72	1.0055
26	10	0.729*	3.49	9.35	1.2827	1.4427	0.0800	2.4785	79.5	0.9948
27	10	0.729*	1.54	9.35	1.2827	1.4427	0.0800	1.9050	90.0	0.9878

* These are PuO₂ in Natural UO₂.

** Cases 1 through 19 are with stainless steel clad, Cases 20 through 27 are zircaloy.

7045U012784



TABLE 4

WESTINGHOUSE UO_2 Zr-4 CLAD CYLINDRICAL CORE CRITICAL EXPERIMENTS^(6,7)

Experiment	Pitch In	Boron Concentration (ppm)	Material Buckling (for LEOPARD CM-2)	Critical No. of Pins	Radius of Fuel Region (cm)	k_{eff} (LEOPARD/PDQ-7)
1	0.600	0	.008793	489.4	19.021	0.9912
2	0.690	0	.009725	317.0	17.605	0.9941
3	0.848	0	.008637	251.6	19.276	0.9927
4	0.976	0	.006458	293.0	23.935	0.9935
5	0.600	306.	.007177	659.9	22.088	0.9927
6	0.600	536.4	.006244	807.2	24.429	0.9937
7	0.600	727.7	.005572	950.2	26.504	0.9940
8	0.600	104.	.008165	546.3	20.097	0.9919
9	0.600	218.	.007599	607.1	21.186	0.9917
10	0.600	330.	.007106	669.5	22.248	0.9916
11	0.600	446.	.006661	735.3	23.315	0.9909
12	0.600	657.1	.005809	895.3	25.727	0.9944
13	0.848	104.	.007320	321.0	21.772	0.9938
14	0.848	218.	.006073	420.5	24.919	0.9925
						0.9928 Mean
						0.0012 Std

Notes(a) Fuel Region Data

Enrichment = 2.719 w/o U-235
 Fuel Density = 10.41 g/cm³
 Pellet Radius = 0.20 in
 Clad IR = 0.2027 in
 Clad OR = 0.23415 in

(b) Thickness of water reflector is that required to attain total radius of 50 cm for model.

$$(c) B_z^{2(PDQ-7)} = .000527 \text{ cm}^{-2}$$

TABLE 5

BATTELLE FIXED NEUTRON POISON CRITICALS⁽¹⁸⁾

Case	Length Times Width*	No. of Assemblies In Array	Absorber Type	Thickness	Distance To Fuel Cluster	Critical Separation of Clusters	k_{eff} LEOPARD/PDQ
020	20 x 17	3	Boral	.713 cm	.645 cm	6.34 cm	0.9932
017	22.21 x 16 ^x	3	Boral	.713	.645	5.22	0.9944
002	20 x 18.88 ⁺	1	Boral	.713	2.732	∞	0.9925
028	20 x 16	3	S.S.	.485 cm	.645 cm	6.88 cm	0.9946
027	20 x 16	3	S.S.	.302	.645	7.43	0.9935
032	20 x 17	3	S.S. 1.1 w/o B	.298 cm	.645 cm	7.56 cm	0.9933
038	20 x 17	3	S.S. 1.6 w/o B	.298	.645	7.36	0.9931
0028	20 x 18.075	1	None	-	-	∞	0.9956
015	20 x 17	3	None	-	-	11.92 cm	0.9942
013	20 x 16	3	None	-	-	8.39	0.9945
022	20 x 15	3	None	-	-	6.39	0.9933
021	20 x 16	3	None	-	-	4.46	0.9946

Statistical Summary:

Series	Number	mean k_{eff}	α
Boral	3	0.9934	0.0008
S.S.	2	0.9941	0.0006
S.S. (Borated)	2	0.9932	0.0001
Fixed Poison			
Total	7	0.9935	0.0007
Non-Poison			
Total	5	0.9944	0.0007
Overall	12	0.9939	0.0008

* This is in units of pitch (Pitch = 2.032 cm)

^x Center assembly was 20x16 and the outer two were elongated at 22.21x16.

⁺ 20x18.88 was one assembly with a boral sheet on two sides.

Fuel region data: Enrichment = 2.35 w/o, Pellet radius = 0.5588 cm,
Clad OR = .635 cm, Wall thickness = .0762 cm, Pitch = 2.032 cm

7045U012784

TABLE 6

SAXTON $\text{PuO}_2\text{-UO}_2$ CRITICAL EXPERIMENTS
(Reference 9)

<u>Expt.</u>	<u>Boron</u> (ppm)	<u>H₂O/UO₂</u> (Volume)	<u>Pitch</u> (Inches)	<u>-k_{eff}</u>	<u>-k_{eff}-1</u>
1	0	1.68	.520	.9912	-.0088
2	0	2.17	.560	1.0029	+.0029
3	337	2.17	.560	1.0084	+.0084
4	0	4.70	.735	.9944	-.0056
5	0	10.76	1.040	1.0008	+.0008



TABLE 7

ESADA PuO₂-UO₂ CRITICAL EXPERIMENTS
(Reference 10)

<u>Expt.</u>	<u>Boron</u> (ppm)	<u>Pu-240</u> (%)	<u>H₂O/UO₂</u> (Volume)	<u>Pitch</u> (Inches)	<u>k_{eff}</u>	<u>k_{eff}-1</u>
1	0	8	1.11	.690	.9902	-.0098
2	0	8	3.49	.9758	1.0055	+.0055
3	526	8	3.49	.9758	.9949	-.0051
4	0	24	3.49	.9758	.9948	-.0052
5	0	8	1.54	.750	.9878	-.0122
6	526	8	1.11	.690	.9945	-.0055

TABLE 8

SUMMARY OF PREDICTIONS FOR k_{eff}
IN CRITICALITY EXPERIMENTS

<u>Experiment</u>	<u>Cases</u>	<u>k_{eff}</u>
Saxton PuO_2-UO_2	5	$0.9995 \pm .0068$
ESADA PuO_2-UO_2	6	$0.9946 \pm .0061$
All PuO_2-UO_2	11	$0.9969 \pm .0066$

TABLE 9

SUMMARY OF REACTIVITY BIASES AND UNCERTAINTIES
FOR GINNA REGION 2 MDR

<u>Description</u>	<u>Reactivity Effect</u>	<u>k_∞</u>
Basic rack cell at 20°C, 4.25 w/o U-235 @ 30,000 MWD/MT 8.430 inch pitch (see Figure 1) Using one-quarter cell model		0.9072
Calculation Biases		
Leopard/PDQ model bias	+0.0031	
Modeling Effect	+0.0005	
Mesh Spacing Effect	+0.0002	
Most Reactive Temperature over operating range	+0.0000	
Most Reactive Water Density	+0.0000	
Region 1 - Region 2	+0.0123	
Interface Effect		
Total Bias	+0.0161	
Basic cell including Biases		0.9223
Tolerances and Uncertainties (95/95)		
Depleted fuel assembly reactivity uncertainties	0.0131	
Maximum error due to pitch tolerance	0.0019	
Maximum error due to SS thickness tolerance	0.0002	
Maximum error due to pellet density tolerance (+ .015)	0.0015	
Maximum error due to pellet diameter tolerance (+ .001")	0.0005	
Calculational Uncertainty (2.82σ)	0.0186	
Total Uncertainty (statistical)	0.0229	
Maximum reactivity change from biases and uncertainties	0.0390	
Maximum k _∞ , including biases and uncertainties		0.9462

TABLE 10

COMPUTED INFINITE MULTIPLICATION FACTORS FOR GINNA MDR

<u>Enrichment w/o</u>	<u>Exposure MWD/MT</u>	<u>Computed k_{∞}</u>
1.75	0	0.8973
1.75	10,000	0.7901
1.75	12,500	0.7649
1.75	15,000	0.7442
3.00	10,000	0.9609
3.00	20,000	0.8655
3.00	25,000	0.8215
3.00	30,000	0.7788
4.25	0	1.1701
4.25	25,000	0.9463
4.25	30,000	0.9072
4.25	35,000	0.8680
4.25	40,000	0.8288
4.25	45,000	0.7903

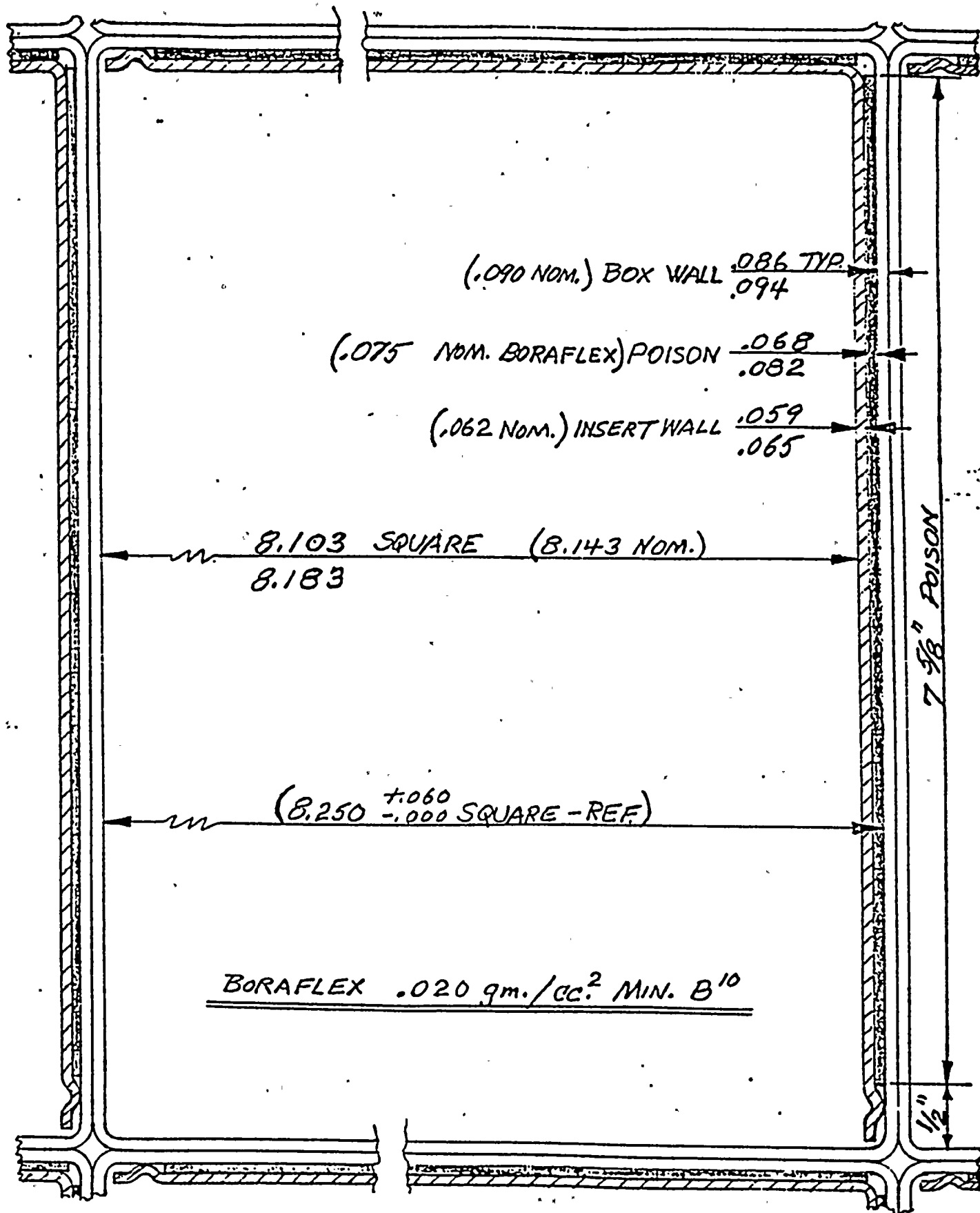


Figure 1. Ginna MDR Spent Fuel Rack Design

FIGURE 2

NET DESTRUCTION OF U-235 VERSUS BURNUP
IN THE YANKEE ASYMPTOTIC NEUTRON SPECTRUM

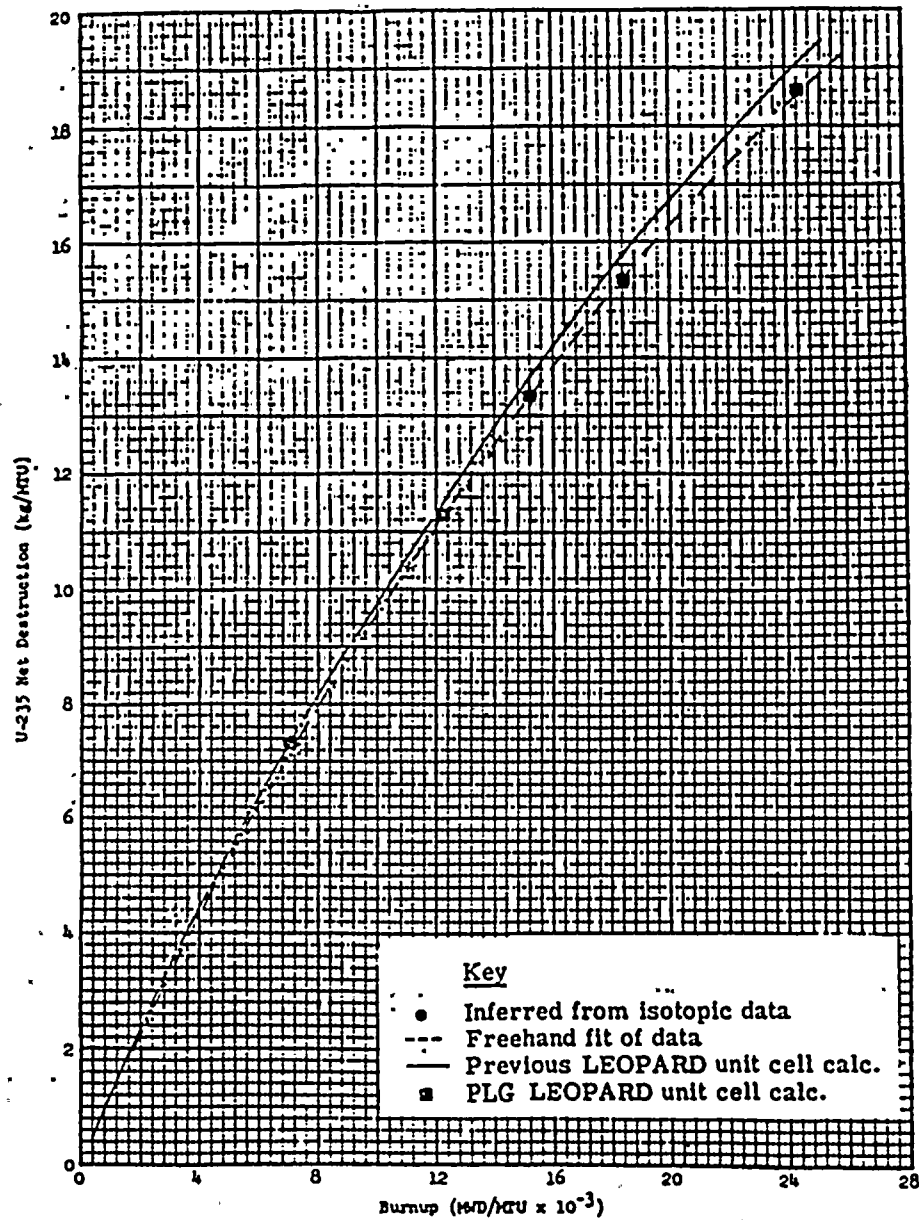


FIGURE 3

SPECIFIC PRODUCTION OF U-236 VERSUS
BURNUP IN THE YANKEE ASYMPTOTIC NEUTRON SPECTRUM

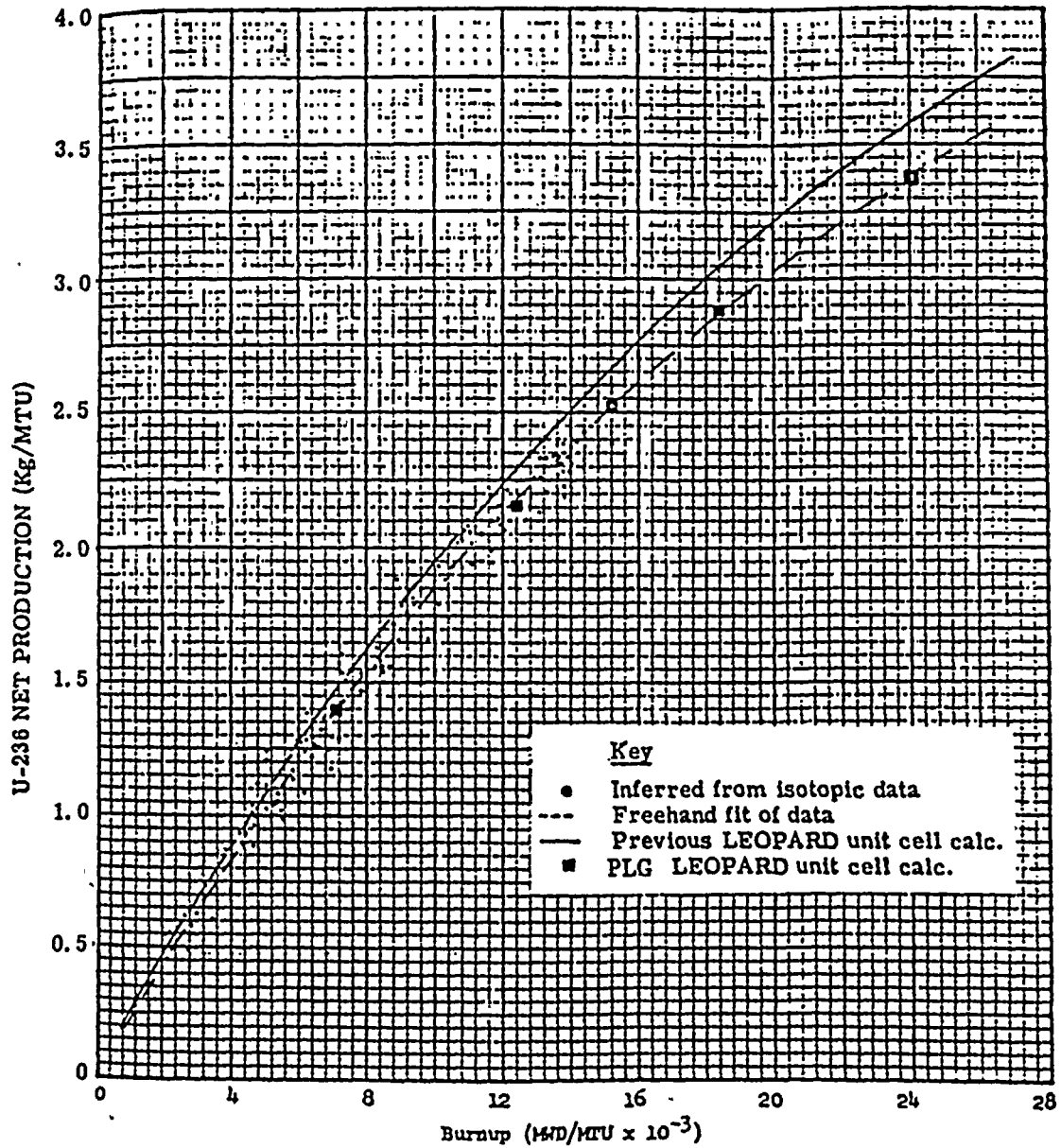


FIGURE 4

NET DESTRUCTION OF U-238 VERSUS BURNUP
IN THE YANKEE ASYMPTOTIC NEUTRON SPECTRUM

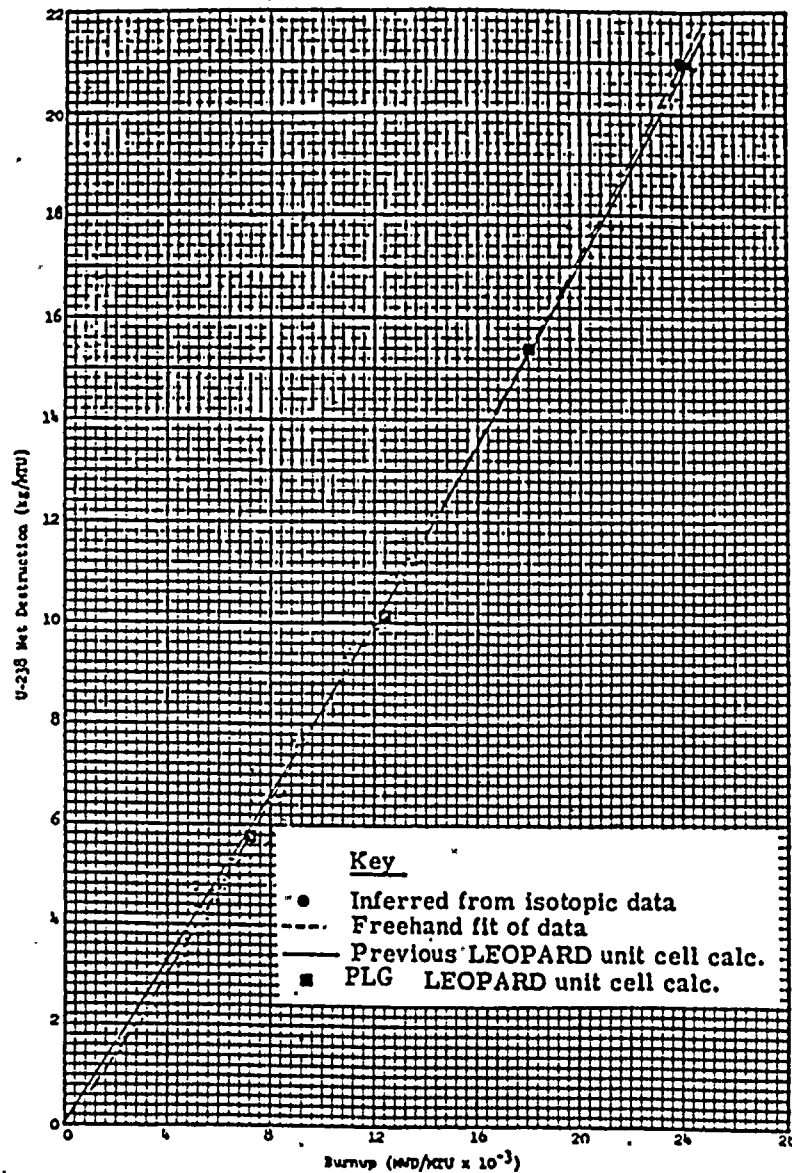


FIGURE 5

SPECIFIC PRODUCTION OF PU-239 VERSUS BURNUP
IN THE YANKEE ASYMPTOTIC NEUTRON SPECTRUM

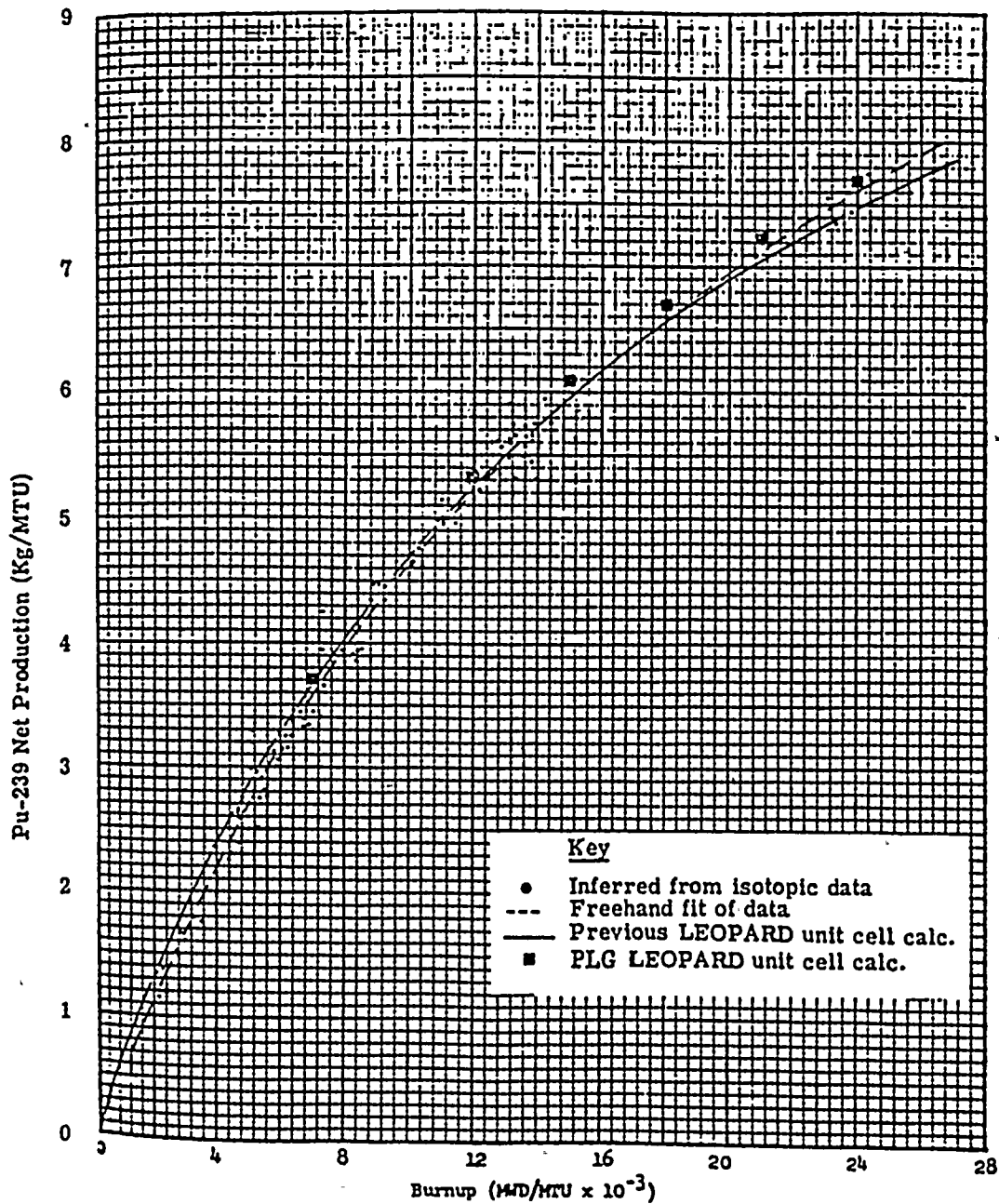




FIGURE 6

SPECIFIC PRODUCTION OF Pu-240 VERSUS BURNUP IN THE
YANKEE ASYMPTOTIC NEUTRON SPECTRUM

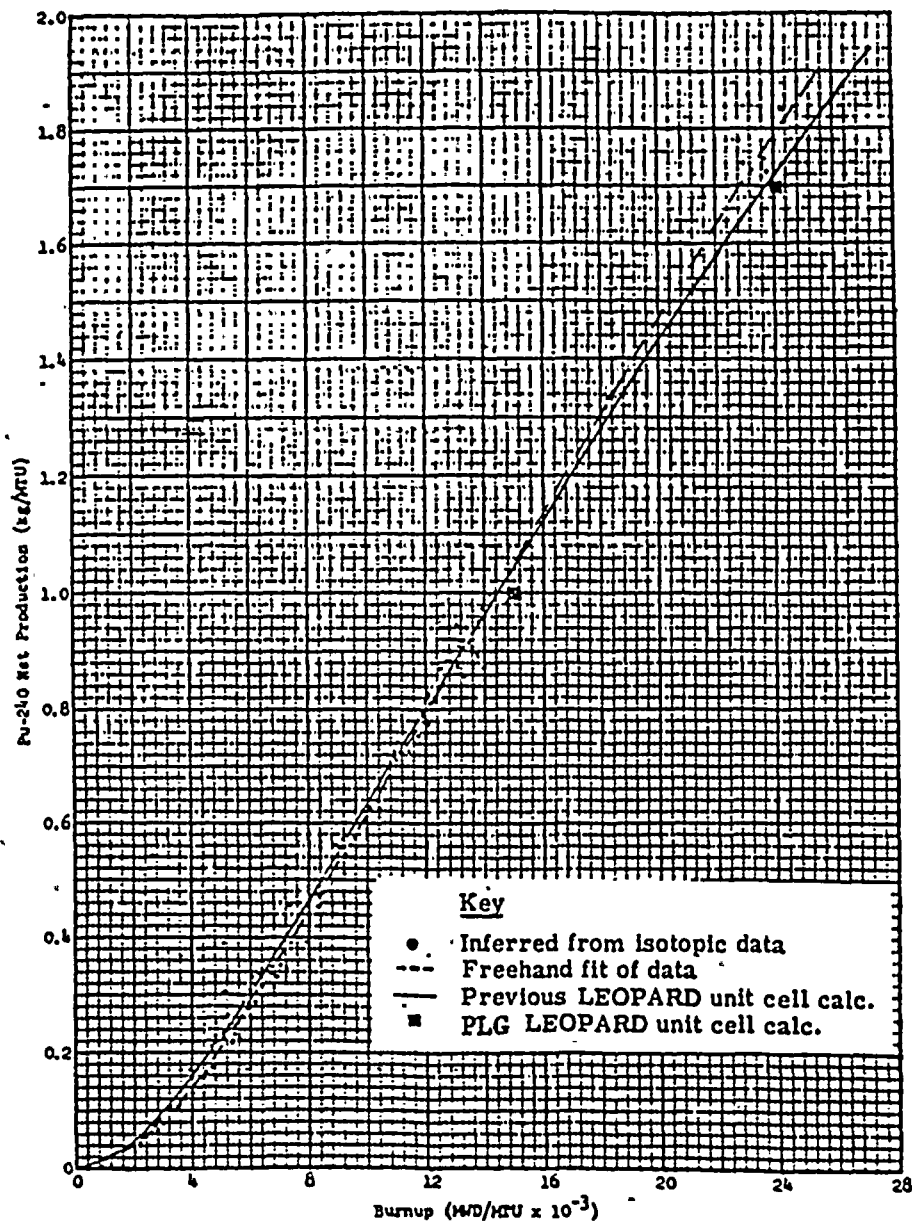


FIGURE 7

SPECIFIC PRODUCTION OF Pu-241 VERSUS BURNUP IN
THE YANKEE ASYMPTOTIC NEUTRON SPECTRUM

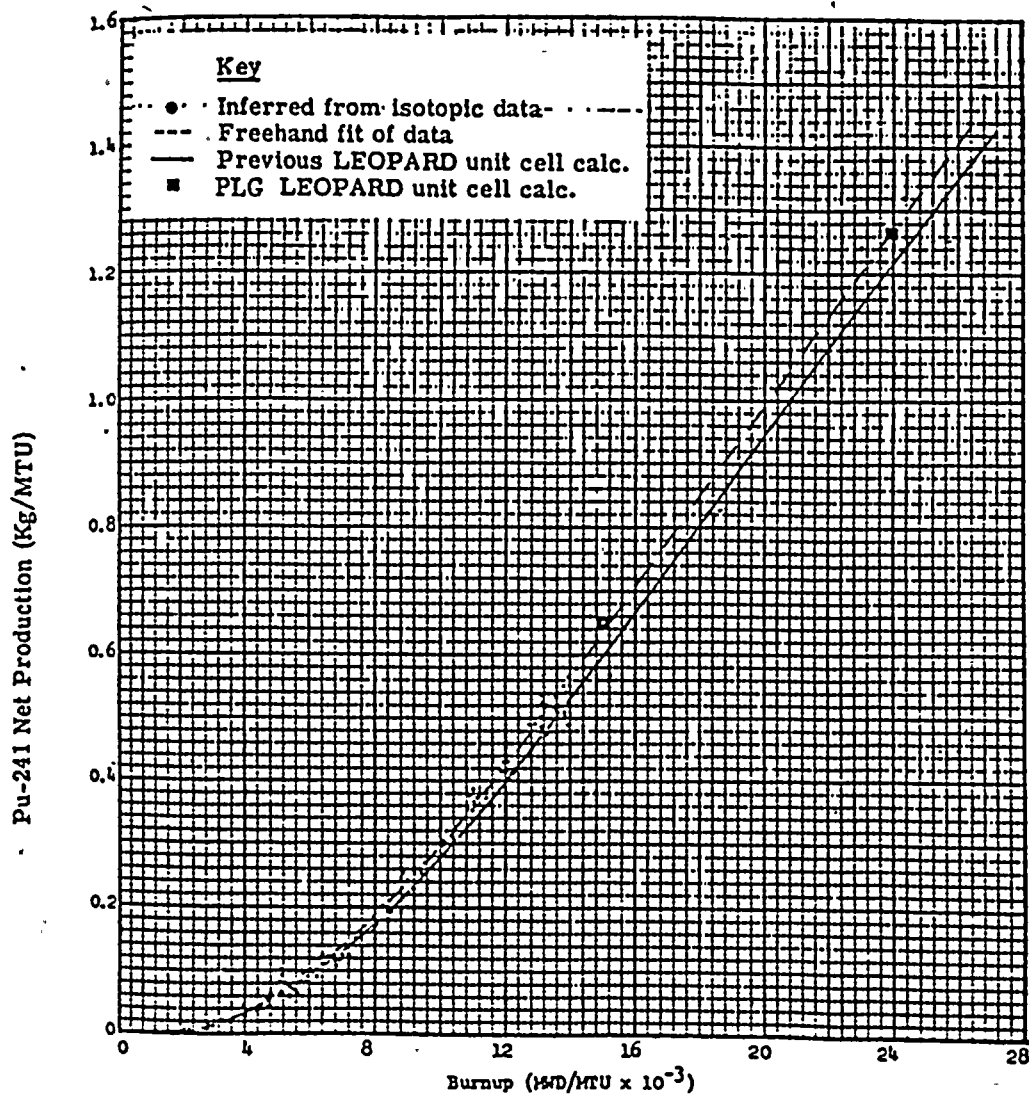


FIGURE 8

SPECIFIC PRODUCTION OF Pu-242 VERSUS BURNUP IN
THE YANKEE ASYMPTOTIC NEUTRON SPECTRUM

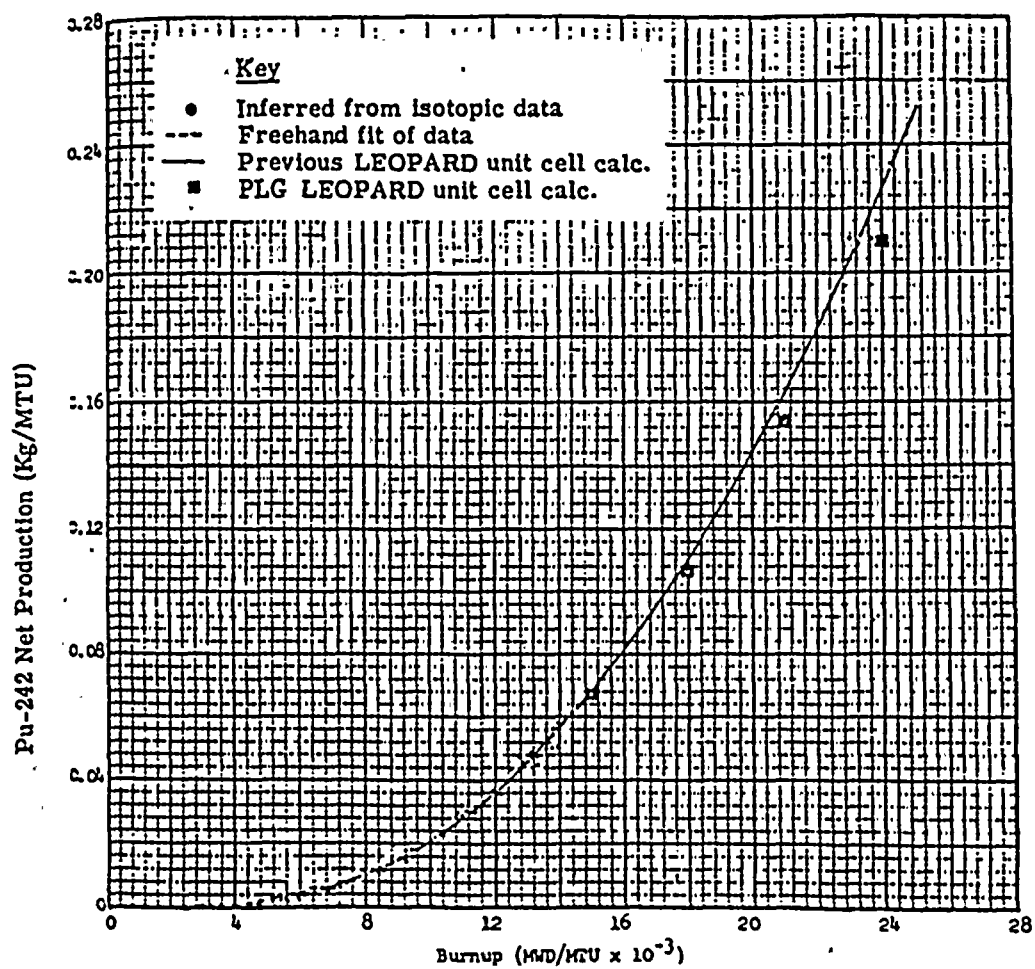




FIGURE 9

SPECIFIC PRODUCTION OF TOTAL Pu AND FISSILE Pu VERSUS BURNUP
IN THE YANKEE ASYMPTOTIC NEUTRON SPECTRUM

Net Production (Kg/MTU)

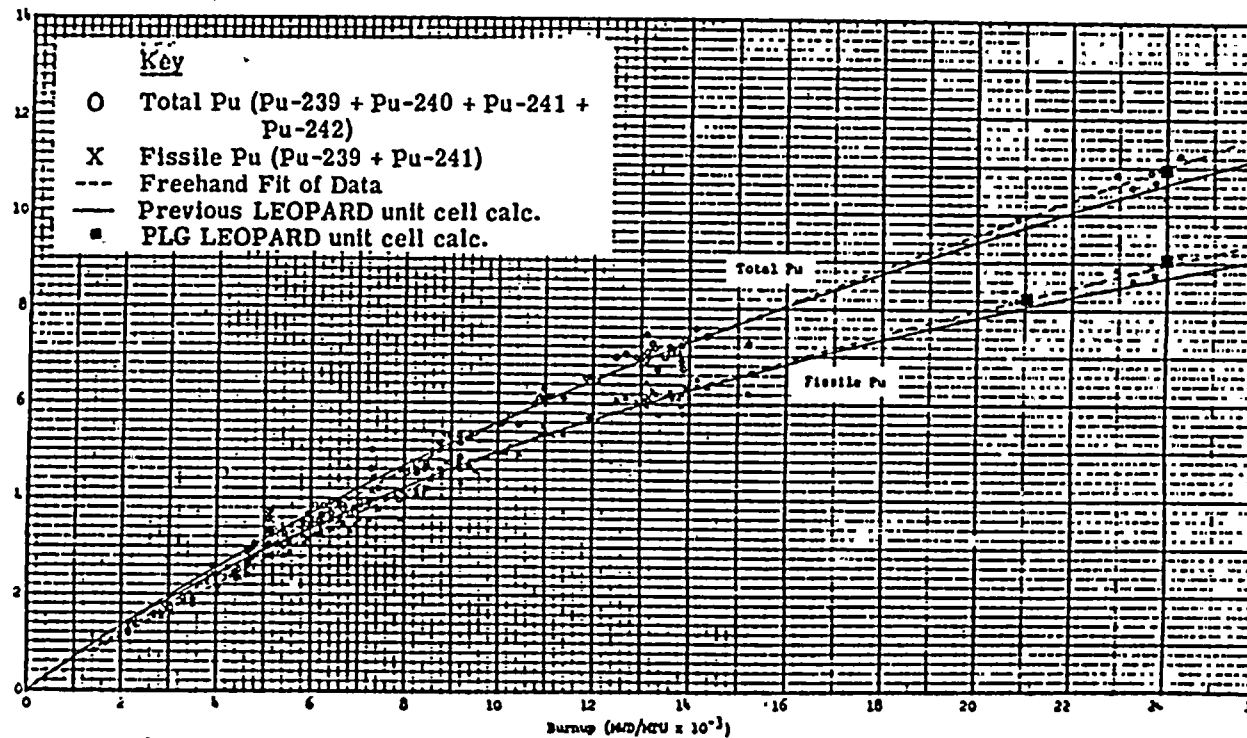


FIGURE 10

ATOM PERCENT OF TOTAL U VERSUS EXPOSURE

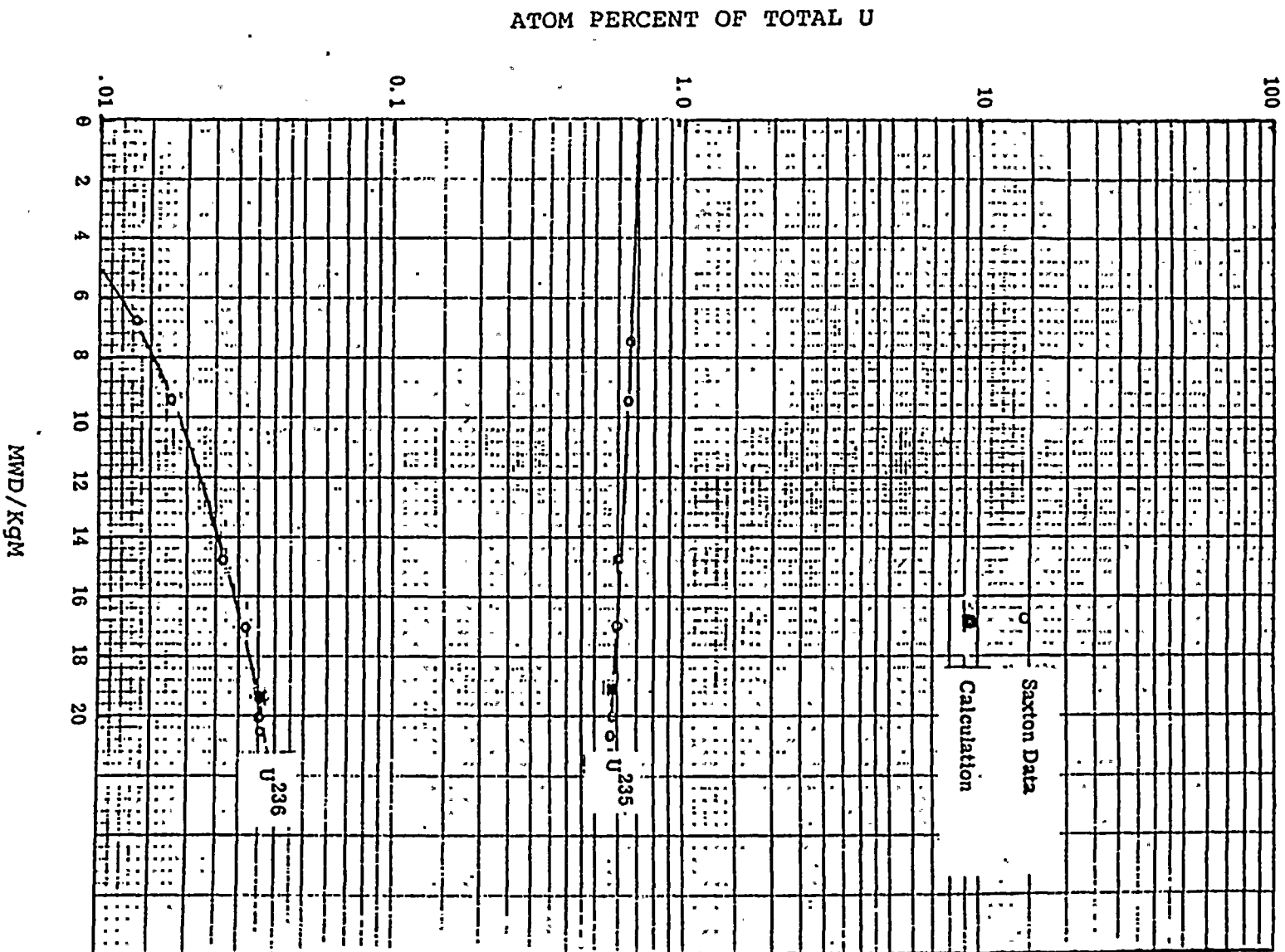


FIGURE 11

Pu-239/U-238 ATOM RATIO VERSUS EXPOSURE

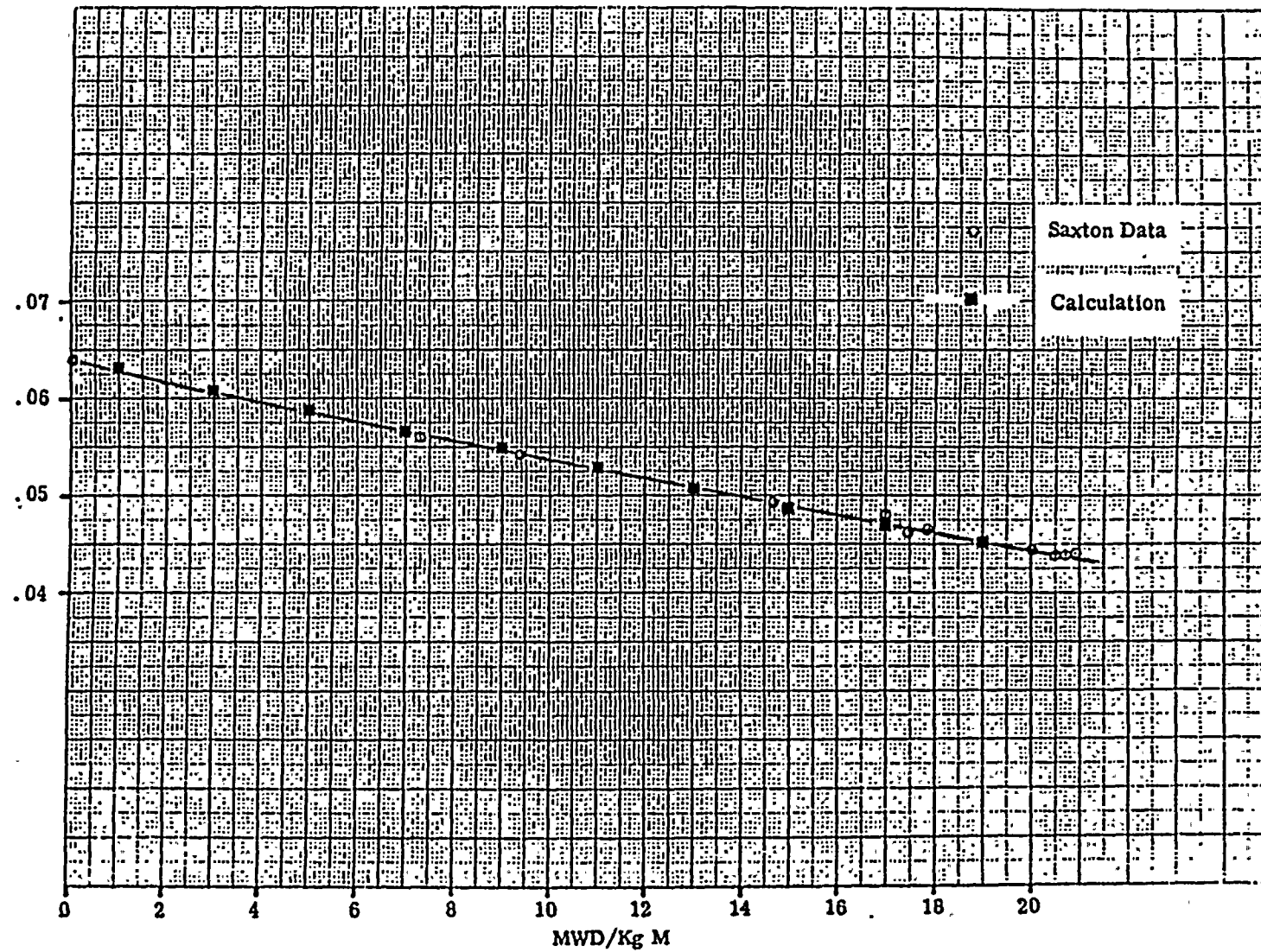
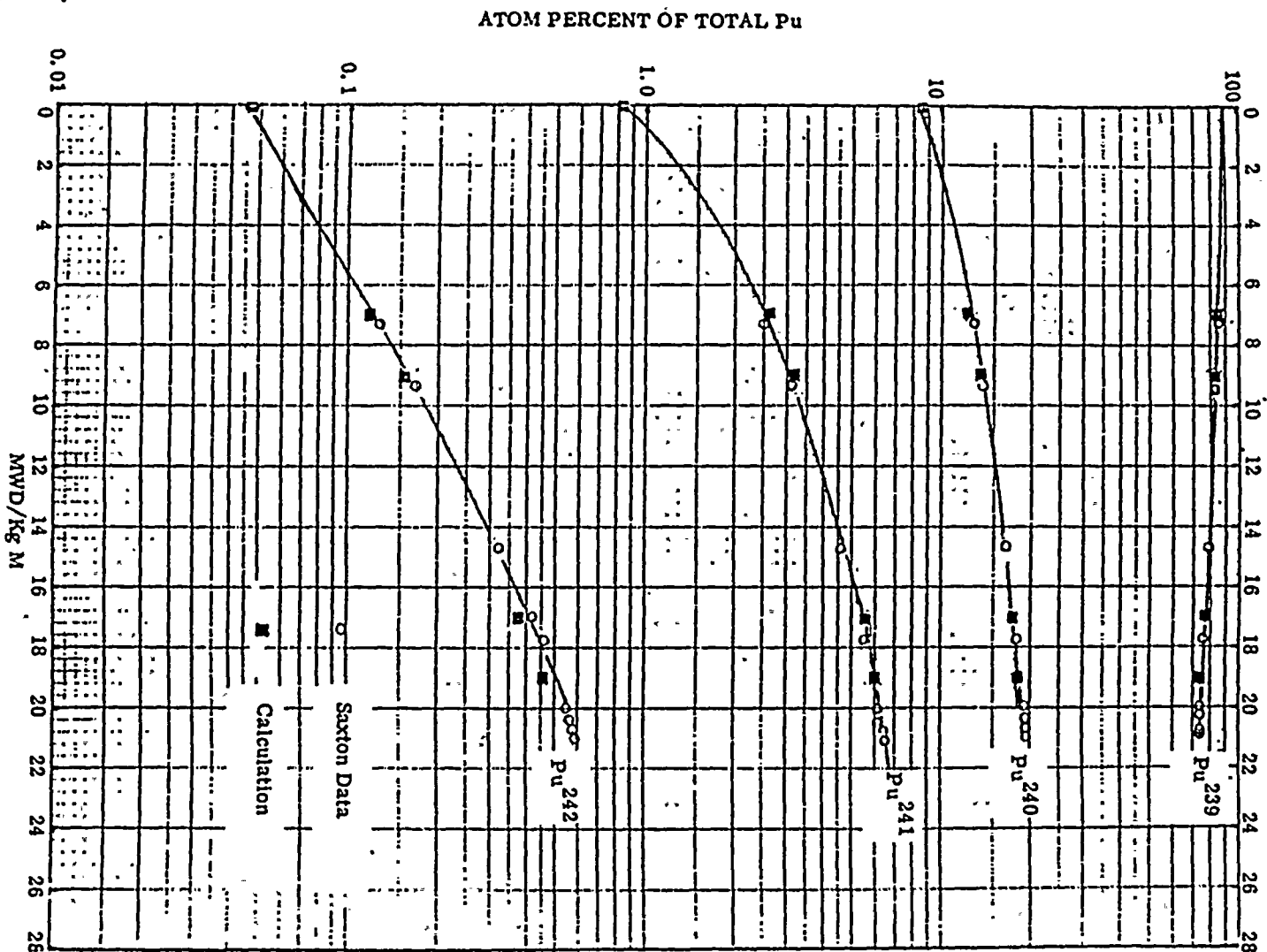


FIGURE 12

ATOM PERCENT OF TOTAL Pu VERSUS EXPOSURE



2200 m/s absorption cross-section, barns/fission

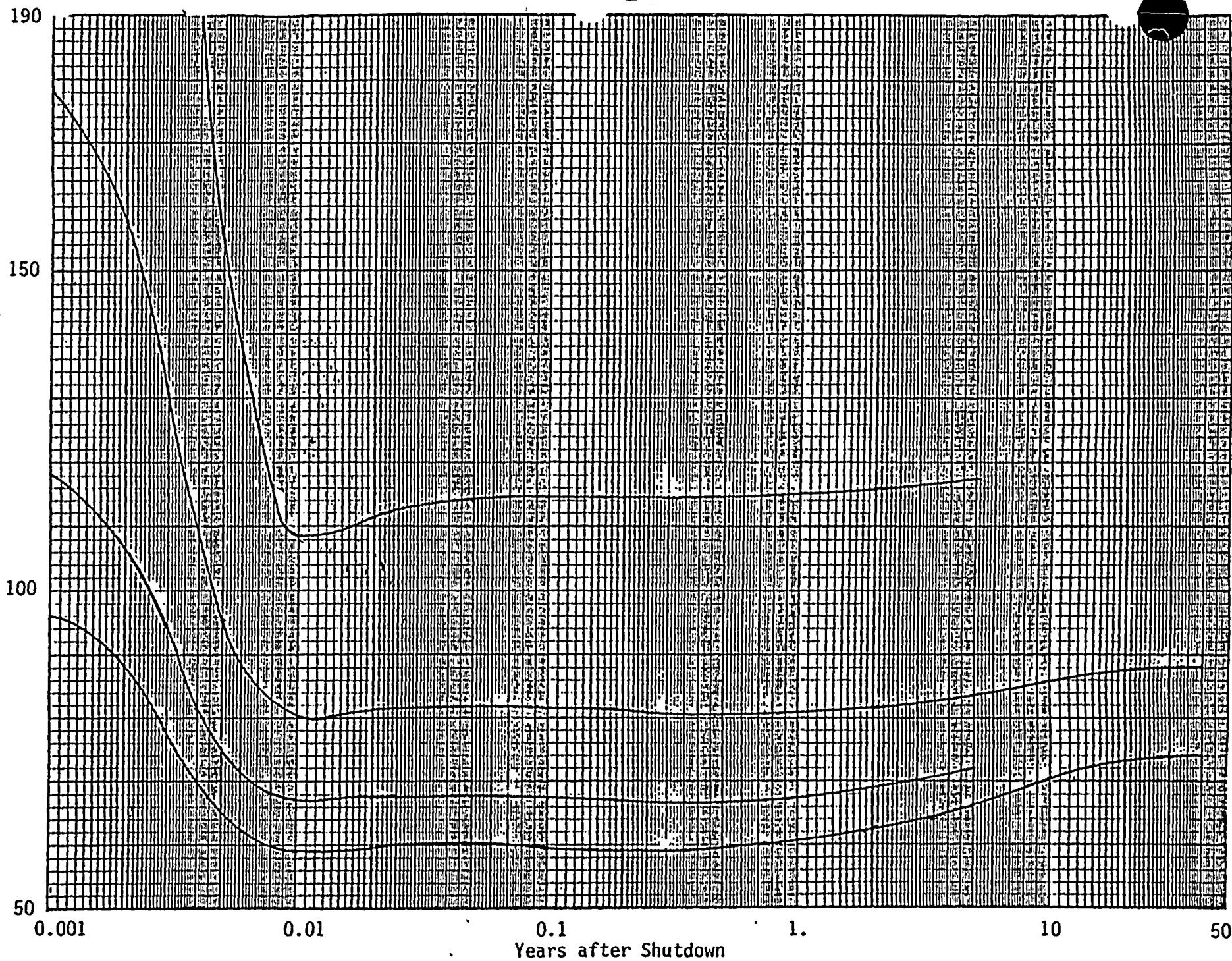
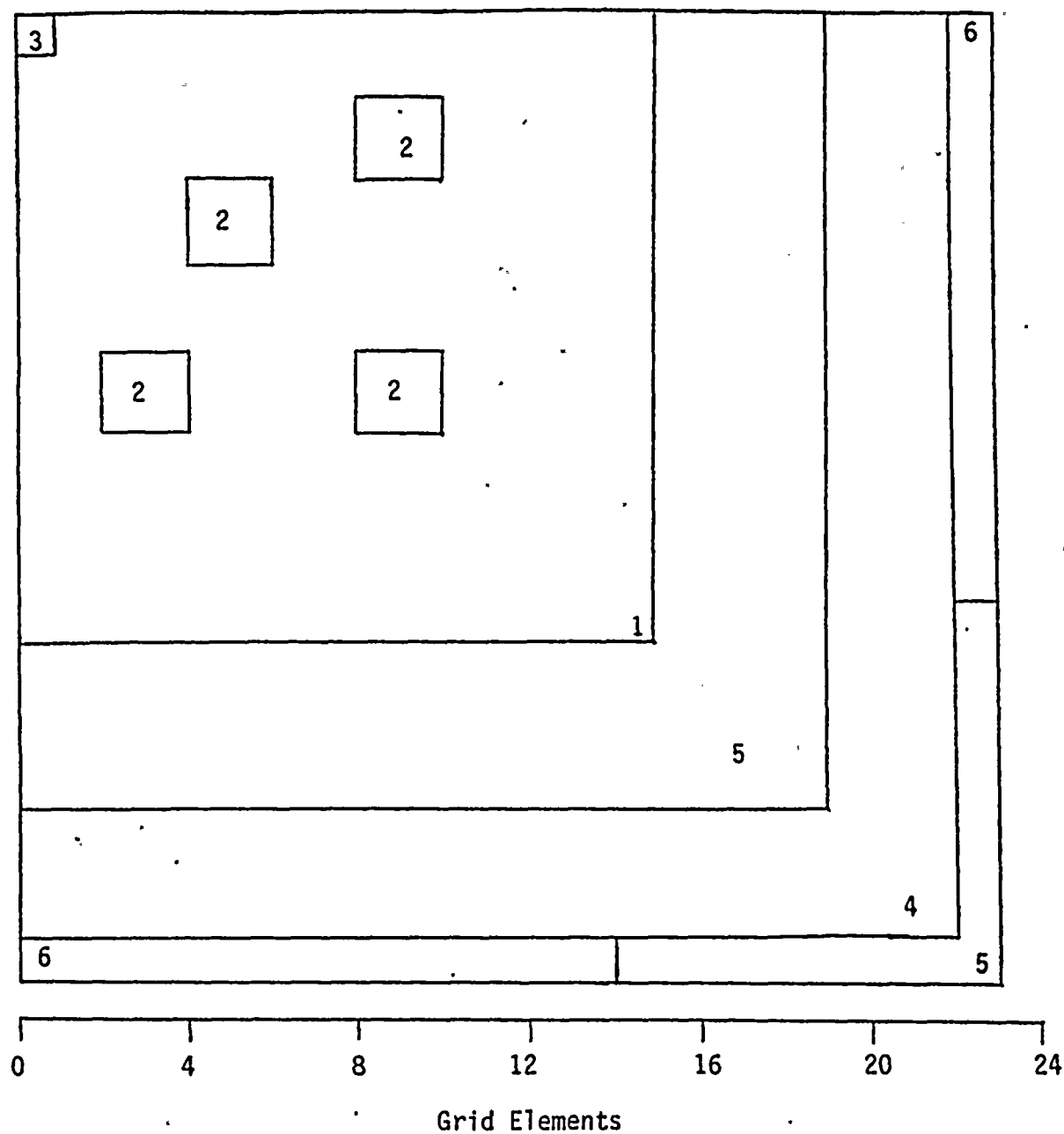


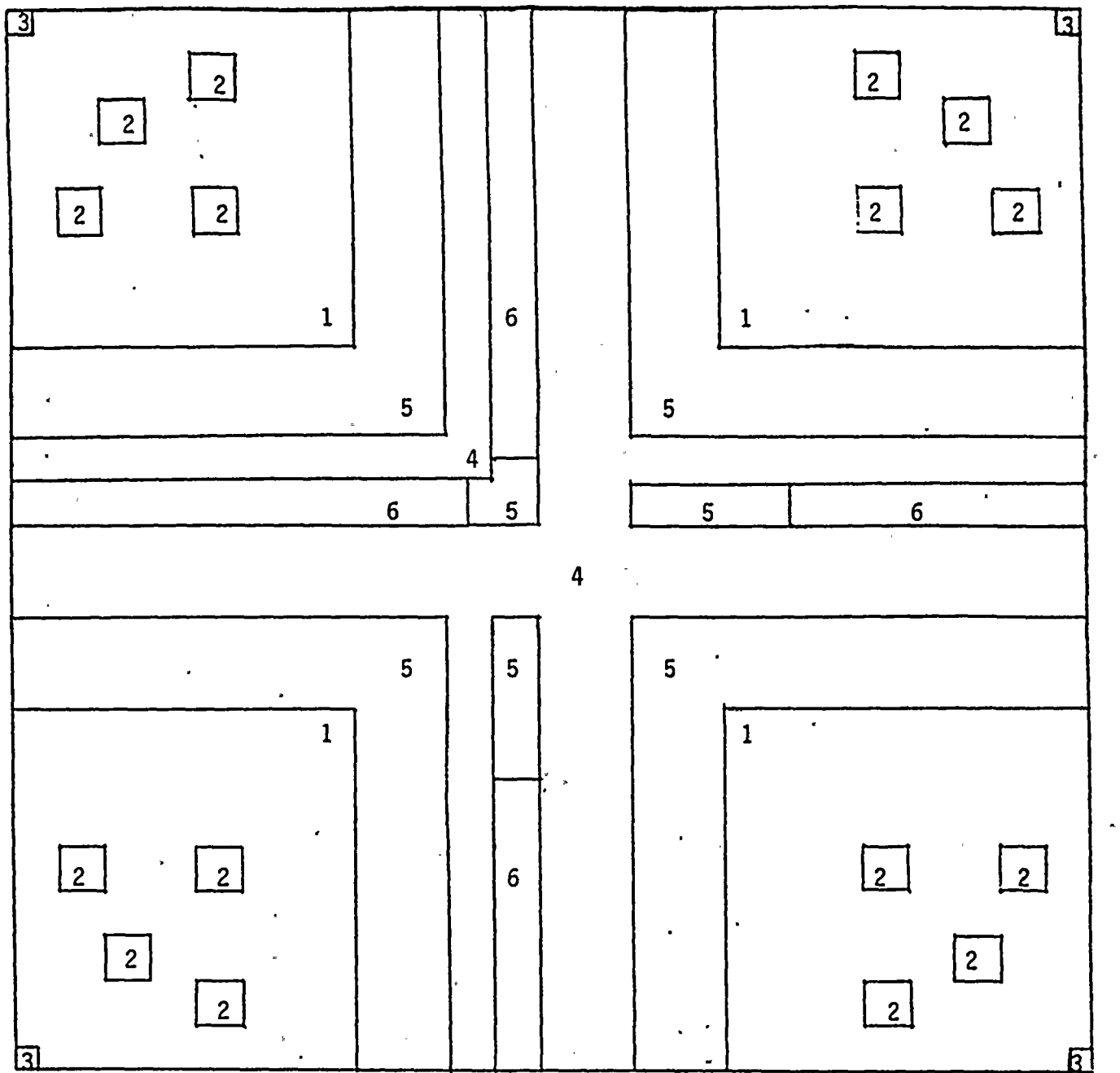
Figure 13. Fission Product Absorption Cross-Sections as a Function of Time After Shutdown



MATERIAL IDENTIFICATION

- | | |
|--------------------------|--------------------|
| 1. Pin Cells | 4. Stainless Steel |
| 2. Guide Tube Cells | 5. Water |
| 3. Instrument Tube Cells | 6. Boraflex |

Figure 14. One-Quarter Rack Cell Model for Ginna MDR



0 10 20 30 40 47

Grid Elements

MATERIAL IDENTIFICATION

- | | |
|--------------------------|--------------------|
| 1. Pin Cells | 4. Stainless Steel |
| 2. Guide Tube Cells | 5. Water |
| 3. Instrument Tube Cells | 6. Boraflex |

Figure 15. Four-Quarter Rack Cell Model for Ginna MDR

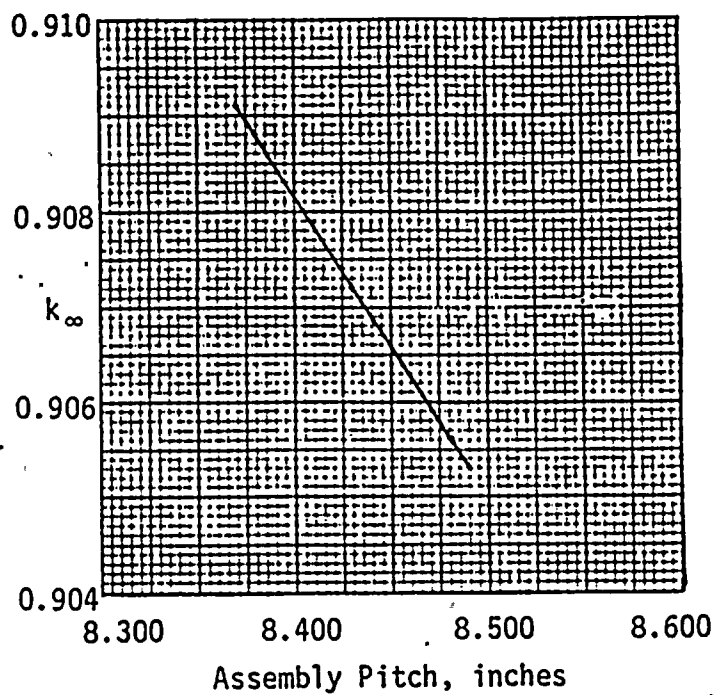


Figure 16. Variation of k_{∞} with Assembly Pitch for Ginna MDR
(4.25 w/o @ 30,000 MWD/MT, 20°C)

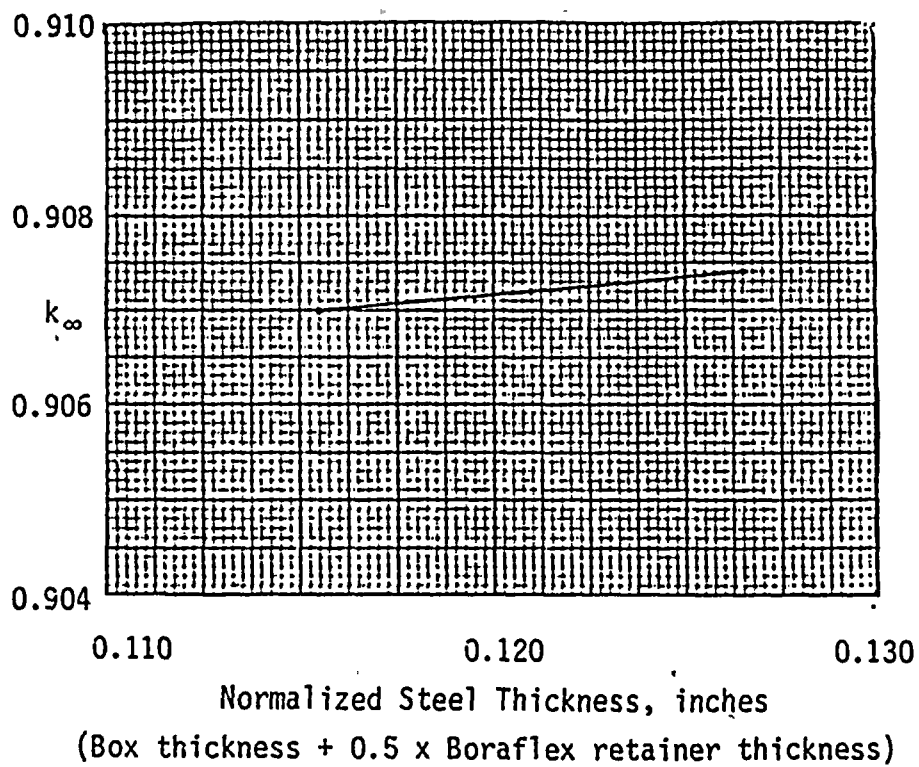


Figure 17. Variation of k_{∞} with Steel Thickness for Ginna MDR
(4.25 w/o @ 30,000 MWD/MT, 20°C)

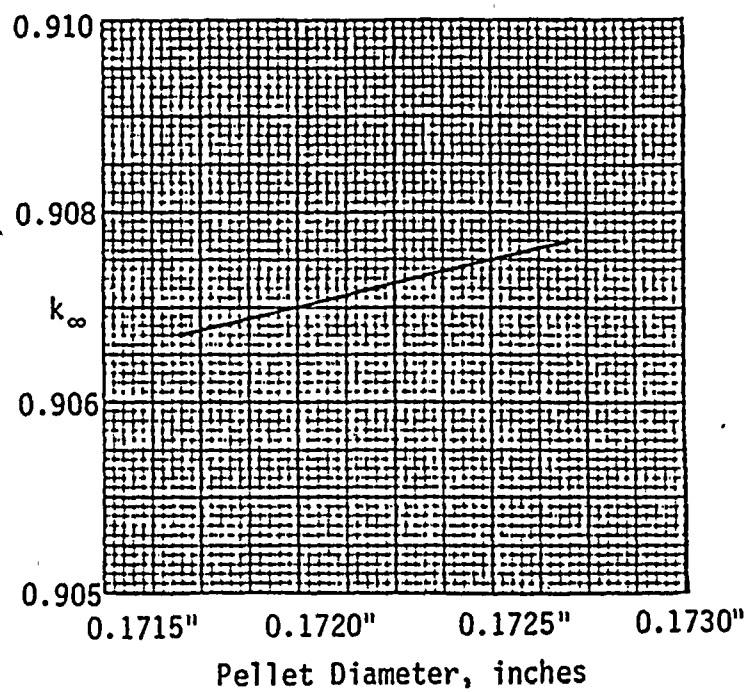


Figure 18. Variation of k_{∞} with Pellet Diameter for Ginna MDR
(4.25 w/o @ 30,000 MWD/MT, 20°C)

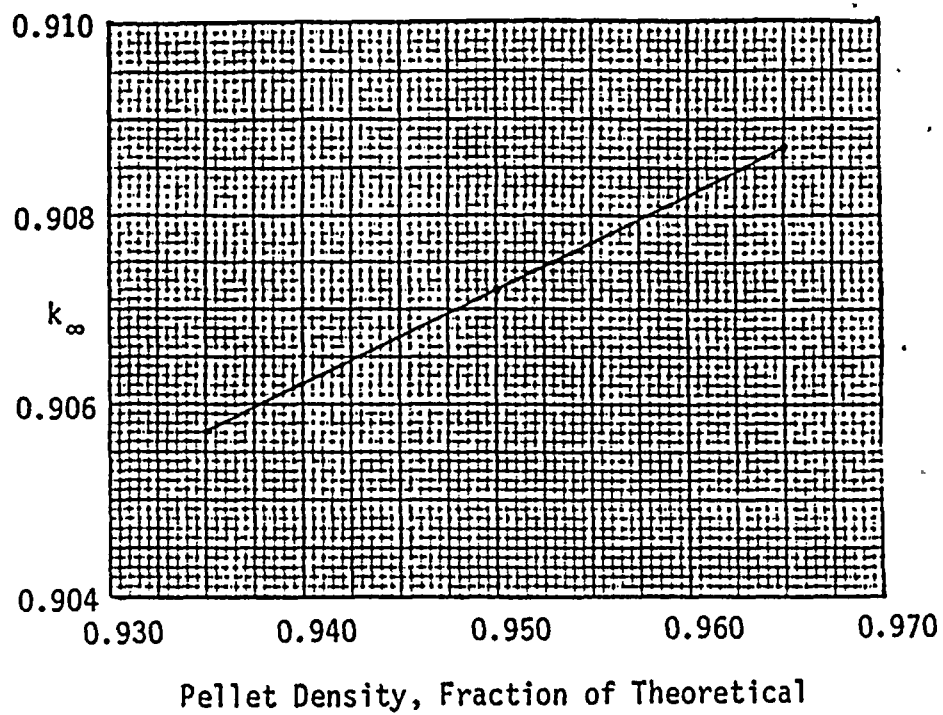
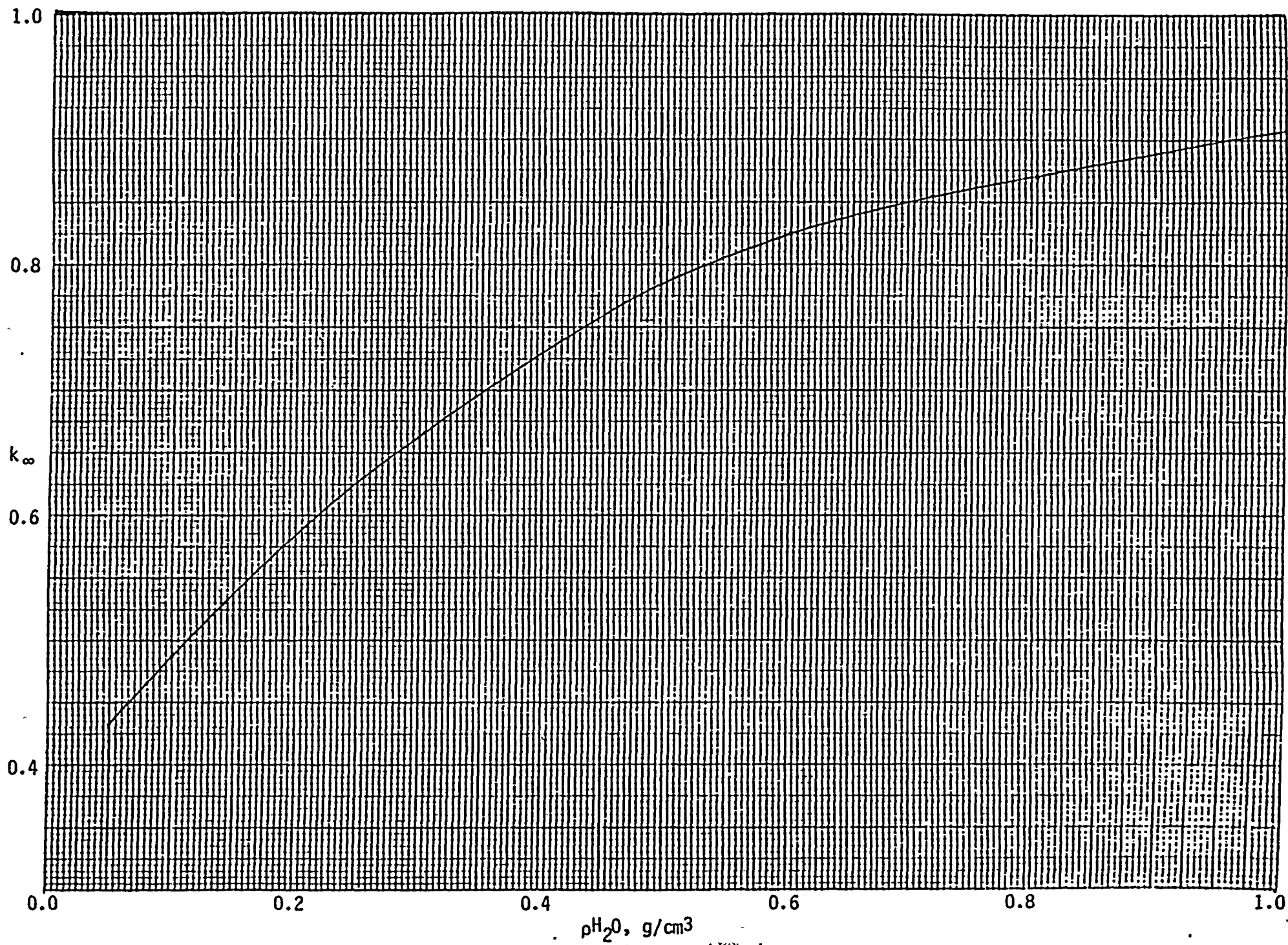


Figure 19. Variation of k_{∞} with Pellet Density for Ginna MDR
(4.25 w/o @ 30,000 MWD/MT, 20°C, Reference Dimensions)

Figure 20. Variation of k_{∞} with water density for Ginna MDR
(4.25 w/o @ 30,000 MWD/MT, 20 C, Reference Dimensions)



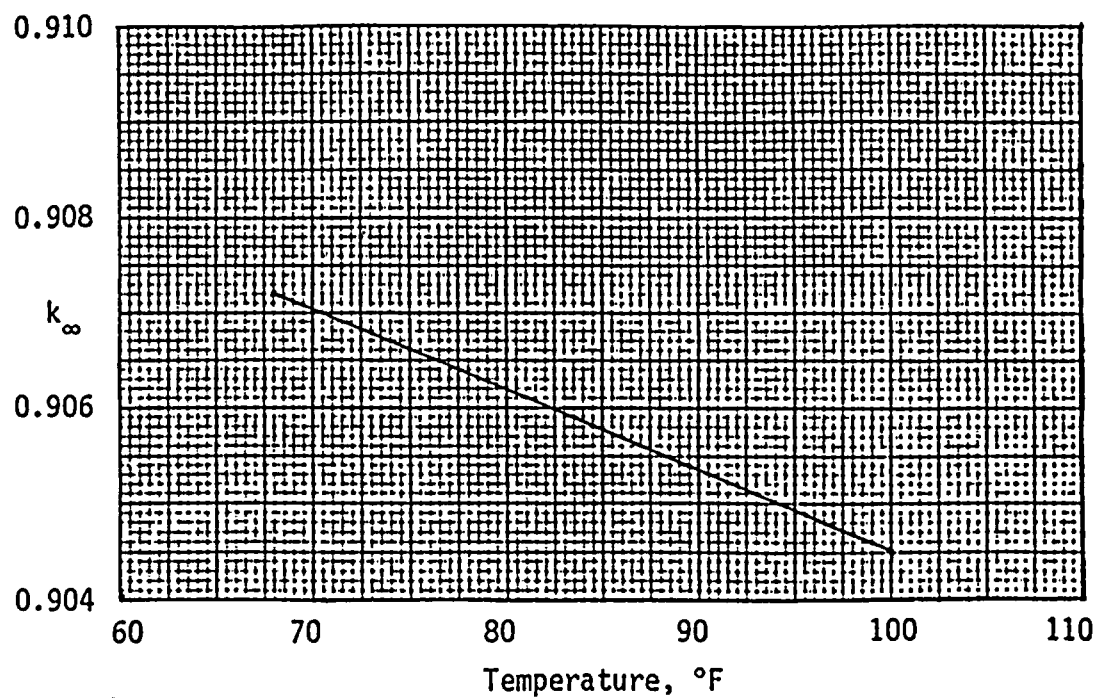
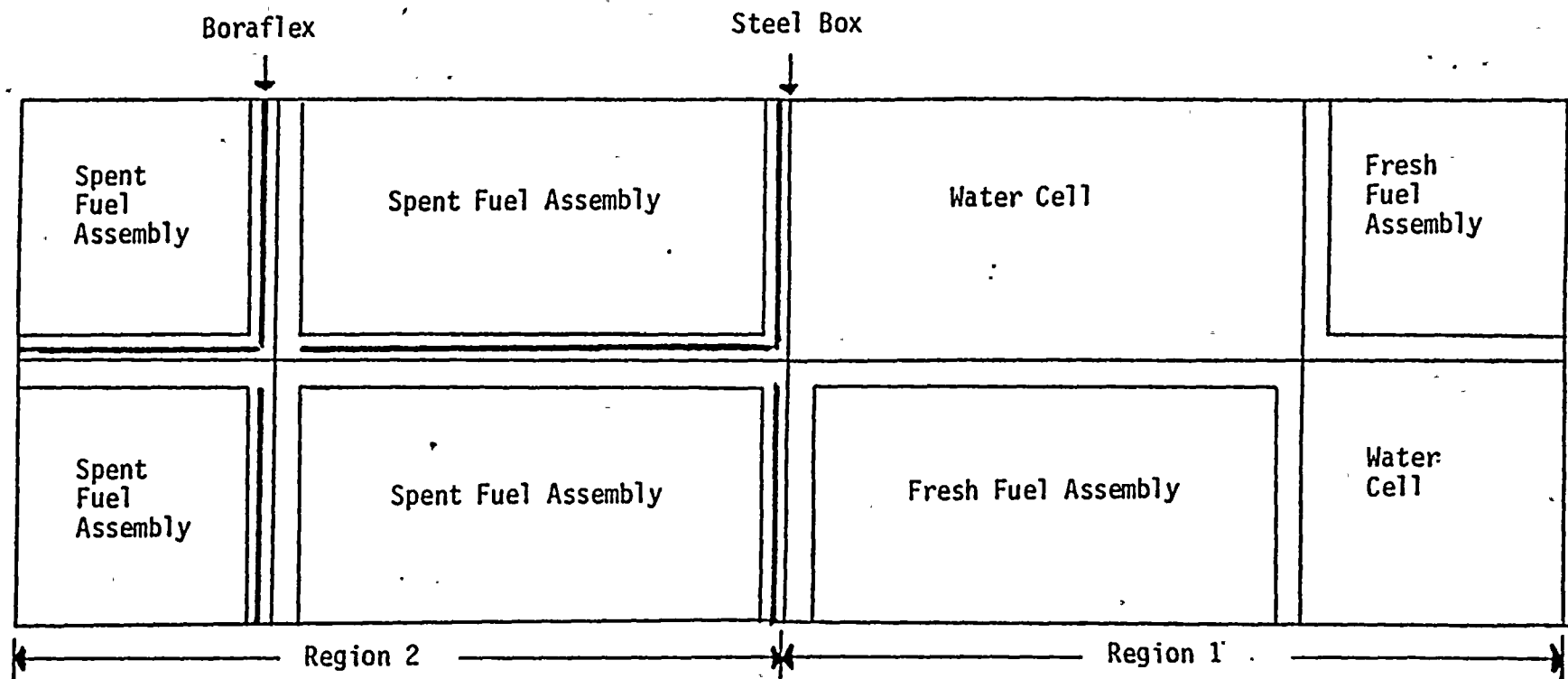


Figure 21. Variation of k_{∞} with Temperature for Ginna MDR
(4.25 w/o @ 30,000 MWD/MT, Reference Dimensions)

Figure 22. Configuration Used to Determine the Effects of the Region 1 - Region 2 Interface



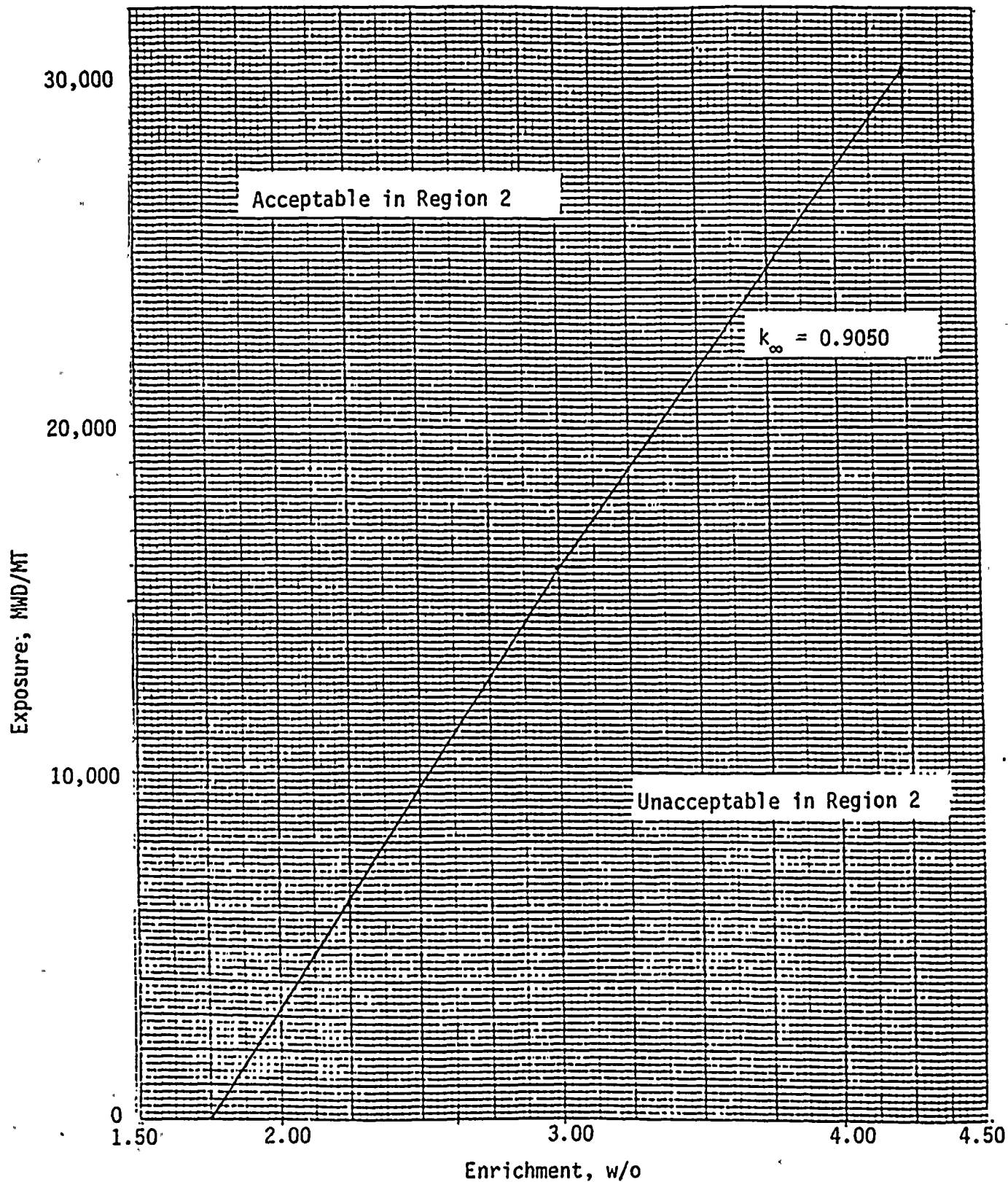


Figure 23. Regions of Acceptability and Unacceptability for Region 2 Spent Fuel

Attachment C

In accordance with 10CFR 50.91 these changes to the Technical Specifications have been evaluated against three criteria to determine if the operation of the facility in accordance with the proposed amendment would:

1. involve a significant increase in the probability or consequences of an accident previously evaluated; or
2. create the possibility of a new or different kind of accident from any accident previously evaluated; or
3. involve a significant reduction in a margin of safety.

The proposed modification would increase the spent fuel storage capacity at Ginna from 595 fuel assemblies to 1016. The safety analysis has shown that the modified racks satisfy NRC Staff accepted criteria for nuclear, structural and thermal hydraulic design. The discussion below examines each of the three criteria stated above and supports the finding that the proposed modification is outside the standards of 10CFR 50.91. Therefore, a no significant hazards finding is warranted.

1. The proposed modification does not involve a significant increase in the probability or the consequences of an accident previously evaluated.

Four potential accident scenarios have been identified: 1) spent fuel cask drop; 2) loss of spent fuel pool forced cooling water; 3) seismic event; 4) spent fuel assembly drop. The probability of these events will not be affected by the amount of fuel stored in the pool.



The consequences of a spent fuel cask drop accident are unchanged by the modification. The current Technical Specifications prohibit the movement of a cask in the auxiliary building. An Application for Amendment to the Operating License has been submitted to the NRC to delete this restriction by modifying the crane to be single failure proof in accordance with the requirements of NUREG-0554. This would obviate the need to evaluate the consequences of a cask drop accident.

The loss of spent fuel pool forced cooling water has been previously evaluated for both the current pool cooling system,^{1,2} and the system to be installed in 1986.^{3,4} The decay heat loads assumed in these analyses bound those that will be experienced due to the increased storage capacity. Therefore the consequences of this accident are unchanged from those previously evaluated.

The structural response of fully loaded storage racks during a seismic event was evaluated in Section 4 of Attachment B to this Application. The results of this evaluation satisfied NRC Staff accepted design criteria. Therefore the consequences of a seismic event are unchanged.

The consequences of a single fuel assembly drop has been evaluated in reference 2 and in Sections 2 and 4 of Attachment B to this Application. The evaluation indicates that Keff remains below .95. Since the proposed modification only affects storage of well cooled fuel, the maximum radiological releases would occur from the drop of an assembly in Region 1 which is unchanged. Therefore the consequences of a fuel assembly drop are unchanged.



2. Create the possibility of a new or different kind of accident from any accident previously evaluated.

RG&E has evaluated the proposed rack modification in accordance with the NRC April 14, 1978 letter "NRC Position for Review and Acceptance of Spent Fuel Storage and Handling Application" and appropriate NRC and industry guides, codes and standards. In its evaluation, RG&E has found no indication that a new or different kind of accident is created.

3. The proposed modification does not involve a significant reduction in the margin of safety.

Under normal operation and accident conditions, the proposed modified storage rack design must satisfy certain criteria in three areas:

1. Nuclear Criticality
2. Thermal Hydraulic
3. Structural Mechanical

In the area of nuclear criticality, the criteria established is that Keff must be less than .95. Section 2 of Attachment B of this Application indicates that this criteria is satisfied and the results are not significantly different than previous analyses.⁵ The criteria itself is unchanged from previous submittals, therefore the margin of safety has not been reduced.

Section 3 of Attachment B of the Application and previous analyses^{1,2,3,4} evaluate the thermal hydraulic considerations of the modification. This evaluation shows that the decay heat loads of previous analyses bound those that could result from the proposed modification. Therefore the margin of safety has not been reduced.

The structural considerations deal primarily with the response of fully loaded racks during a seismic event. Section 4 of Attachment B to the Application presents the structural mechanical evaluation of the racks and indicates that the appropriate criteria established by NRC guidance and industry practice has been satisfied. In addition, these analyses establish the acceptability of pool floor loads under worst case conditions. With the appropriate criteria satisfied, there is no significant reduction in the margin of safety.

